

AIX-MARSEILLE UNIVERSITY  
FACULTY OF SCIENCE OF LUMINY  
ECOLE DOCTORALE DES SCIENCES DE LA VIE ET DE LA SANTE

**The microRNA miR-449 controls the development of multiciliated cells in the mucociliary epithelium of the amphibian *Xenopus laevis* by modulating the activity of multiple targets**

Presented in public on 5<sup>th</sup> December 2014 by:  
ANNA ADAMIOK

A DISSERTATION FOR THE DEGREE OF DOCTOR OF PHILOSOPHY

Jury composed by:

Dr. Paris A. Skourides  
Dr. Jean-Pierre Tassan  
Prof. Sophie Chauvet  
Dr. Vincent Bertrand  
Dr. Andrea Pasini

Rapporteur  
Rapporteur  
Examiner  
Examiner  
Thesis supervisor

## Acknowledgements

First of all, I would like to thank my current supervisor Dr. Andrea Pasini and previous supervisor Laurent Kodjabachian for their help and all meaningful discussions that we had during my PhD.

I am grateful to Andrea for the time he dedicated to reading and criticizing my writing. While writing this thesis, Andrea's comments have been invaluable. I would like to thanks Laurent for giving me the opportunity to work at his team and for supporting my scientific carrier by founding my attendance to conferences.

I would like to thank Dr. Paris A. Skourides and Dr. Jean-Pierre Tassan for kindly accepting to be my rapporteurs as well as Prof. Sophie Chauvet and Dr. Vincent Bertrand for being my examiners.

Next, I would like to thank all of my colleagues in the lab. Especially, a previous post-doc from Laurent's team Patricia Castillo-Briceno, who became my best friend. I would like to thanks Patricia and her husband Francisco, for help in my professional and personal life. Marie Cibois and Virginie Thome for introducing me to *Xenopus* and all protocols of the lab, also for help with french administration. Diego Revinski and Piereluigi Scerbo for the incredible atmosphere their made in the team. Thanks for all discussions and nicely spent time after work. Thanks Pigi for your songs. Celine Burckle thanks for help while preparing the internal seminar.

I would like to thanks my mother, incredible strong and positive woman, for her endless support and present in my life. For all her advices and love.

Finally, I would like to thanks all my friends. From Poland and France, Grenoble and Marseille. Especially, Joanna Andrecka, thanks to her I am started my PhD. Anna Wolnik thanks for all visits and invitations, calls and messages, and spent together amazing holidays! People I met in EMBL Grenoble, my previous supervisor Dr. Ramesh Pillai and colleagues: Steffi, Philipp, Raman, Jordi, Elisa, Zhaolin, Simon, Micheal and my dear Juliette.

Of course thank to my friends who I met and working with in Luminy/Marseille. Especially, I would like to thank Eunice and Mayyasa for redaction my thesis and all the adventures we had while being together. Also, My flatmate Akankshi Munjal for sharing the apartment with me for almost 3 years.

# Table of Contents

|   |           |
|---|-----------|
| <b>I. Introduction</b>  | <b>8</b>  |
| <b>1. Cilia</b>   | <b>9</b>  |
| 1.1 Discovery of cilia  | 9         |
| 1.1.1. Definition and structural description of cilia                                 | 9         |
| 1.1.1. A The centriole  | 9         |
| 1.1.1. B The centrosome   | 10        |
| 1.1.1. C The basal body   |           |
| 1.1.1. D The transition zone  | 14        |
| 1.1.2 Motile vs primary cilia   | 17        |
| 1.1.3. Multiple vs solitary cilia   | 18        |
| <b>1.2 Cilia function in vertebrate development and physiology</b>                    | <b>20</b> |
| 1.2.1. Multiple cilia   | 20        |
| 1.2.2. The special case of nodal cilia  | 21        |
| 1.2.3. Cilia as mediators of signaling pathways                                       | 22        |
| 1.2.3.A The primary cilia and the Hedgehog (Hh) signaling pathway                     | 22        |
| 1.2.3.B The primary cilia and the Planar Cell Polarity signaling pathway              | 23        |
| 1.2.3.C The primary cilia and the Platelet-derived growth (PDGF)<br>signaling pathway | 26        |
| 1.2.3 D The primary cilia and the Fibroblast Growth Factor (FGF)<br>signaling pathway | 26        |
| 1.2.4. The primary cilia and their sensory function                                   | 27        |
| 1.2.5 .The ciliopathies   | 30        |

|   |           |
|---|-----------|
| <b>2. Ciliogenesis - from centriole to cilia</b>                                  | <b>33</b> |
| <b>2.1 Ciliogenesis vs. multiciliogenesis</b>                                     | <b>33</b> |
| 2.1.1. Centrioles/centrosomes function and biogenesis                             | 33        |
| 2.1.2. Different centriole biogenesis pathways                                    | 33        |
| 2.1.2. A) Centriole duplication through the centriolar pathway                    | 34        |
| 2.1.2. B) Centriole amplification through the centriolar pathway                  | 35        |
| 2.1.2. C) Centriole amplification through the acentriolar pathway                 | 36        |
| 2.1.3. The conversion of centrioles to basal bodies                               | 37        |
| 2.1.4. Actin cytoskeleton reorganization  | 38        |
| 2.1.4. A) Description of actin  | 38        |
| 2.1.4. B) Actin and cilia   | 40        |
| <b>2.1.5 Basal bodies docking and polarization at the plasma membrane surface</b> | <b>43</b> |
| <b>2.1.6. Cilia axoneme growth</b>  | <b>45</b> |
| 2.1.6. A) Intraflagellar transport  | 45        |
| 2.1.6. B) Vesicle transport   | 47        |
| 2.1.6. C) Control of proteins transfer within the cilium                          | 48        |
| 2.1.6. D) Control of the cilia length   | 49        |
| <b>2.1.7. Polarized beating</b>   | <b>50</b> |
| <b>3. Mechanisms of ciliary gene regulation</b>                                   | <b>52</b> |
| <b>3.1 Transcriptional level</b>  | <b>52</b> |
| 3.1.1. Rfx  | 53        |
| 3.1.2. FoxJ1  | 56        |
| 3.1.3. Myb  | 58        |
| 3.1.4. E2F  | 59        |
| <b>3.2. Post-transcriptional level</b>  | <b>60</b> |
| 3.2.1. Small non-coding RNAs: Definition and biogenesis                           | 60        |
| 3.2.1.1. Mechanisms of miRNA-mediated gene regulation                             | 62        |
| 3.2.1.1 A miR-34  | 63        |
| 3.2.1.1 B miR-449   | 64        |

|  |     |
|--|-----|
| <b>3.3 Regulatory proteins</b>   | 66  |
| 3.3.1 Multicilin   | 66  |
| 3.3.2. CCNO  | 67  |
| <br>   |     |
| <b>3. The embryonic epidermis of <i>Xenopus laevis</i> as model for studying the formation of mucociliary epithelia</b>  | 68  |
| <br>   |     |
| <b>4.1 The <i>Xenopus</i> mucociliary epithelium (MCE)</b>   | 70  |
| 4.1.1. Structure and function  | 72  |
| 4.1.1. A Mucus-secreting cells   | 72  |
| 4.1.1. B Multiciliated cells   | 72  |
| 4.1.1. C Ionocytes   | 73  |
| 4.1.1. D Small secretory cells   | 74  |
| <b>4.2. Multistep formation</b>  | 75  |
| 4.2.A. Layer segregation   | 75  |
| 4.2.B. Cell fate specification   | 77  |
| 4.2.C. Cell intercalation  | 78  |
| 4.2.D. Cell differentiation  | 79  |
| <br>   |     |
| <b>5. Aim of the work: identification and functional analysis of new miR-449 targets required for the development of the <i>Xenopus</i> mucociliary epithelium</b> | 81  |
| <br>   |     |
| <b>II. Results</b>   | 82  |
| <br>   |     |
| <b>6. Submitted data – additional information on R-Ras</b>   | 83  |
| Manuscript   | 86  |
| *Additional data on Delta1   | 122 |
| <b>7. Unpublished data on Rho- a GDP dissociation inhibitor beta – Arhgdib</b>   | 123 |
| 7.1. Arhgdib, a putative miR-449 target  | 123 |
| 7.2. Spatiotemporal expression of Arhgdib in whole-mount embryos   | 125 |
| 7.3. Spatiotemporal expression of Arhgdib in explanted ectoderm  | 126 |

|  |     |
|--|-----|
| <b>8. Unpublished, preliminary data on Steel a KIT ligand</b>  | 128 |
| 8.1. Steel - a putative miR-449 target   | 128 |
| 8.2. Spatiotemporal expression of <i>Xenopus</i> Steel1 and Steel2<br>in whole-mount embryos   | 130 |
| 8.3. Spatiotemporal expression of Steel1 RNA by using double<br>fluorescent <i>in situ</i> hybridization (FISH) on sectioned embryos | 133 |
| 8.4. Spatiotemporal expression of Steel1 RNA following<br>a miR-449a inactivation  | 136 |
| 8.5. Using "protector morpholinos" to specifically and selectively inhibit<br>the interaction between miR-449a and Steel1            | 138 |
| 8.6. Spatiotemporal expression of Steel1 following Steel1 Po injection   | 140 |
| 8.7. Effect of Steel1 protection from miR-449 binding on MCC<br>intercalation and distribution                                       | 143 |
| 8.8. Effect on the Steel1 overexpression on MCCPs distribution<br>and intercalation  | 144 |
| 8.9. Elucidating the existence of soluble or membrane bound form<br>of Steel1 in <i>Xenopus laevis</i> embryos                       | 145 |
| <b>III. Materials and methods</b>  | 148 |
| <b>IV. Discussion</b>  | 152 |
| <b>V. Conclusions and perspectives</b>   | 167 |
| <b>VI. References</b>  | 168 |

# **INTRODUCTION**



# 1. Cilia

## 1.1. Discovery of cilia

Cilia were discovered almost coincidentally in 1676 by Anton van Leeuwenhoek, who described them as "...a second sort of animalcules...provided with diverse incredibly thin little feet, or little legs [cilia], which were moved very nimbly ..., and wherewith they brought off incredibly quick motions (Haimo and Rosenbaum, 1981)".

The importance of the cilium has been ignored for a long time. Only in the 20th century, technical advances such as electron microscopy and immunocytochemistry have allowed a fine description of the ciliary structure and composition (Davis et al, 2006).

After the initial discovery, cilia have mostly interested scientists because of their ability to move. Recent discoveries, have found that cilia also play major movement-independent roles during development and postnatal life. It has been revealed that multiple human genetic disorders are caused by dysfunction of the cilia. Therefore, loss of ciliary function became an object of interest for biomedical research. Nowadays, many genetic and biochemical approaches are applied in order to identify the components of the ciliary proteins (Sharma et al., 2008).

### 1.1.1. Definition of cilia

Currently, cilia are defined as microtubule-based organelles, which protrude from the cell apical surface and anchor to the cytoskeleton through a structure called basal body. The size of cilia is variable and species specific, ranging in length from 3 to 30µm with a diameter of 200-300 µm. They are present on the surface of a wide range of cell types (Davis et al 2006; Hoyer-Fender, 2010; Gerdes et al, 2009).

Cilia have arisen early in eukaryotic evolution therefore can be found across a broad phylogenetic spectrum, with some exceptions including *Cyanidioschyzon*, *Dictyostelium* and *Saccharomyces* (Cavalier-Smith, 2002; Davis et al, 2006).

Interestingly, in vertebrates cilia are present almost ubiquitously, while in

invertebrates especially in *Drosophila* they have been found only in some cell types, for instance in the sensory neurons and sperm (Davis et al, 2006)

### **1.1.1. A The centriole**

Cilia elongate from the basal body, a structure derived from the centriole. For most of the cell cycle centrioles exist in pair called centrosome. The two centrioles from the pair are named mother (Fig.1) and daughter centriole (Dawe et al, 2007). Expectedly, these two centrioles can be distinguished from each other. They differ in age, thereby the mother centriole is formed at least two cell cycles before the daughter. Interestingly, the two centrioles from the pair (which are called as a centrosome) are orthogonally oriented with the lumen of procentriole facing the wall of the mother (Kuriyama and Borisky, 1981).

The two centrioles from the pair display structural and functional differences. For example, the mother centriole is characterized by the presence of fibrous distal and subdistal appendages (Hoyer-Fender, 2010). When an older centriole from the pair (the mother centriole) differentiates into basal body, two sets of fibrous appendages convert into basal foot and transition fibers (Tang and Marshall, 2012).

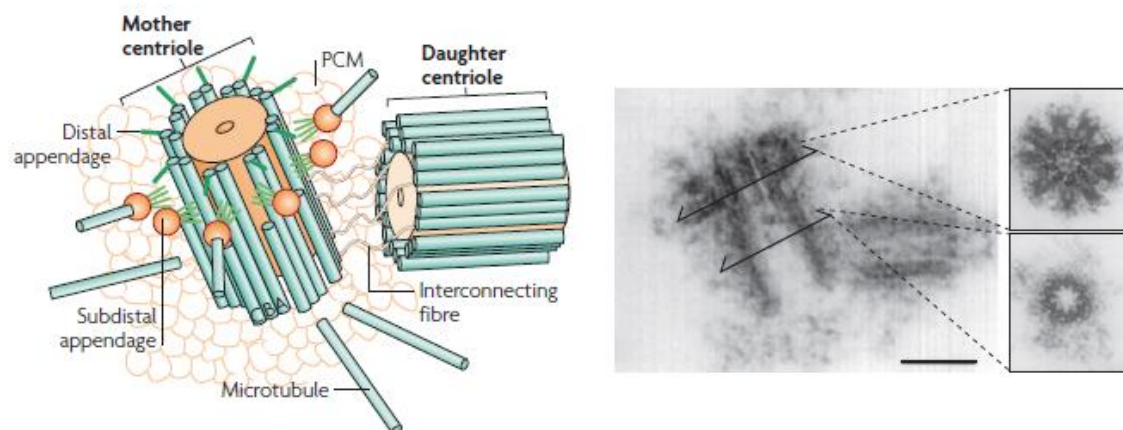
In primary cilia, the basal foot, which assembles from sub-distal appendages of the mother centriole, plays a role in microtubules anchoring (Kobayashi et Dynlacht, 2011) while, the basal foot of the motile cilia in multiciliated epithelium additionally controls ciliary beating by pointing out the right direction of the fluid flow (Tang et Marshall, 2012). Interestingly, in primary cilia up to five basal feet have been found to project from the single basal body, whereas, the basal body of motile cilia has only a single basal foot (Hoyer-Fender, 2010).

During the centriole maturation the distal appendages, which represent the second fibrous structures of the mother centriole transform into the transition fiber. The main function of the transition fiber is recruitment of the basal bodies to the membrane during cilia assembly (Kobayashi et Dynlacht, 2011).

### 1.1.1. B The centrosome

Centrioles from the pair are connected by the cohesion fibers and form a structure called the centrosome (Paintrand et al, 1992) (Fig.1). However, the assembly and organization of centrosome depend not only on the presence of the centrioles, but also on the existence of the pericentriolar material (PCM) (Fig.1). Interestingly, the PCM surrounding the centrioles, also participates in the nucleation and organization of the mitotic and interphase microtubules (Paintrand et al, 1992).

Centrosomes are essential for ciliogenesis. Their importance is reflected for example by the name, which means central body (in Latin centrum and Greek soma). Centrosomes are well-conserved structures required for the proper cilia formation in the evolutionarily distant species (Sluder, 2005).

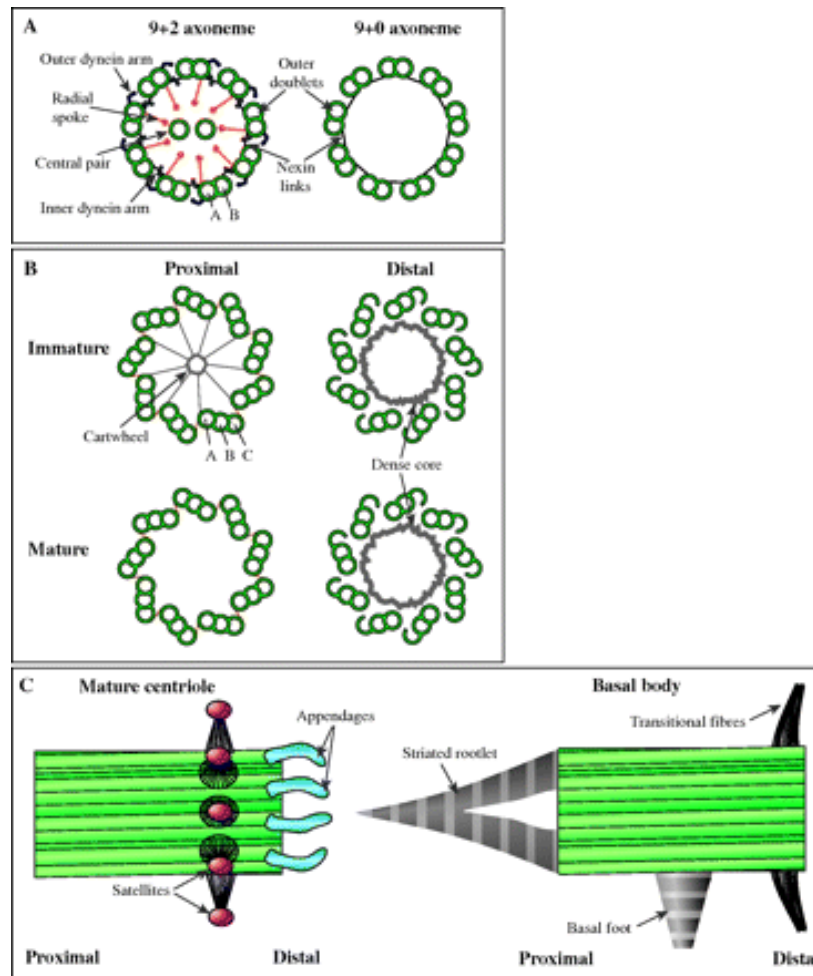


**Figure 1.** A) Schematic view of the structure of centrosome. B) Electron micrograph of the centrosome. The main cross-section shows the subdistal appendages, where the smaller images on the side show the cross-section of the proximal part of the centriole. Scale bar 0,2 $\mu$ m. (Battencourt-Dias et Glover, 2007).

Centrosomes play also important roles in orchestrating the cell cycle progression. They are replicated synchronously with the cell cycle and they also provide binding scaffold for numerous proteins involved in cell cycle progression and checkpoint control. For example, checkpoint kinase 1 (Chk1) in *Xenopus* eggs (Kramer et al, 2005), cell cycle modulator Cdc14b in zebrafish (Clement et al, 2011,

Avashti and Marshall, 2012) and spindle checkpoint regulator BubR1 in zebrafish and human are associated with the centrosomes.

Moreover, during mitosis, centrosomes organize the mitotic spindle. Their malfunction causes random distribution of chromosomes, which leads to aneuploidy (Loncarek and Khodjakov, 2009).



**Figure. 2.** Schematic representation of the ultrastructure in cross-sections of motile and immotile (A) as well as immature and mature cilia (B) The arrows point to characteristic structural features (C) The comparison of the mature centriole and basal body (Dawe et al, 2007).

### 1.1.1. C The basal body

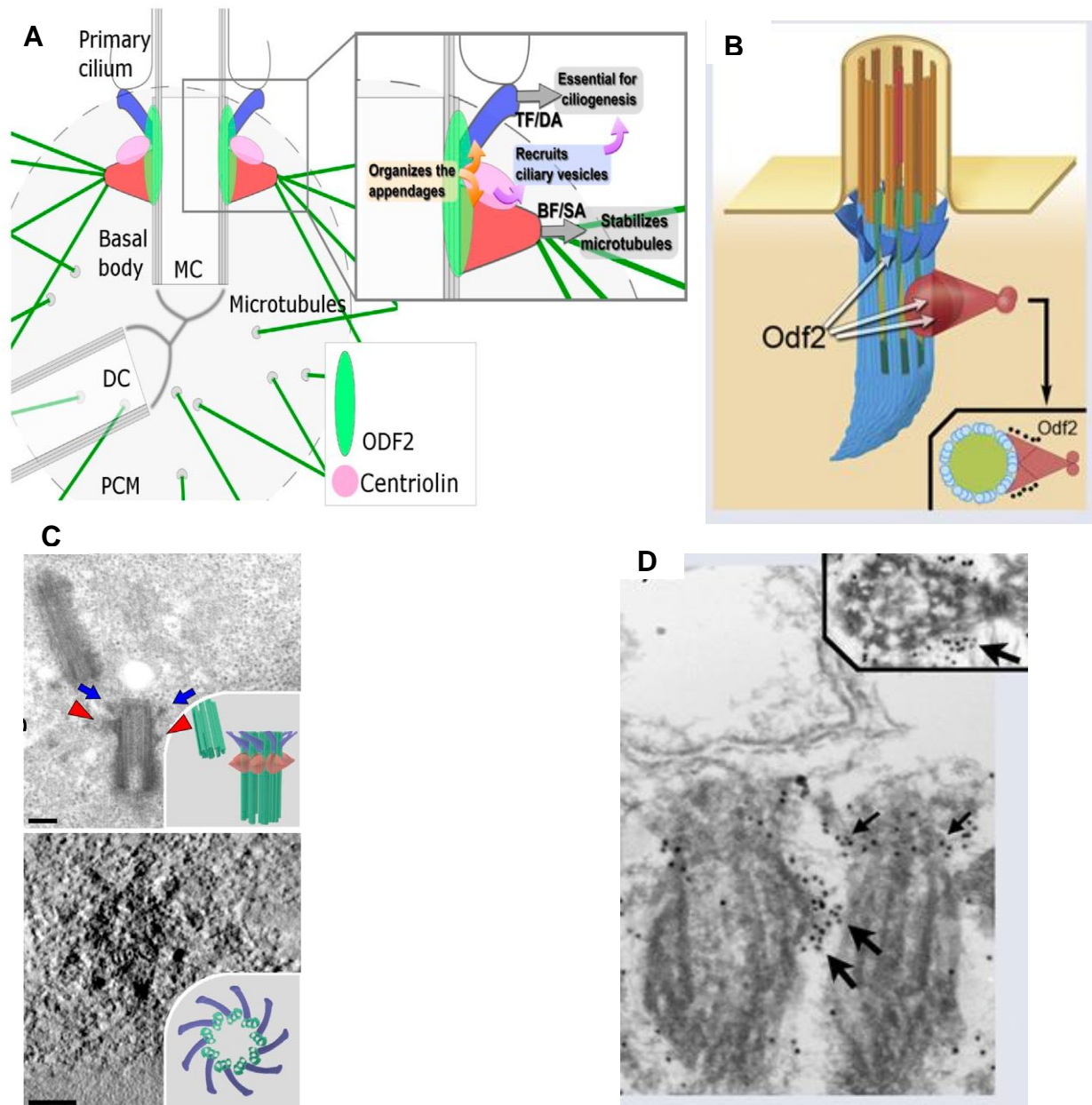
The mother centriole converts into the basal body. These two structures differ from each other, the basal body exhibiting additional structural features and a different repertoire of proteins. Also, they are found in different location. Centrioles exists close to the nucleus, while the basal body is docked at the plasma membrane. The basal body also undergoes specific posttranslational modifications such as acetylation and polyglutamylation of  $\alpha$  and  $\beta$ tubulins (Westermann et Weber, 2003).

The basal bodies possess the transitional fibers (corresponding to the distal appendages of the mother centriole), the basal foot/feet (corresponding to sub-distal appendages), and the striated rootlets (Fig.2 and 3).

The striated rootlets are structures, which extend from the proximal end of the basal bodies toward the cell center. The function of the striated rootlets is to anchor the basal body (and by extension the cilium complex) to the cell. One of the well-known component of the striated rootlets is rootletin, which is commonly used as a marker in immunohistochemistry to stain for the basal body (Hoyer-Fender, 2010).

The distinction between centrioles and basal bodies refers also to the expression levels of different proteins. For example, the proteins called CP110 and Cep97, suppress cilia assembly by forming a cap at the distal end of the mother centriole in primary cilia (Kobayashi and Dynlacht, 2011). Also, Cep64 and Odf2 localize to mother centriole appendages, where they are involved in the formation of basal body (Kumimoto et al, 2012). Their function is described in details in the chapter 2.

Interestingly, the basal body of primary cilia is composed of two centrioles, which are connected to each other. On the other hand, the basal body of motile multiple cilia is composed only of one centriole (Fig.3) (Kumimoto et al, 2012; Tateishi et al, 2013).



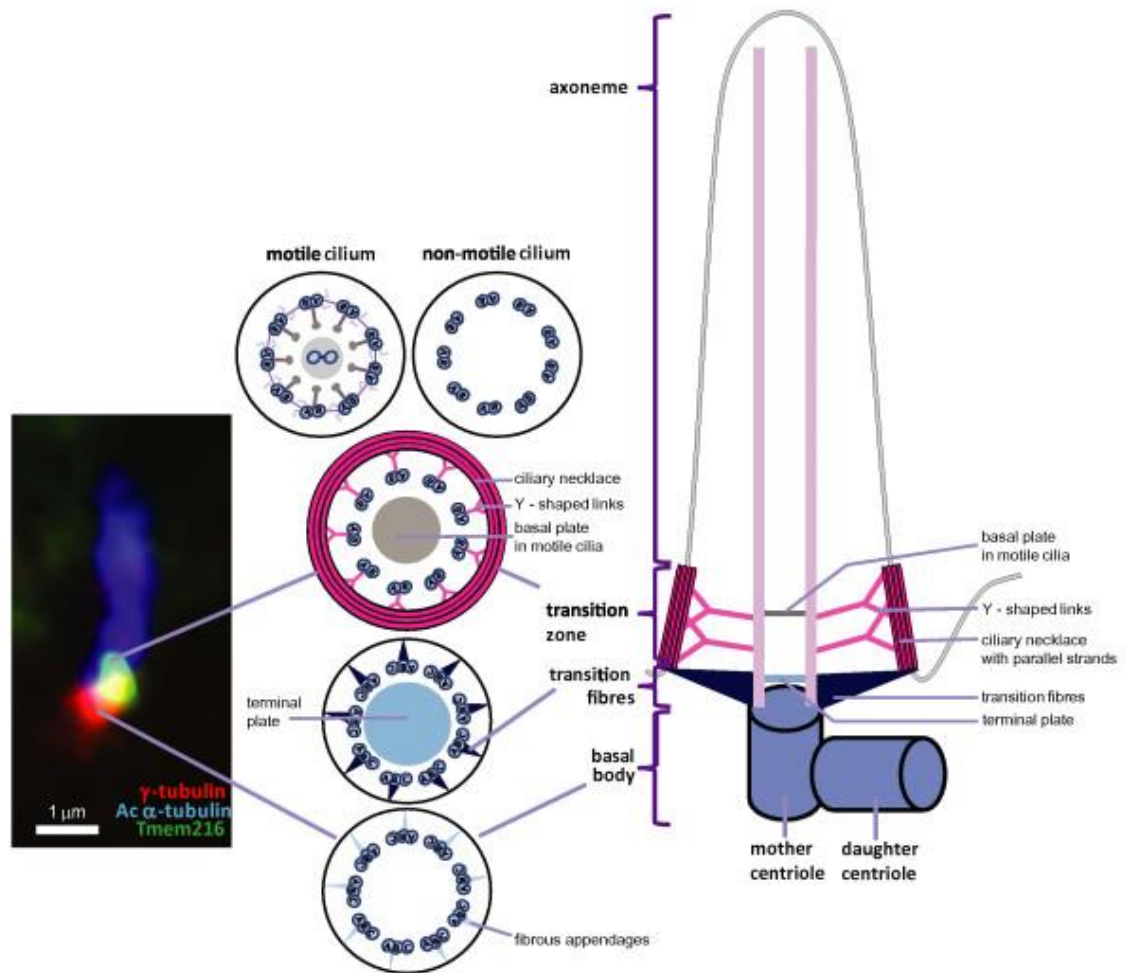
**Figure 3.** A) Schematic drawing of the specific roles of the appendages of ciliary basal bodies in primary cilia. In the proposed model, separate domains in Odf2 serve as the molecular platform on which the appendages are constructed. The BF/SAs (red) stabilize MTs, whereas the TFs/DAs (blue) are essential for ciliogenesis. B) Schematic drawings of basal bodies of multiple motile cilia show a marker of basal foot – ODF2. Inset is a crosssectional view of a basal body at the level of the basal foot. C) Electron micrograph showing transition fiber (TFs blue) and/or basal feet (BF red) on primary cilia basal bodies (longitudinal section). Electron tomograph showing cross section of primary cilia basal body D) Immunoelectron microscopic labeling for Odf2. Large arrows indicate immunogold signal in the basal feet. Small arrows show immunogold signals on anchoring fibers. Inset is a cross-

sectional view of basal bodies at the level of the basal feet (A, C Kunimoto et al, 2012; B, D Tateishi et al, 2013).

#### **1.1.1. D The transition zone**

The basal body converted from mother centriole exhibits nine sets of microtubule triplets at the proximal end, however at the distal ends doublets of microtubules exist (Hoyer-Fender, 2012). This shift of microtubules organization from triplets to doublets takes place within the axoneme in the proximity to the structure called transition zone. Together with the transition fibers, the transition zone forms so-called "ciliary gate". The ciliary gate constitutes a barrier, which allows the selective passage of materials into the cilium (Fig.4) (Szymanska et Johanson, 2012).

The aspect of the transition zone varies among species and cell-types, however its structural components appear to be conserved. Y-shaped linkers and the ciliary necklace are characteristic structures of the transition zone (Fig.3) (Szymanska et Johanson, 2012). Y-shaped linkers connect the outer doublets of microtubules to the plasma membrane and the ciliary necklace. The latter one is a specialized structure consisting of several parallel strands of intra-membrane particles, which encircles the ciliary membrane. In the motile cilia, the ciliary necklace converges with the minus end of the microtubules from the central pair (Szymanska et Johanson, 2012). It is speculated that the ciliary necklace participates in the nucleation and stabilization of the central pair of microtubules (Gilula et Satir, 1972). However, the molecular composition of ciliary necklace is unknown (Szymanska et Johanson, 2012).



**Figure 4.** Schematic representation of the ciliary ultrastructure with cross-sections at the level of the basal body, the transition fibers, the transition zone and the axoneme. The structure of motile and non-motile cilia is shown. On the left, is an enlarged immunofluorescence micrograph of a single primary cilium on an IMCD3 epithelial cell immunostained for axonemal marker acetylated-tubulin, the basal body marker  $\gamma$ tubulin and transmembrane protein TMEM216 which localizes to the transition zone. Scale bar = 1  $\mu$ m (Szymanska and Johanson, 2012).



### 1.1.2. Motile vs primary cilia

Cilia are divided into two main subgroups according to their ability to move. Moreover, this classification is based on the configuration of the microtubules. Therefore, motile and immotile cilia can be distinguished. The first ones are able to beat, while the immotile cilia, also called primary cilia, are involved in signal sensing (Takeda et Narita, 2012). Interestingly, these two types of cilia share the common structural core. Accordingly, all cilia contain the axoneme, constituted of a ring of nine outer doublets of microtubules (Fig.2 and 3), which in turn consist of so-called A and B tubules.

The differences between motile and immotile cilia are related to the presence of additional structural and molecular features, which are a requisite for motility. Motile cilia contain two extra inner microtubules at the center of the axoneme called the central pair. In this case, the axonemal configuration is called 9+2 (Yuan et Sun, 2013). Other characteristic features of the motile cilia are the dynein motors, the radial spokes and the nexin links (Fig.1, Fig.2) (Yuan et Sun, 2013). The dynein motors are arranged in two rows, composed of the inner (IDA) and outer dynein arms (ODA). Dynein arms are able to form a link between two adjacent outer microtubule doublets (Fig.2) (Dawe et al, 2006; Lin et al, 2012). Also, nexin links the outer doublets with each other and facilitates the role of dyneins. On the other hand, the radial spokes located at the nine outer doublet microtubule, interact with the central pair and regulate the activity of the dynein motors (Lin et al., 2012). Dynein, which are arranged along the length of A-tubule of each outer doublet, "walk" along the B-tubule of neighboring outer doublet and cause the two doublets to "slide" one in relation to other (Lin et al., 2012; Dawe et al., 2006; Davis et al., 2006). Because of the presence of the nexin arms (and to a lesser extent of the radial spokes), the sliding of the doublets is only limited, and this relative rigidity results in a flexing of the whole axoneme (Lin et al., 2012; Dawe et al., 2006; Davis et al., 2006).

The primary cilia which lack the central pair of microtubules and exhibit the 9+0 axonemal configuration do not possess dynein complexes and consequently do not exhibit the beating activity (Dawe et al., 2006).

Interestingly, the 9+2 microtubule organization appeared earlier in the evolution than the 9+0 configuration (Yuan et Sun, 2013).

Some exceptions have been found to the paradigm of the correlation between

the 9+2 axonemal organization and the cilia beating ability. One of the most striking examples is the vertebrate node, a ciliated embryonic organ that establishes the left-right asymmetrical body patterning. The nodal cilia exhibit the 9+0 axonemal configuration, however they are motile and beat with a circular motion that generates a directional fluid flow (Nonaka et al, 1998). Another example is the mouse choroid plexus epithelia, where cilia exhibit 9+1 and 9+0 microtubule organization, but are partially motile (Fig.3) (Narita et al, 2010).

The kinocilium in the mammal inner ear displays 9+2 microtubule organization, however it is not motile. Additionally, in non-metazoans many motile cilia have atypical axonemal configurations, such as 14+0 or 3+0 microtubule organization of flagella on the sperm of protura and parasitic protozoans (Dawe et al, 2007).

### **1.1.3. Multiple vs solitary cilia**

Cilia can be also categorized according to their number as solitary or multiple cilia (Fig.4). Accordingly, motile cilia can be present in a single or in many copies per cell, while immotile cilia (primary cilia) are present in a single copy (Fig.4) (Takeda et Narita, 2012). Here, few examples of different cilia will be given.

#### **Multiple cilia**

The multiple motile cilia cover, for example, the epithelium of the upper airways of human and the embryonic and larval skin of amphibians. Such multiple beating cilia are also present in the ventricles of the brain and oviducts of vertebrates. Their characteristic feature is the generation of cilia-driven fluid flow (Satir et Christensen, 2007; Roy 2009, Choksi et al, 2014).

Most of the multiple cilia are motile, however two cases of immotile multiple cilia have been found. These are the Grüneberg ganglion neurons and the olfactory sensory cilia (Fig.3) (Takeda et Narita, 2012).

The Grüneberg ganglion neurons (discovered in 1973) are involved in the detection of the alarm pheromone in mice. Cilia of Grüneberg ganglion neurons are

multiple, but in contrary to typical multiple cilia are present in the dozens not hundreds per cell (Takeda et Narita, 2012).

Another example of multiple immotile cilia are the olfactory sensory cilia in vertebrates. They exhibit motility in the aquatic vertebrates (Rhein et al., 1981), but they are often non-motile in the terrestrial vertebrates (Takeda et Narita, 2012).

### **Solitary cilia**

The solitary immotile cilia (primary cilia) play very important roles in vertebrate development. They participate in many different signaling pathways by transmitting signals, hence they are also called the cell's antennas. The primary cilia are present almost ubiquitously in different cell types of vertebrates (Ishikawa et Marshall, 2011).

The nodal cilia are another type of cilia, which are solitary and motile (Fig.5). They possess dual function. They are involved in the generation of the fluid flow and sensing of signals. These cilia are located on the ventral cells of the mammalian node as well as in the epithelium of Kupffer's vesicle in fish and the gastrocoel roof plate (GRP) in frogs.

Another examples of the motile monocilia are prototypical flagella on protozoans and sperm cells, as well as cilia present in the pronephric kidney tubules of zebrafish embryos (Fig.5) (Choksi et al, 2014).

| Axoneme<br>Number | 9+0                              | 9+2  |
|-------------------|----------------------------------|--|
|                   |                                  |  |
| Solitary          | Most Cell Types (I)              | Inner Hair Cells (V)   |
|                   | Embryonic Node (II)              | Sperm (VI)   |
| Multiple          | Grüneberg Ganglion Neuron (III)  | Olfactory Neurons (VII)                                      |
|                   | Choroid Plexus Epithelium ? (IV) | Tracheal Epithelium<br>Ependyma<br>Oviduct Epithelium (VIII) |

**Figure 5.** New classification of cilia/flagella in vertebrates based on the axoneme structure, number of projections on a single cell and motility. Motile cilia are indicated in red, immotile ones in blue. According to this classification, one can identify the following eight categories of cilia/flagella: (I) Solitary 9+0 non-motile cilia (authentic primary cilia), (II) Solitary 9+0 motile cilia (classic nodal cilia), (III) Multiple 9+0 non-motile cilia, (IV) Multiple 9+0 motile cilia, (V) Solitary 9+2 non-motile cilia, (VI) Solitary 9+2 motile cilia (so-called flagella), (VII) Multiple 9+2 non-motile cilia, (VIII) Multiple 9+2 motile cilia (conventional motile cilia) (Takeda et Narita, 2012).

## 1.2 Cilia function in vertebrate development and physiology

Cilia are multifunctional structures involved in many developmental and physiological processes. To illustrate their functional diversity, few examples from different tissues will be presented in this chapter.

### 1.2.1 Multiple cilia

The majority of multiple cilia are motile. Their coordinated and directional beating allows them to generate efficient fluid movement required for the proper development and function of different tissues and organs (Satir et Christensen, 2007).

Multiple cilia line the surface of different types of the epithelium. For example, in many vertebrates, cilia-driven fluid flow is used for lung clearance from the inhaled

particles in airway epithelium, but also for the transport of the egg within the epithelium of the female reproductive tract and proper circulation of cerebrospinal fluid within the brain ventricles (Satir et Christensen, 2007).

Additionally, multiple-motile cilia can serve also a source of the movement for protists (Dawe et al, 2007).

The mechanical function of multiple motile cilia is well-known. However, it has been suggested that they might also play sensory functions. In mammals, motile cilia of the airway epithelium display both the mechanosensation and chemosensation functions. Shah and colleagues showed that these cilia sense the entering of noxious substances. In turn, this recognition initiates a defensive mechanism, which mechanically eliminates the offending compound (Shah et al, 2009). This is supported by the fact that the airway epithelial cells express the sensory bitter taste receptors localized to the motile cilia. It is also known that the bitter compounds increase the intracellular  $\text{Ca}^{2+}$  concentration, which stimulates ciliary beat frequency (CBF) (Shah et al, 2009). It has been suggested to define all types of cilia as sensors with an additional function of motility, which is restricted to a subset of motile cilia.

### **1.2.2 The special case of nodal cilia**

A special case of the solitary and motile cilia is represented by the nodal cilia. They exist, for example, in the gastrocoel roof plate in frogs or Kupffer's vesicle in teleost fishes (Choksi et al, 2014).

These cilia established the left-right body asymmetry through their coordinated clockwise beating, which generates a leftward directional movement of the fluid surrounding the node (Nonaka et al, 1998). Therefore, the nodal cilia of zebrafish are tilted posteriorly in order to produce a leftward fluid flow (Nonaka et al, 2005). In the mouse node, it was shown that the cilia-driven flow triggers a rise in intracellular calcium in the cells located at the left side of the node, subsequently leading to asymmetric gene expression and morphogenesis (Basu et Brueckner, 2008).

### 1.2.3. Cilia as mediators of the signaling pathways

Primary cilia were firstly observed in the renal epithelium and thyroid gland (Zimmermann, 1898). However, their biomedical relevance was disclosed many years later, through the discovery of cyst formation in mouse kidney induced by perturbation of the function of the ciliary protein called *ift88* (ORPK) (Pazour et al, 2000; Schrick et al, 1995).

Afterwards, it was shown that the primary cilia are required for the response to many developmental signals from different pathways including the Hedgehog (Hh), the Planar Cell Polarity (PCP), the Platelet-derived growth factor (PDGF) and the Fibroblast Growth Factor (FGF) signaling pathways. Thus, primary cilia possess a role as the nexus for the signal transduction during the development (Goetz and Anderson, 2010).

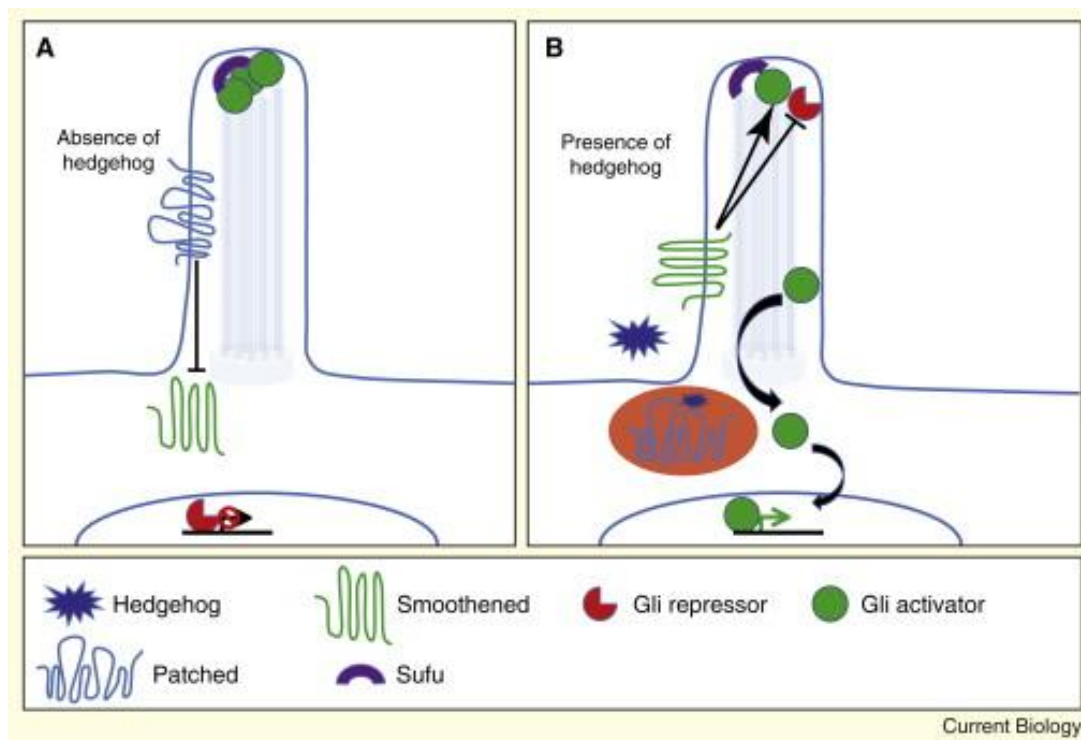
### 1.2.3. A The primary cilia and the Hedgehog (Hh) signaling pathway

The Hedgehog (Hh) signaling pathway is known to control cell fate decisions in many different tissues. Hh ligands, such as Desert hedgehog (Dhh), Indian hedgehog (Ihh), or Sonic hedgehog (Shh) bind to their receptor Patched (Ptch), causing the repression of the downstream protein Smoothened (Smo) and activation of the Gli transcription factors (Gli 1-3), thus inducing the transcription of the Hh target genes. Inversely, in the absence of Hh ligands, the Gli transcription factors are proteolytically processed to a repressor form (GliR), which keeps the Hh target genes off (Fig.6) (Davis et al, 2006).

The implication of the primary cilia in the reception of multiple signals during development was revealed for the first time in cilia mutants, in which the embryonic patterning was defective due to impairment in Hh signaling pathway. Mouse neural tube mutants called *wimble* and *flexo* with mutated Intraflagellar Transport (IFT) genes show phenotypes characteristic of Sonic hedgehog signaling defects (Huangfu et al, 2003). Subsequent data confirmed that cells lacking cilia are not able to respond to the Hh signaling pathway. Additionally, it was shown, that Smo

localization to the cilium in vertebrates is a prerequisite for Smo proper function (Corbit et al, 2005).

In other publication, it was demonstrated that the IFT proteins of primary cilia interact with the Gli transcription factors. For example, IFT88 is required for proper function of the Gli repressor and activator. As a result, IFT mutants show Hh loss of function phenotypes in some cell types and Hh gain-of-function phenotypes in others. For example, GliA controls neural patterning and mutation of IFT88 shows loss of the Hh signaling pathway in the neural tube, while other IFT mutant displays pre-axial polydactyly characteristic of loss of GriR (Liu et al, 2005).



**Figure 6.** Hedgehog signaling and the cilium. A) In the absence of Hh ligand the repressor form of Gli transcription factor inhibits Hh responsive gene transcription, while Gli activator is maintained in the cilia via Sufu binding. In this situation Patched receptor inhibits the Smo transmembrane protein B) The presence of Hh ligand causes translocation of Ptch receptor out of the cilia membrane, thus activating Smo protein and leading to the translocation of the Gli activators to the nucleus, where expression of Hh responsive genes is activated (Berbari et al, 2009).

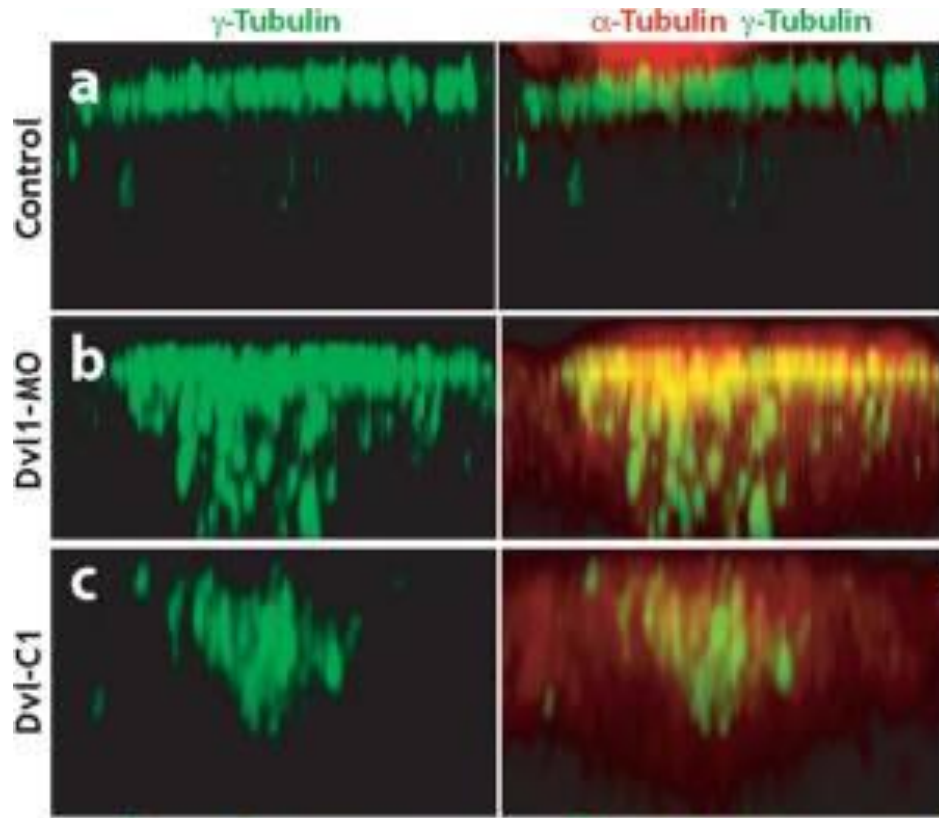
### **1.2.3. B The primary cilia and the Planar Cell Polarity signaling pathway**

Initially, the Planar Cell Polarity (PCP), which is an ability of cells to be oriented relative to an axis along the plane of the tissue, has been found in *Drosophila* (Vladar et al, 2009).

The PCP pathway acts through receptors such as Frizzled (Fz) or Van Gogh (Vangl) and downstream effectors including Dishevelled (Dsh), Inturned (Int) or Fuzzy (Fuz). However, the complete list of the PCP core proteins is much longer (Wallingford et Mitchell, 2011; Park et al, 2008).

The most significant function of the PCP for the ciliogenesis is its participation in cilia assembly through the control of cilia polarized organization (Mitchell et Park, 2012). Several other evidences support the existence of a link between the PCP and cilia. For example, it was shown that Dvl mediates the docking of basal bodies at the apical surface of the multiciliated cells in *Xenopus* epidermis (Fig.7) (Park et al, 2008). Also, Dvl controls the planar polarization of basal bodies, hence the ciliary beating (Park et al, 2008; Mitchell et al, 2009).





**Figure 7.** Dishevelled is essential for basal bodies docking at the apical surface of the multi-ciliated cells in *Xenopus laevis* larval skin. A) Wilde type embryos B) Dvl morphants C) Dvl truncated form. Basal bodies in green stained with  $\gamma$ tubulin, the cilia stained in red with  $\alpha$ tubulin (Park et al, 2008).

A good example of a direct functional link between the cilium and PCP is the mouse vestibular system, which contains hair cells similar to those present in the cochlea. The PCP complex acts here before stereocilia bundle development to provide an underlying polarity to all cells in the vestibular epithelia (Deans et al, 2007).

### **1.2.3. C The primary cilia and the Platelet-derived growth factor (PDGF) signaling pathway**

The well-known function of the PDGF signaling is its involvement in the embryonic development, also a link to the ciliogenesis has been found (Zaghloul et Brugmann, 2011). The PDGF protein family consists of five ligands, which can be recognized by three receptors. It has been shown that one of the PDGF receptors called PDGFR $\alpha\alpha$  is localized and enriched in the primary cilium of mouse embryonic fibroblasts (Tallquist and Kazlauskas, 2004).

In postmitotic cells, PDGFR $\alpha\alpha$  binding to its ligand PDGF-AA cause an activation of the downstream MEK/ERK/Akt signaling (Scheider et al, 2005). In IFT mutant quiescent cells PDGFR $\alpha\alpha$  signaling was abrogated and receptor accumulates at the microtubule-organizing center (MTOC) rather than in the cilia. Therefore, the cilia are required for PDGFR $\alpha\alpha$  signaling (Scheider et al, 2005).

### **1.2.3. D The primary cilia and the Fibroblast Growth Factor (FGF) signaling pathway**

The FGF signaling is essential for regulating cilia length and function (Neugebauer et al, 2009). The FGF pathway is composed of several ligands and receptors. The most important receptor for ciliogenesis is Fgfr1. It was shown that disruption of FGF signaling through Fgf receptor 1 reduced the expression of ift88, and of two master regulators of the ciliary gene expression, namely the foxj1 and rfx2 transcription factors. In zebrafish, loss of function of Fgfr1 and its ligands in Kupffer's vesicle caused kidney cysts, shortened cilia and randomized organ laterality, reflecting the phenotype seen in the ift88 mutants (Zaghloul et Brugmann, 2011; Neugebauer et al, 2009).

It was suggested that the FGF ligands: Fgf8 and Fgf2/4 through binding to the receptor Fgfr1 maintained a transcriptional network which allows normal expression of IFT proteins, required for the ciliary axoneme growth (Neugebauer et al, 2009).

#### 1.2.4. The primary cilia and their sensory function

Primary cilia are important not only for signal transduction, but also for the detection of other stimuli, such as fluid shear, mechanic deformation (movement, vibration, touch) light or odorants.

For example, the primary cilia in renal epithelium play a mechanosensory role. These cilia deflect in response to fluid movement initiated by an intracellular calcium signal (Praetorius et Spring, 2003). The involvement of primary cilia in renal cystic disease relies on the activity of two genes, Polycystins1 and 2 (PC1, PC2). In the absence of PC1 and PC2 genes calcium signaling induced in cilia is lost (Nauli et al, 2003).

Moreover, cilia play a role in the sensing of pressure, touch and vibration. All of these functions were particularly well demonstrated in invertebrates, including *Drosophila melanogaster* and *C.elegans*. For example, in flies, vibration is detected by the chordotonal organ, which consists of sensory neurons. These neurons extend cilia. Vibrations result in the changes of cilia shape, through their stretching, thus initiating a rapid electrical response via ion channels located in the axoneme (Ernstrom et Chalfie, 2002).

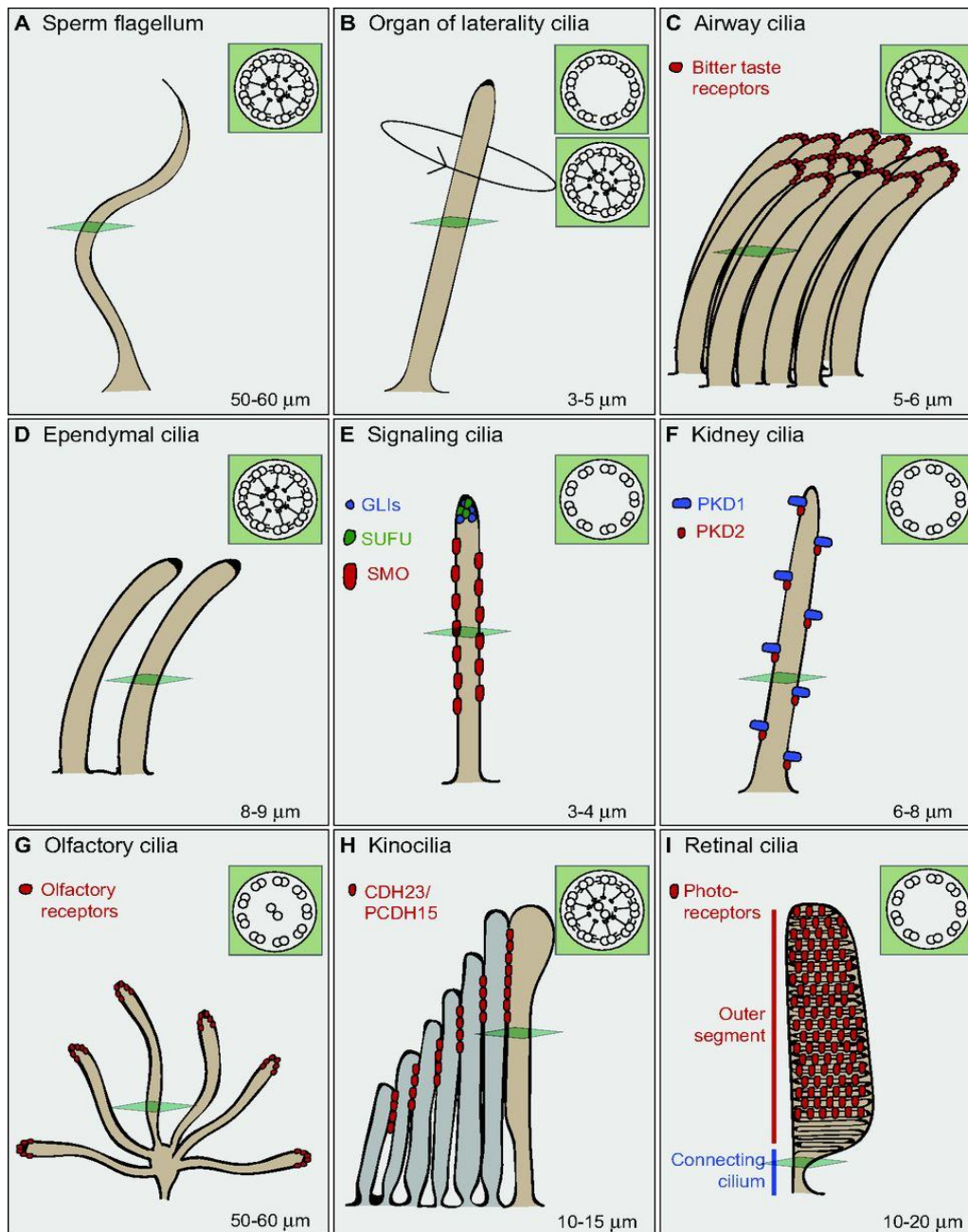
Another example of mechanosensory function of the primary cilia are the hair cells in the organ of Corti in the cochlea. The hair cells bear on their apical surfaces stereocilia, and a primary cilium called kinocilium. The sense of the hearing depends on the hair cells, which transduce sounds with their hair bundles, containing actin-based stereocilia and microtubule-based kinocilia, through the mechanotransduction channel (Shin et al, 2005).

In mammals, the mechanosensation is likely to be operated by similar mechanism since the Bardet-Biedl syndrome related to impaired cilia gives defects in the mechanosensation. However, no direct association of cilia with mechanosensitive organs of mammalian skin has been reported (Berbari et al, 2009).

The detection of light in mammals occurs through the photoreceptors, which for their proper function use modified primary cilia (Fig.8I). The degeneration of photoreceptors is commonly associated with cilia disorders including Bardet-Biedl syndrome (BBS) and nephronophthisis.

Blindness is also associated with an impaired kinesin subunit of the kif3a mutants required for IFT within primary cilia of the photoreceptor (Berbari et al, 2009).

The olfactory sensory cilia (Fig.8G) are responsible for the odorant detection. The olfactory signaling is initiated when the odorants are in contact with the epithelium. Therefore, odorants can be considered as the ligands for G-protein coupled receptors found in the sensory neuron's cilia (Fig.8G). Interestingly, anosmia is commonly found in mouse cilia mutant and in BBS patients (Kulaga et al, 2004).



**Figure 8.** Diversity of vertebrate cilia with indication of the axonemal configuration, number per cell and length. Key proteins or receptors that localize to cilia are illustrated. Motile vs immotile. Solitary vs multiple. (A) The sperm flagellum moves with a whip-like motion. (B) Motile nodal cilia, by contrast, move in a vortical manner to establish left-right asymmetry. (C) Bitter taste receptors localize to human airway cilia. (D) Biciliated ependymal cells function to circulate CSF in the spinal canal. (E) Components of the hedgehog signaling pathway, including GLI proteins, SUFU (suppressor of fused homolog) and SMO (smoothened), localize to solitary signaling cilia. (F) By contrast, mechanosensory proteins, such as PKD (polycystic kidney disease) 1 and PKD2, localize to renal cilia to sense urine flow. (G) Olfactory neurons localize olfactory receptors to the distal ends of their cilia in order to sense odorant molecules. (H) The kinocilium serves to polarize the actin-based stereocilia (gray) during development of auditory hair cells. CDH23, cadherin 23; PCDH15, protocadherin 15. (I) Retinal cells have a specialized connecting cilium that gives way to the outer segment - a membrane-dense protrusion packed with photoreceptor molecules (Choksi et al, 2014).

### 1.2.5. Ciliopathies

Ciliopathies are defined as congenital disruptions of ciliary structure or function, which cause pleiotropic developmental disorder (Ko, 2012). However, this definition is collective, since ciliopathies comprise different syndromes and phenotypes.

The definition of ciliopathies as a link between pathological phenotypes and ciliary dysfunction, was proposed in the 1970s by Bjorn Afzelius, who showed that the lack of outer dynein arms caused diminished motility of cilia (Gerdes et al, 2011). This discovery was supported by the successive revelation of cilia-specific proteins, which defects are related to human disorders (Fig.9) (Hildebrandt et al, 2011; Gerdes et al, 2011).

Ciliopathies are associated with diverse clinical features including abnormalities in neural tube closure and patterning, polydactyly, cystic kidney, liver diseases, retinal degeneration, anosmia, cognitive defects, obesity and randomization of the left-right body axis (Sharma et al, 2008). Therefore, ciliopathies affect most of the organs, for example, kidney, brain, limb, eye, liver or bone (Ko, 2012).

Additionally, ciliopathies can be classified into two categories, namely into the motile and immotile cilia-related disorders (Ko, 2012).

Sensory and signaling defects in primary cilia cause kidney cyst formation. The most common kidney ciliopathy, which causes renal failure is called nephrocystin NPHP. It is an autosomal recessive cystic kidney disease caused by mutations in 11 NPHP genes. All of NPHP proteins localize to the cilium, transition zone and centrosome (Fig.9) (Hildebrandt and Zhou, 2007).

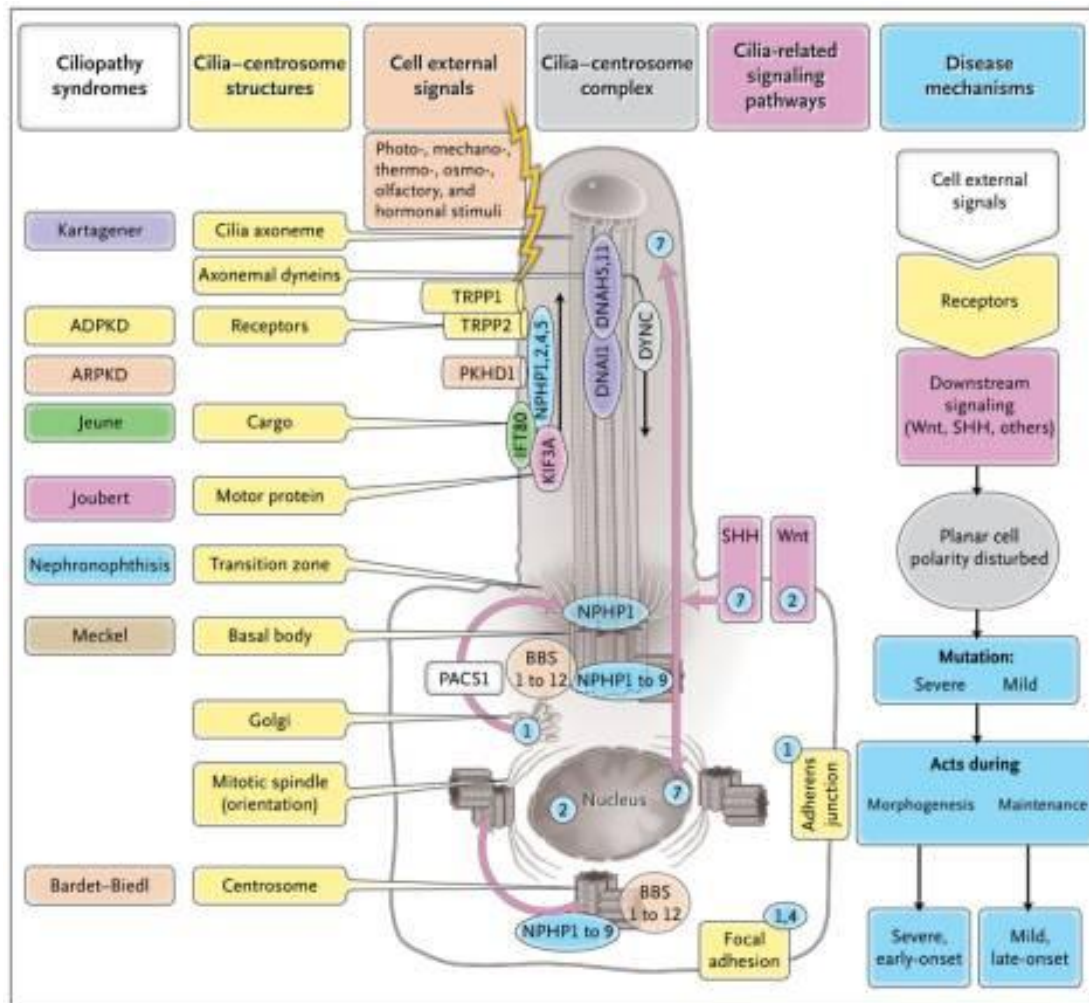
Another, ciliopathy is Bardet-Biedl (BBS) syndrome, a rare disorder related to the mutations of any of the 14 known BBS ciliary genes. The Bardet-Biedl syndrome was linked to ciliopathies, when BBS proteins were found in the ciliated sensory neurons of *C.elegans* (Ansley et al, 2003). The BBS phenotypes include retinal degeneration, renal cysts, polydactyly, cognitive impairment, diabetes and obesity (Zaghloul and Katsanis, 2009), (Yuan and Sun, 2013).

Other examples of ciliopathies are the Joubert and Meckel-Gruber syndromes. The first one is characterized by impaired development of the cerebellum and brain stem, which is manifested by the lack of balance and coordination of the patients.

Meckel-Gruber syndrome (MGS) is characterized by renal cyst formation, encephalocele, polydactyly and situs inversus (Yuan and Sun, 2013).

However, not only dysfunctions of the primary cilia, but also impairments of motile cilia are associated with numerous pleiotropic human disorders. For example Primary Ciliary Dyskinesia (PCD) characterized by recurrent airway infections and sterility, is caused by impairment of the ciliary motility. The majority of PCD-related mutations have shown to affect genes coding for components of the motile cilia such as the dynein arms and central pair apparatus (Yuan and Sun, 2013).

Very often the PCD is accompanied by another disease named heterotaxy (Htx) which is a rare congenital defect of visceral organs, such as the heart, liver and gut. Heterotaxy shows disruptions in normal left-right patterning during embryogenesis (Yuan and Sun, 2013).



**Figure 9.** Ciliopathy Proteins and Their Relationship to the Cilium–Centrosome Complex (CCC)

Single-gene ciliopathies are shown, with colors matching the respective gene products located at the CCC machinery. Subcellular components of the CCC can be seen within a ciliated epithelial cell and include polycystin-1 (TRPP1), polycystin-2 (TRPP2), fibrocystin-polyductin (PKHD1), intraflagellar-transport (IFT) cargo, kinesin anterograde motor components (KIF3A), and cytoplasmic dynein (DYNC). Receptors on cilia perceive cell extracellular signals and process them through the Wnt, sonic hedgehog, and focal adhesion signaling pathways. These pathways play a role in planar cell polarity, which is mediated partially through the orientation of centrosomes and the mitotic spindle poles. Depending on the severity of mutations within the same gene (e.g., in nephronophthisis type 6 [NPHP6]), they may act either during morphogenesis to cause a severe, early-onset, developmental disease phenotype (e.g., Meckel's syndrome) or during tissue maintenance and repair to cause a mild, late-onset, degenerative disease phenotype (e.g., the Senior–Løken syndrome). The numbers in blue circles denote subcellular sites of different nephrocystins (NPHP1, 2, 4, 5, and 7) (Hildebrandt et al, 2011).



## **2. Ciliogenesis – from centrioles to cilia**

### **2.1 Ciliogenesis vs Multiciliogenesis**

Ciliogenesis is a multistep process consisting of several characteristic stages. Briefly, the process of cilia generation starts with the exit of centrioles from the mitotic cycle. This is followed by migration of the centriole to the cellular cortex and its maturation into a basal body. Each basal body provides the base for the growth of a single ciliary axoneme.

In most of the cases ciliogenesis results in the formation of a single cilium per cell. However, in some cell types, a single cell produces hundreds of cilia. These cells are collectively called multiciliated cells (MCCs). The process of multiple cilia formation is called multiciliogenesis.

The main difference between ciliogenesis and multiciliogenesis is the number of cilia produced per cell. The main steps in the process of cilia formation are rather the same in the ciliated (CCs) and multiciliated cells (MCCs), with the exception in the mechanisms of centriole duplication/amplification.

In the following chapter, each step of ciliogenesis/multiciliogenesis will be described and emphasis will be put on the case of multiple cilia formation.

#### **2.1.1. Centrioles duplication/amplification**

The first step of ciliogenesis requires the exit of centrioles from the mitotic cycle, to allow them to duplicate and play a role of axoneme base.

The new centrioles are generated during a process called centriole duplication or amplification pathways. There are two different pathways of centrioles biogenesis: centriolar and acentriolar (another name is *de novo*) pathway. The main difference between them is the presence of the preexisting centrioles in the former one (Fig.10). Physiologically, the acentriolar pathway seems to be exploited exclusively by the multiciliated cells for amplification of their centrioles, however this is still under the speculation.

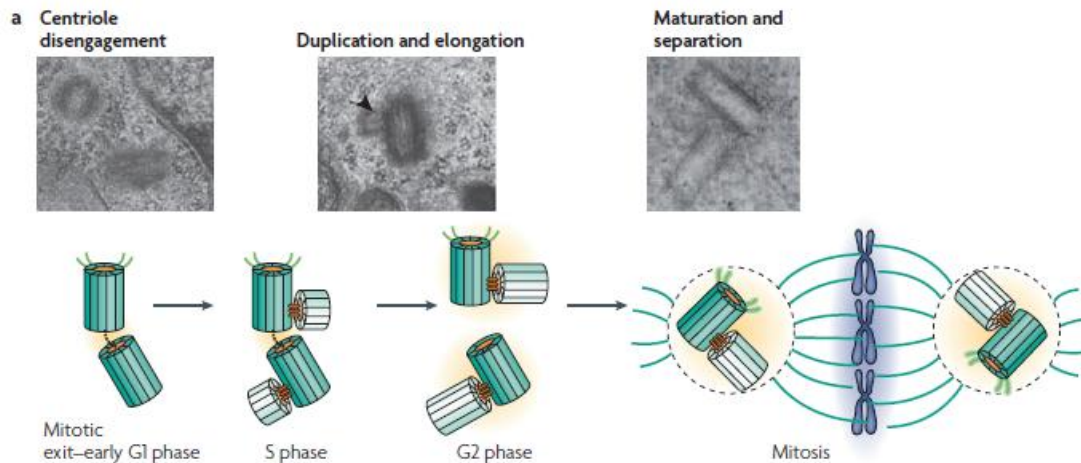
## **2.1.2. Different centriole biogenesis pathways**

### **2.1.2. A) Centriole duplication through the centriolar pathway**

In the centriolar/canonical duplication pathway, centrioles are generated from preexisting centrioles in the S phase of the cell cycle. Then, they grow and reach their final size in M phase. The newly formed centriole is tightly associated with parental centriole until late M phase (Fig.10). The paired centrioles then dissociate (centriole disengagement) and lose their orthogonal positioning (Battencourt-Dias et Glover, 2007). This process is subdivided into three essential events: centriole disengagement, centriole duplication and elongation, centrosome maturation and separation (Fig.10) (Tsou et Stearns, 2005; Battencourt-Dias et Glover, 2007).

The process of centriole dissociation is controlled by a protease called separase, which prevents premature centriole disengagement before anaphase (Tsou et Stearns, 2005). Centriole disengagement is a prerequisite for another round of centriole duplication as well as for the conversion of the mother centriole to basal body in G0 phase (Kobayashi and Dynlacht, 2011; Tsou et Stearns, 2005).

Additionally, it has been shown that the full process of centrioles maturation from procentrioles requires 1,5 cell cycle and is under the control of cell cycle regulators, including CDK10.



**Figure 10.** Centriole duplication pathway. Upper panel shows the micrographs from transmission electron microscopy (TEM), which indicates the three essential steps of the centriologenesi. Lower panel shows schematic structure of the centrioles during the duplication pathway related to the cell cycle (Battencourt-Dias et Glover, 2007).

### 2.1.2. B) Centriole amplification through the centriolar pathway

The mechanism of centriole amplification has been explained by the simultaneously nucleation of multiple daughter centrioles from a single mother centriole, thus forming a structure called rosette. The proteins Plk4, Cep152 or Sas6 are found in association with the rosettes (Peel et al, 2007).

Polo-like kinase (Plk4) is a key kinase involved in the initiation step of the centriole duplication. Plk4 phosphorylates several centriolar proteins including Cep152, responsible for procentriole nucleation, and GCP6, a component of the  $\gamma$ -TuRC microtubule-nucleating complex (Avidor-Reiss and Gopalakrishnan, 2013). Plk4 also phosphorylates regulators of centriolar proteins like the E3-ubiquitin ligase FBXW5, which participates in Sas6 degradation (Puklowski et al, 2011). On the other hand, Sas6 participates in formation of the cartwheel, the first structure in the developing centriole that manifests nine-fold symmetry (Avidor-Reiss and Gopalakrishnan, 2013).

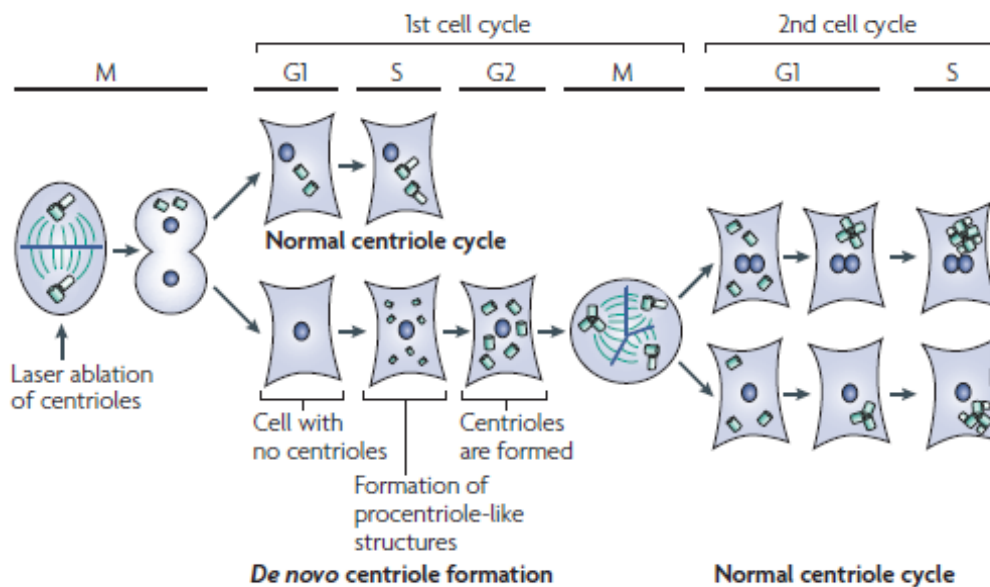
The overexpression of the rosette proteins caused the formation of multiple daughter centrioles around a single mother centriole or the re-duplication of mother centrioles in the same cell cycle (Peel et al, 2007, Rodrigues-Martins et al 2007, Loncarek and Khodjakov, 2009).

### **2.1.2. C) Centriole amplification through the acentriolar pathway**

The centriole amplification pathway results in the generation of hundreds of cilia per cell. Centriole amplification occurs through the acentriolar, *de novo* or deuterosome-mediated centriole biogenesis, where new centrioles are generated in the absence of any preexisting procentrioles (Fig.11). Centrioles arise from amorphous electron-dense granules consisting of the different centrosomal proteins, which fuse to larger structures called deuterosomes (Vladar and Stearns, 2007).

The deuterosomes are non-microtubule based structures and their components are largely uncharacterized. So far, only two deuterosome-specific protein has been revealed: CCDC78 and Deup1. CCDC78 (coiled-coil domain containing protein 78) was found highly up-regulated in *Xenopus laevis* multiciliated cells, where it localizes weakly to the centriolar foci, but strongly to the deuterosome foci in MCCs. CCDC78 provides the scaffold to which Cep152 is recruited to the deuterosome and is essential for centriole amplification (Klos Dehring et al, 2013). Also, Deup1 (parologue of Cep63 in vertebrates) through interaction with Cep152 enables massive centriole amplification in multiciliated cells (Zhao et al, 2013).

Interestingly, when compared the deuterosome-mediated and the canonical centriole amplification pathways at molecular level, they are quite similar. Plk4, Sas6 and Sas4 kinases are involved in the regulation of both pathways (Klos Dehring et al, 2013).



**Figure 11.** De novo vs centriolar centriole formation pathway (Battencourt-Dias et Glover, 2007).

### 2.1.3. The conversion of centrioles to basal bodies

Proper ciliogenesis requires the conversion of centrioles to basal bodies, which is a reversible process. When cells reenter the cell cycle, the primary cilia disassemble, then basal bodies migrate near the nucleus, where they act as a mitotic apparatus. In other words, cilia disassembly results in basal bodies transition to the centrioles.

This shift from centriole to basal body is under the control of diverse proteins and signaling pathways. For example, two distal centriolar proteins discussed in previous chapter: CP110 and Cep97 (Kobayashi and Dynlacht, 2011).

Notably, several other proteins are involved in the formation of basal bodies. Odf1 (oral-facial-digital syndrome 1) protein, participates in centriole length control and cilia formation (Singla et al, 2010). ODF2 (Outer dense fiber protein 2) has been shown to be involved in the assembly of the distal and subdistal appendages (basal foot and transition fibers) during ciliogenesis in mouse. Furthermore, ODF2 appears

to be essential for the basal body docking in mouse tracheal MCCs. Since the basal foot points the direction of cilia beating during the effective stroke, ODF2 protein becomes an important basal body polarization marker (Fig.3) (Ishikawa et al, 2005, Kunitomo et al, 2011).

Another centriolar protein called Cep164, which localizes to the distal appendages is also essential for cilia formation (Graser et al, 2007).

Therefore, the above evidences suggest, that the appendage-specific proteins required for basal body formation are involved in the process of conversion. However, the exact mechanism of their action is not yet known (Kobayashi et Dynlacht, 2011).

On the other hand, basal bodies transition to centriole is under the control of protein kinase Aurora A, which activates a deacetylase for tubulin called HDAC6. HDAC6 deacetylates axonemal microtubules and disassembles the cilia (Pugacheva et al, 2007).

#### **2.1.4. The actin cytoskeleton reorganization**

Another the crucial steps of ciliogenesis is the formation of a dense meshwork of actin at the apical surface of ciliated cells. It is not clear when exactly this process occurs during multiciliogenesis. Therefore, we suggested that actin reorganization takes place in the same time when the basal bodies migrate and dock.

##### **2.1.4. A) Description of actin**

Actin is the most abundant protein in the animal kingdom, required for many different biological processes such as environmental forces sensing, membrane vesicles internalization, movement and division of cells (Pollard and Cooper, 2009).

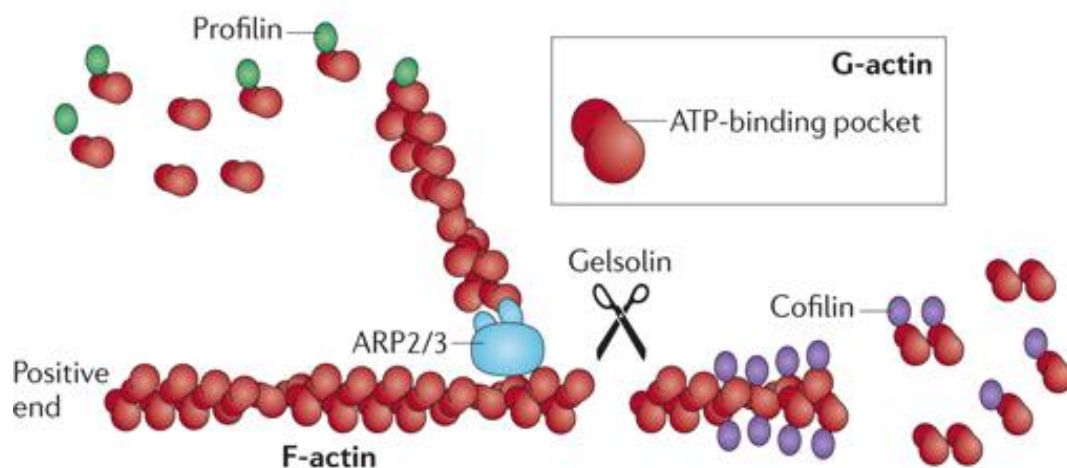
Actin exists in two different forms, globular (G-actin) and filamentous (F-actin). The globular form is characterized by the presence of an ATP pocket (cleft), which is used for the spontaneous polymerization of monomers into filaments (Fig.11). Upon addition of the monomer the hydrolysis of ATP to ADP modifies its structure and affinity for F-actin. The process of constant addition of monomers on one end of the

growing filament and dissociation from the other end is named treadmiling (Pollard and Cooper, 2009).

Actin can spontaneously polymerize, therefore the first step of monomer assembly is initiated and regulated by the ARP2/3 complex, formins and spiore/cordon bleu (Pollard, 2007). However, these proteins are not required for regulation of the actin dynamics, which is controlled by different set of regulators such as profilins (polymerization), cofilins (depolymerization) and gelsolin (sever and cap actin filaments) (Fig.12) (Taylor et al, 2011).

Actin filaments are associated with each other and are cross-linked through the interaction with scaffolding proteins. These actin cross-linkers also provide anchorage of actin to the plasma membrane. The best known cross-linkers of actin are actinin, filamin and the molecular motor Myosin II, which increase the stiffness of the actin mesh.

Interestingly, the function of actin varies and is dependent on its subcellular localization. For example, during ciliogenesis cortical actin promotes the docking of basal bodies, while actin stress fibers are negative regulators of cilia formation.

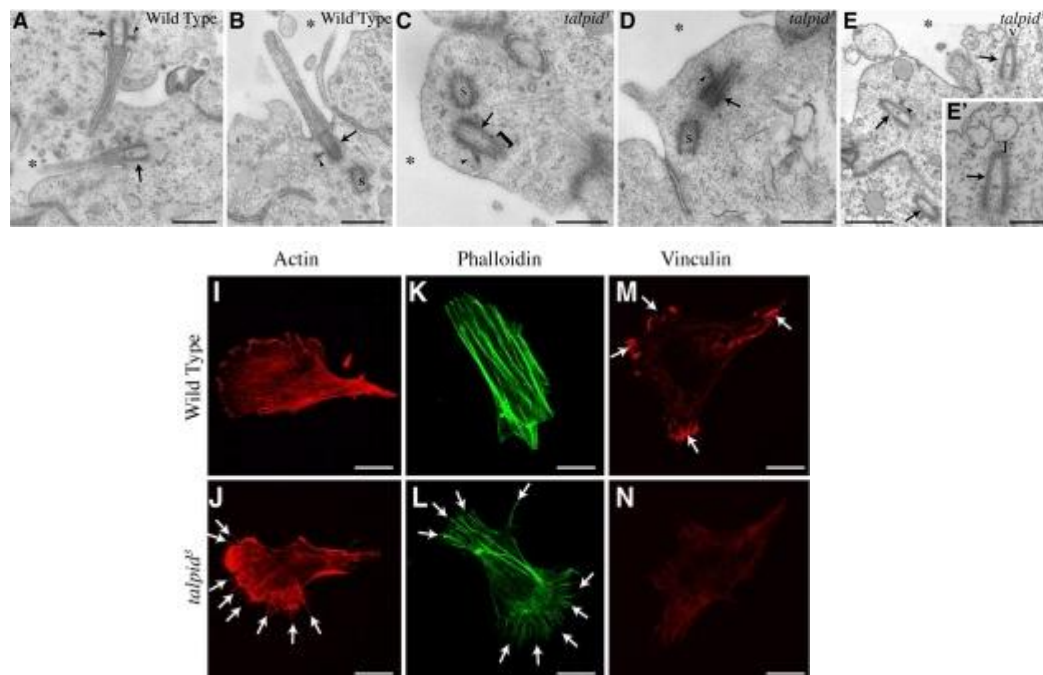


**Figure 12.** Filamentous actin formation through polymerization/depolymerization activity. G-actin monomers polymerization is initiated by the Arp2/3 complex binding. Profilin promotes polymerization, while cofilin support depolymerization (Taylor et al, 2011)

#### 1.2.4. B Actin and cilia

The link between actin and ciliogenesis was first revealed in the chicken *Talpid3* mutants, characterized by defects in primary cilia formation and actin organization (Fig.13). In these mutants, properly matured basal bodies could not dock to the apical cell membrane (Yin et al, 2009).

Also, recent studies showed that actin is responsible for the anchoring of basal bodies to the cell membrane in the multiciliated cells of the frog mucociliary epithelium (Antoniades et al, 2014).

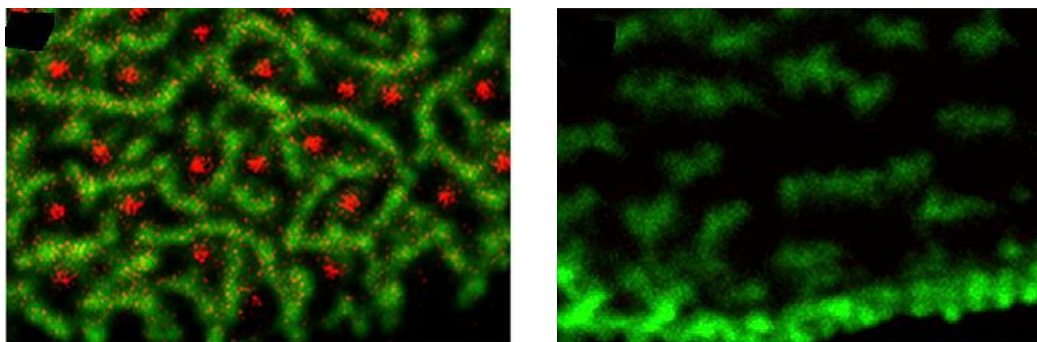


**Figure 13.** Transmission electron microscopy section through the neuroepithelium of wild type (A-B) and *talpid3* mutants (C-E'). In the mutant chicken embryos primary cilia formation is affected by loss of basal bodies orientation towards the apical surface and disruption of the E) vesicle fusion with the basal body. Arrows indicate basal bodies, s –sister centriole. F) Actin cytoskeleton of wild-type (A, K, M) and *talpid3* mutant (J, L, N) cells from limb buds in primary culture. Arrows in J, L indicate actin-containing filopodia in the mutant cells. The focal adhesions expressing Vinculin are present only in the wild type embryos (arrows in M) (Yin et al, 2009).



In multiciliated cells actin plays multiple roles. For example, actin together with myosin controls the transport of basal bodies to the cell apical surface, which is a prerequisite to their docking. On the other hand, cortical actin of the MCCs promotes the anchorage of the basal bodies to the plasma membrane, which is a prerequisite to ciliary axoneme growth (Klotz et al, 1986; Dawe et al, 2007; Boisvieux et al, 1990; Ioannou et al, 2013). This enrichment of cortical actin at the apical surface of MCCs is colloquially named actin cap or actin web-like structure (Pan et al, 2007).

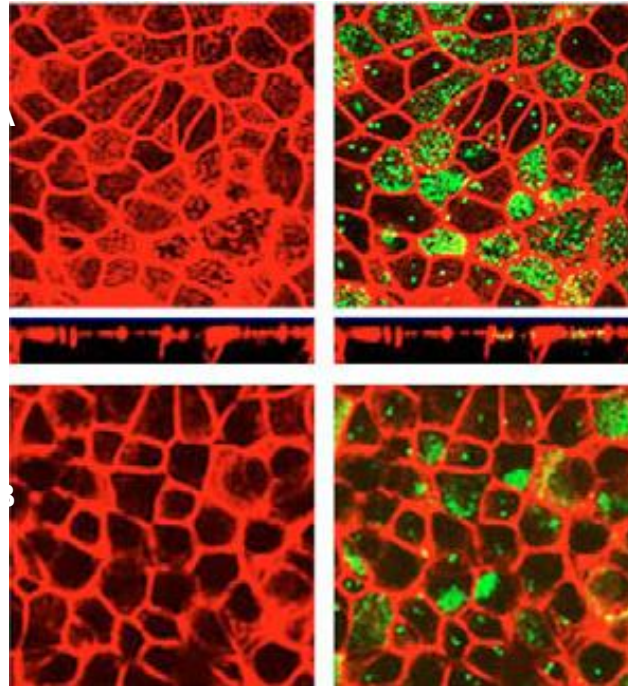
It was shown recently that in *Xenopus* MCC actin exists in two different pools, named the apical and subapical actin network (Fig.14). These distinct actin networks are involved in different processes. The apical pool of actin mostly participates in the basal bodies docking, while the subapical pool regulates the spaced pattern and the cell-wide polarity of basal bodies (Antoniades et al, 2014, Ioannou et al, 2013, Werner et al, 2011).



**Figure 14.** Apical A) and subapical B) pools of actin at the surface of *Xenopus* multiciliated cells. F-actin stained with Phalloidin in green, basal bodies indicated by injection of Centrin2 -RFP (Antoniades et al, 2014).

Currently, several lines of evidence from different model organisms support F-actin involvement in the process of cilia generation. New molecular regulators of the actin cap formation are becoming revealed. One well-known regulator of the actin meshwork is RhoA GTPase, a member of the family of Rho GTPases (Fig.15). It was

shown in mouse airway epithelial cells that RhoA controls the formation of actin cap in ciliated cells (CCs). The cells treated with specific inhibitors of RhoA function lost their actin cap. Therefore, basal bodies were unable to be docked at the apical surface of plasma membrane (Fig.15) (Pan et al, 2007).



**Figure 15.** Actin organization at the apical surface of the ciliated cells in mouse primary culture airway epithelial cells before (A) and after (B) treatment with Clostridium botulinum C3 exotoxin, which specifically inactivates RhoA. F-actin stained with phalloidin in red, basal bodies stained with  $\gamma$ tubulin in green (Pan et al, 2007).

Moreover, it was shown that RhoA acts downstream of the PCP signaling pathway effector Dishevelled (Dvl). In *Xenopus* Dvl morphants, the activation of RhoA was disrupted, although its localization was unaffected. Therefore, RhoA inactivation seems to be sufficient for the disruption of the apical actin network (Park et al, 2008).

PCP pathway proteins like *Xenopus* Inturned and Fuzzy are also essential for the apical enrichment of actin through controlling RhoA localization (Park et al, 2006, Gomperts et al, 2004).

Actin is also regulated by Ezrin, a component of the ERM (ezrin-radixin-moesin) complex (Pan et al, 2007). Ezrin is expressed for example at the apical surface of ciliated cells and associated with basal bodies in the pulmonary epithelium (Gomperts et al, 2004). The knock-out of Forkhead box transcription factor J1 (Foxj1 required for motile cilia formation) promotes the expression of calpastatin, an inhibitor of the protease calpain, resulting in strong decrease in the expression of ezrin as well as of the ezrin binding phosphoprotein-50 (EBP-50) (Gomperts et al, 2004).

The actin cap formation is not only under the control of Rho GTPases. For example, a flagellar protein first discovered in *Chlamydomonas* and called the Nucleotide binding protein 1 (Nubp1), stabilises actin in a RhoA independent manner during frog ciliogenesis (Ioannou et al, 2013; Pazour et al, 2005). The knock-down of Nubp1 caused defects in the apical actin organization, but also impaired an internal actin network essential for basal bodies migration. Furthermore, it was suggested that after basal bodies docking internal actin remodeled into the subapical actin (Ioannou et al, 2013).

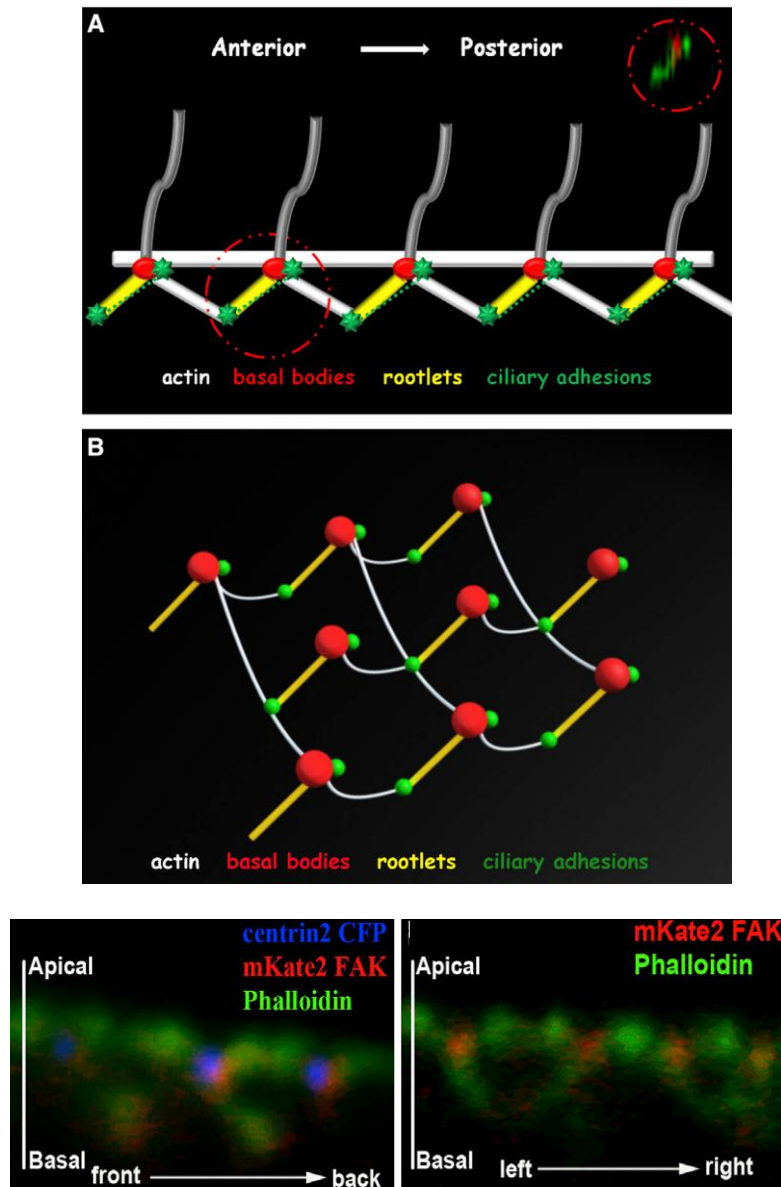
### **2.1.5 Basal body docking and polarization at the plasma membrane surface**

It is important to better understand the relation between actin and the basal body, given that the formation of a dense actin meshwork at the apical cells surface is required for basal body anchoring.

One explanation for the existence of a link between the basal bodies and actin cytoskeleton is provided by the finding of the so-called “ciliary adhesion” (CA) complex, constituted of proteins also involved in the formation of focal adhesions (Fig.16). As it was shown in *Xenopus laevis* epithelial cells, the focal adhesion proteins, including Focal Adhesion Kinase (FAK), Paxilin and Vinculin are associated with basal bodies in the CA complex, which permits the docking of basal body to the apical actin cap (Fig.16) (Antoniades et al, 2014).

However, to allow ciliary growth, basal bodies need not only to be docked, but also polarized and oriented in respect to the cell. In ciliated cells, the proper polarity is maintained by three modes of planar polarity: rotational, tissue-level and translational planar polarity (Wallingford, 2010).

The rotational planar polarity is manifested by the positioning of the basal bodies-specific structures such as the basal foot, which points the direction of effective stroke, and the rootlet, which points away from it. Therefore, the rotational planar polarity is a specific alignment of multiple basal bodies within each single multiciliated cell (Wallingford, 2010).



**Figure 16.** A) Schematic view of the CA complexes interaction with basal bodies and apical/subapical pool of actin. B) Proposed arrangement of the subapical actin network (Antoniades et al, 2014).

The second mode of polarization called tissue-level polarity (inter-cellular polarity) refers to all MCCs within the tissue, which have their aligned basal bodies oriented in the same direction (Wallingford, 2011).

The third mode called translational planar polarity exist in for example ependymal cells, where basal bodies are present in a cluster, only partially covering the apical surface and the position of these clusters is planar polarized. Clusters initially form in the center of each cell, and as polarity becomes entrained, the cluster migrates to the posterior apex of each cell (Mirzadeh et al, 2010).

The proper polarity and orientation of basal bodies is controlled by the Planar Cell Polarity (PCP) signaling cascade (Wallingford, 2010). Disruption of the PCP protein Dishevelled (Dvl) randomized the rotational polarity within each multiciliated cell and consequently impaired directional fluid flow (Wallingford, 2010).

The rotational and tissue-level polarities are controlled by IFT88. Interestingly, IFT88 mutation significantly impairs cell polarity, but does not affect the localization of core PCP proteins, thus suggesting that the role of IFT in cell polarity is independent of PCP signaling pathway (Jones et al, 2008).

#### **2.1.6. Cilia axoneme growth**

When the apical and subapical actin is properly organized and basal bodies are docked at the plasma membrane, the cilia axoneme can grow. The axonemal growth takes place within the region limited by the ciliary membrane, a lipid bilayer extended from the plasma membrane (Yuan and Sun, 2013).

The ciliary axoneme growth is achieved mainly through the Intraflagellar Transport (IFT), but it is also supported by the vesicle transport.

##### **2.1.6. A) Intraflagellar transport (IFT)**

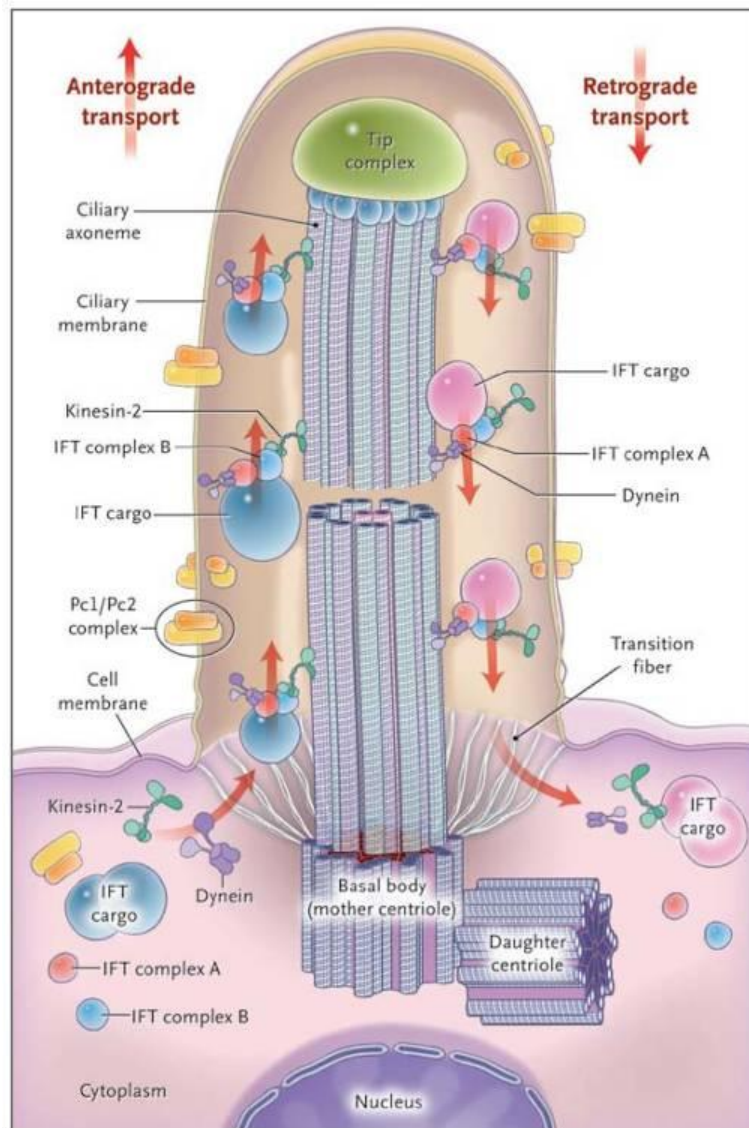
Intraflagellar transport was described for the first time by differential interference contrast (DIC) microscopy in the flagella of the green alga *Chlamydomonas reinhardtii* (Kozminski et al, 1993).

IFT transports the ciliary proteins from the cytoplasm to the tip of the cilium. This movement is bidirectional and occurs along the axoneme within the multiprotein complexes called IFT particles or IFT trains (Fig.17). Transmission electron microscopy and electron tomography allowed to distinguish two classes of IFT trains. The first class consists of long (around 700 nm) and less electron-opaque IFT trains, while, the second class is characterized by short and highly electron-opaque IFT trains. Long IFT trains contribute to anterograde transport from the base to the tip of cilia, whereas the short IFT trains contribute to retrograde transport (Ishikawa and Marshall, 2011).

Furthermore, IFT trains consist of biochemically distinct complexes named A and B IFT complexes. These two complexes are constructed from 20 proteins, which are enriched in protein-protein interacting domains (Ishikawa and Marshall, 2011). Both complexes are involved in the intraflagellar transport IFT complex A is required for retrograde transport, while IFT complex B contributes to anterograde transport and ciliary assembly. For example, the loss of any protein of the IFT complex B results in short or missing cilia. Therefore, the knock-down of one of the component of IFT complex B called IFT20 in mammalian cells suppresses ciliary assembly (Follit et al, 2006).

The movement of ciliary proteins occurs through the activity of two motor families: the dynein-2 and kinesin-2 family. Each protein family is involved in cargo transport, but at different level. Dyneins control the anterograde transport of ciliary proteins from the cytoplasm to the tip of the cilium, whereas kinesins are involved in the retrograde transport from the tip to the base of the cilium (Fig.17) (Ishikawa and Marshall, 2011).

Additionally, IFT particles can directly bind cargoes. IFT train components were found to co-immunoprecipitated with dynein in *C. reinhardtii* flagella extracts (Qin et al, 2004).



**Figure 17.** Anterograde and retrograde IFT (Hildebrandt et al, 2011).

#### 2.1.6. B) Vesicle transport

The vesicle transport is another mode of transport used by cilia to transfer their proteins within the axoneme. This was found in *Caenorhabditis elegans* OSM-9 mutants, where impaired distribution of the ciliary membrane OSM-9 channels caused disruptions of the IFT. Therefore, it was proposed that IFT-dependent transport of cargo requires interaction with other transport systems present in the cilium (Qin et al, 2005).

More evidences of the IFT machinery involvement in the vesicle trafficking came from studies on IFT20, a component of IFT complex B, which localizes to the Golgi apparatus, cilia and basal bodies (Follit et al, 2006). In mammalian cells the strong knockdown of IFT20 represses ciliary assembly, but did not affect Golgi structure. On the other hand, the moderate knockdown did not impact ciliary assembly, but reduced the amount of polycystin-2 that localized to the cilia. Altogether, these results suggested that IFT20 is required for the delivery of ciliary membrane proteins from Golgi complex to the cilium (Follit et al, 2006).

Another example of membrane proteins known to be involved in the vesicle transport from the Golgi apparatus to the cilia are BBS (Ishikawa and Marshall, 2011).

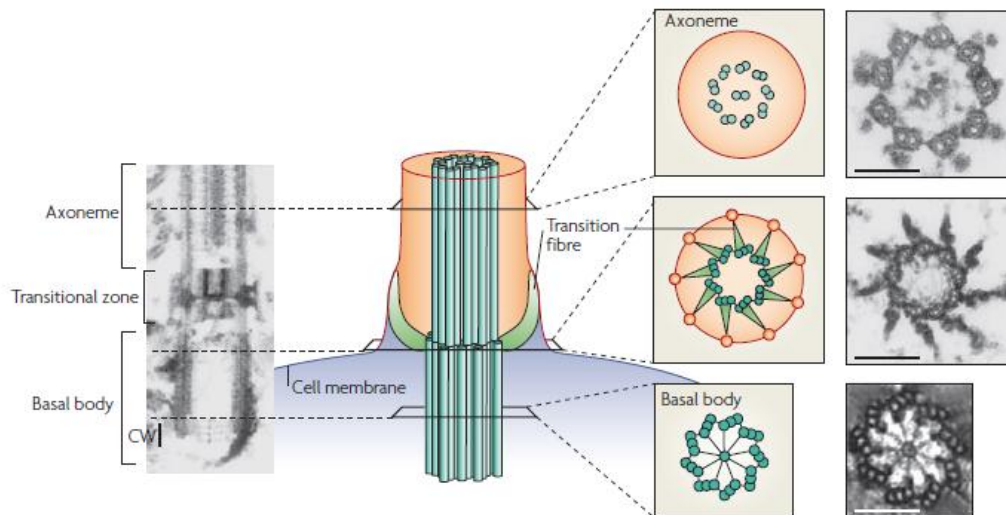
#### **2.1.6. C) Control of proteins transfer within the cilium**

The transport of proteins in and out the cilium allows axoneme to grow. How is this transfer controlled?

The selectivity barrier at the ciliary base called transition zone controls the proteins transfer within the axoneme (described in the chapter 1) (Fig.18) (Szymanska et Johansen, 2010; Dishinger et al, 2010).

The transfer of the ciliary proteins can be controlled by the IFT machinery itself. Therefore, IFT controls ciliogenesis by changing various parameters such as the size and speed of its trains, the periodicity of train entry and the cargo selection. For example, IFT train size decreases as flagella length increases during flagella regeneration in *C. reinhardtii* (Engel et al, 2009).





**Figure 18.** Transmission electron microscopy and schematic sections of ciliary axoneme at the level of axoneme, transition zone and basal bodies (Battencourt-Dias et Glover, 2007).

#### 2.1.6. D) Control of the cilia length

Not only the growth, but also the length of the cilia is tightly controlled. Ciliary length can be controlled by three different levels of regulation, such as: synthesis of the ciliary components, IFT and turnover at the ciliary tip.

Interestingly, each type of cilia possesses different molecular modes of controlling its length. In motile cilia the limiting/accelerating factors of growth are hydrodynamic interactions with the surrounding fluid. The velocity of cilia-driven fluid flow increases with the ciliary length (Marshall and Rosenbaum, 2001).

In primary cilia, where fluid flow is not generated, the length is regulated by signaling molecules, including Retinitis Pigmentosa1 (RP1) and the MKS1, MKS3 proteins related to Meckel-Gruber syndrome (Ishikawa and Marshall, 2011, Williams et al, 2010).

Another explanation for the control of ciliary length is based on the observation that the cilium is continuously growing, even after reaching its final length (Marshall and Rosenbaum, 2001, Ishikawa and Marshall, 2011). The continued assembly is balanced by disassembly, which occurs by removal of the microtubule subunits from the ciliary tip. However, ongoing turnover or disassembly of microtubules does not

occur through spontaneous depolymerization, but rather requires an active mechanism, which is likely controlled by a Kinesin -13 molecular motor. It was shown that the overexpression of the Kinesin-13 family of motors in the parasite *Leishmania major* results in flagellar shortening, while the knockdown yields longer than normal flagella (Blaineau et al, 2007).

Another way of controlling ciliary length implies the process of microtubule disassembly (Marshall et al, 2001). This finding came from the observation that the total number of IFT particles in the cilium is not related to the cilia length. Hence, since the number of the particles is constant, the frequency with which particles deliver cargoes to the tip decreases as the ciliary length increases. It was concluded, that transport is a rate-limiting factor during cilia growth and at steady-state the assembly rate is a decreasing function of the length (Ishikawa and Marshall, 2011).

#### **2.1.7. Polarized beating**

The main function of the motile cilia is the propulsion of the water or body fluids (mucus, urine, cerebrospinal liquid) through polarized and coordinated beating. Ciliary beating is highly coordinated and the so-called ciliary beat frequency (CBF) phenomenon allows to respond quickly and for prolonged time periods to various stimuli (Schmid and Salathe, 2011).

However, the periodic ciliary beating is not feasible without the internal apparatus of cilia, where the nine outer microtubule pairs of cilia axoneme are linked to each other by nexin, whereas the central pair is connected through radial spokes to surrounding microtubules (Satir and Christensen, 2007, Braiman and Priel, 2008).

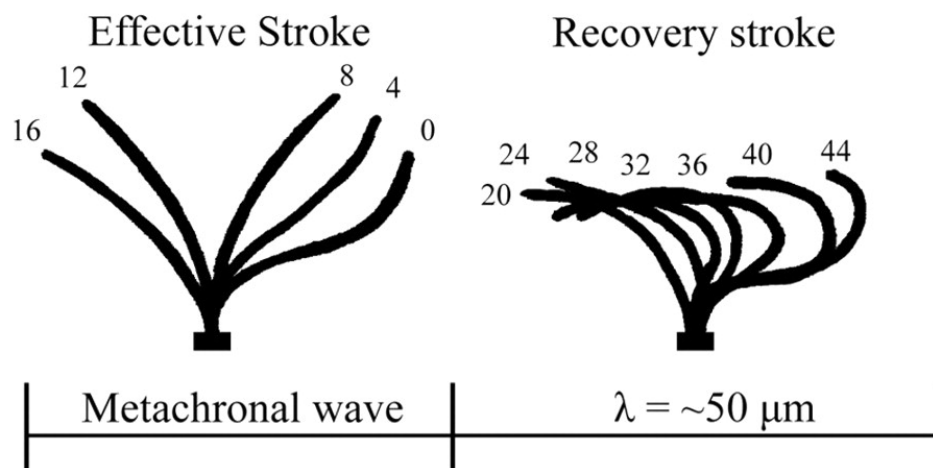
The motor protein Dynein consisting of the inner (IDA) and outer (ODA) arms plays an important role in the cilia beating. Dynein is found on each doublet of microtubules of motile cilia. The energy generated by ATP hydrolysis allows dynein to produce the active sliding of adjacent microtubule doublets and thus cilia can be bent repetitively (Satir and Christensen, 2007).

Interestingly, the ciliary beating machinery of motile cilia functions in two different modes. The first mode, which has been described above, gives a low rate of beating that requires ATP and the ciliary motors. The second mode is characterized by a high rate of beating, and it involves a mechanism regulated by secondary

messengers like  $\text{Ca}^{2+}$ , cGMP and cAMP with a relatively large variety of different receptors, like the purinergic, adrenergic and cholinergic receptors (Braman and Priel, 2008, Schmid and Salathe, 2011; Ma et al, 2002).

Also, the beat by itself can be physically characterized. For example in mucus-propelling cilia the beating consists of two distinct strokes: the fast effective stroke and the slower recovery stroke (Fig.19) (Sanderson and Sleight, 1981). During the effective stroke, the cilia are in an upright position and move perpendicular to the cell surface, which allows them to propel mucus (Fig.19). During the recovery stroke, cilia are bent and incline to the cell surface avoiding the contact with the mucus layer (Fig.18) (Sanderson and Sleight, 1981).

Moreover, the motile cilia of multiciliated cells are tightly packed, and this in turn requires the special arrangement and synchronization of their beating. This is achieved by the generation of the metachronal wave (also called metachronism). In most of the cases the metachronal wave is generated in the opposite direction to propulsion. Metachronism allows single cilia from multiciliated cell to participate in the propulsion without impeding each other's motion (Eshel and Priel, 1987, Braiman and Priel, 2007).



**Figure19** . Traces of a single cilium depicting its position at 4-ms intervals during a complete beat cycle. Planarian cilia beat with an asymmetric waveform consisting of an effective and a recovery stroke; the effective stroke is completed in  $\sim 15$  ms representing one-third of the ciliary beat cycle. Adopted by (Sanderson and Sleight, 1981).

### 3. Mechanisms of ciliary gene regulation

#### 3.1 Transcriptional level

There are at least two levels of ciliary genes transcriptional regulation. The first level is chromatin remodeling, which involves chromatin and its regulators that modify nucleosomes accessibility during gene activation and gene repression (Lee et Young, 2013). The second regulatory mechanism involves transcription factors (Lee et Young, 2013). Unlike chromatin regulators, transcription factors exert their regulatory activity by binding enhancer elements on the DNA and recruiting co-factors and RNA polymerase II, thus controlling the initiation and/or elongation of the DNA transcription (Lee et Young, 2013).

The transcriptional regulation of ciliary gene expression was documented for the first time in *Chlamydomonas* and sea urchin. It was shown that induced deflagellation (loss of the axoneme) causes the accumulation of  $\alpha$  and  $\beta$ -tubulin mRNA and the increased transcription of their new mRNAs (Keller et al, 1984). Moreover, it was shown that inhibition of  $\alpha$  and  $\beta$ -tubulin transcription results in defects in cilia assembly (Damen et al, 1994).

To, our present knowledge the transcriptional regulation of the motile cilia formation is under the control of at least four families of transcription factors: Rfx, FoxJ1, Myb, E2F (Stubbs et al, 2012; Choksi et al, 2014; Tan et al, 2013; Ma et al, 2014; Thomas et al, 2010) (Table 1).

| Cilia type                                 | Organism                             | Transcription factor(s) required | References  |
|--|--------------------------------------|----------------------------------|---|
| Airway motile multicilia                   | Mouse                                | FOXJ1                            | (Brody et al., 2000; Chen et al., 1998)                             |
| Epidermal motile multicilia                | <i>Xenopus</i>                       | FOXJ1<br>RFX2                    | (Stubbs et al., 2008)<br>(Chung et al., 2012)                       |
| Sperm flagellum                            | Mouse                                | FOXJ1                            | (Chen et al., 1998)   |
| Oviduct motile multicilia                  | Mouse                                | FOXJ1                            | (Brody et al., 2000; Chen et al., 1998)                             |
| Brain ependymal multiple motile cilia      | Mouse                                | RFX3<br>FOXJ1                    | (El Zein et al., 2009)<br>(Brody et al., 2000; Chen et al., 1998)   |
| Brain ependymal monocilia/multicilia       | <i>Xenopus</i>                       | FOXJ1                            | (Hagenlocher et al., 2013)  |
| Spinal canal ependymal motile cilia        | Zebrafish                            | FOXJ1A                           | (Yu et al., 2008)   |
| Nodal motile monocilia                     | Mouse                                | RFX3<br>FOXJ1                    | (Bonnafe et al., 2004)<br>(Alten et al., 2012)                      |
| Kupffer's vesicle motile monocilia         | Zebrafish                            | RFX2<br>FOXJ1A                   | (Bisgrove et al., 2012)<br>(Stubbs et al., 2008; Yu et al., 2008)   |
| Gastrocoel roof-plate motile monocilia     | <i>Xenopus</i>                       | RFX2<br>FOXJ1                    | (Chung et al., 2012)<br>(Stubbs et al., 2008)                       |
| Pronephric motile multicilia and monocilia | Zebrafish                            | RFX2<br>FOXJ1A<br>FOXJ1B         | (Liu et al., 2007)<br>(Yu et al., 2008)<br>(Hellman et al., 2010)   |
| Immotile signaling cilia                   | Mouse<br>Zebrafish<br><i>Xenopus</i> | RFX4<br>RFX2<br>RFX2             | (Ashique et al., 2009)<br>(Yu et al., 2008)<br>(Chung et al., 2012) |
| Otic vesicle kinocilia                     | Zebrafish                            | FOXJ1B                           | (Yu et al., 2011)   |
| Chordotonal organ sensory motile cilia     | <i>Drosophila</i>                    | FD3F                             | (Cachero et al., 2011; Newton et al., 2012)                         |
| Sensory neurons                            | <i>Drosophila</i>                    | RFX                              | (Dubruille et al., 2002)  |
|  | <i>C. elegans</i>                    | DAF-19                           | (Swoboda et al., 2000)  |
| Olfactory motile cilia                     | Zebrafish                            | FOXJ1A                           | (Hellman et al., 2010)  |

**Table1.** Ciliary transcription factor(s) needed to produce different cilia types in selected organisms (Choksi et al, 2014).








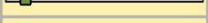


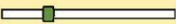




### 3.1.1. RFX

The RFX family of transcription factors plays a major role in the regulation of ciliogenesis in vertebrates, but also invertebrates including *C.elegans* and *Drosophila* (Fig. 20, 21). Members of the Rfx family regulate the expression of the components of both motile and immotile cilia (Swoboda et al, 2000).

The Rfx transcription factors are characterized by the presence of a winged-helix DNA-binding domain (DBD), which allows them to interact with a DNA target site called the X-box. In vertebrates, the RFX family consists of eight members: Rfx1-8 and can be subdivided into two groups based on the functional connections to ciliogenesis. The first subgroup comprises Rfx2-4, while the second subgroup includes Rfx1,5-8 (Fig.20). Unlike the members of the second subgroup, those of the first subgroup undergo homo- and hetero-dimerization and are known to control ciliogenesis (Thomas et al, 2010; Choksi et al, 2014).

Several lines of evidence support a regulatory function of Rfx2 in vertebrate ciliogenesis. Rfx2 is expressed in *Xenopus* in ciliated tissues including neural tube, gastrocoel roof plate, epidermal multiciliated cells and kidneys. Rfx2 is also a crucial

factor in spermatogenesis and it was shown to be enriched in the pronephric kidney tubules of the zebrafish embryo (Chung et al, 2012; Choksi et al, 2014). Knockdown of Rfx2 in *Xenopus* embryos causes phenotypes re-conducible to ciliary defects, such as left-right asymmetry defects and disruption of neural tube closure. This suggests that Rfx2 affects cilia development in the neural tissues through the Hedgehog signaling (Chung et al, 2012), while Rfx2 knock-down in *Xenopus* mucociliary epithelium leads to defects in motile cilia assembly (Chung et al, 2012).

|             | Organisms  | RFX TFs | Protein domains   | Expression patterns  | Ciliary phenotypes  |  | Key ciliary target genes                                       |
|-------------|--|---------|---|--|---|--|--|
|             |  |         |   |  | Organism wide   | Cilia specific   |  |
| Vertebrates | <i>H. sapiens</i><br><i>M. musculus</i><br><i>X. laevis</i><br><i>D. rerio</i> | RFX1    |    | Brain  | Homozygous lethal   | Not known  | <i>ALMS1</i>   |
|             |  | RFX2    |    | Organs of laterality<br>Brain<br>Kidney<br>Testis<br>Epidermis | Left-right asymmetry defects<br>Defective neural tube closure<br>Perturbed HH signaling                             | Truncated, dysfunctional motile cilia<br>Fewer and truncated immotile cilia                            | <i>IFT122</i><br><i>IFT172</i><br><i>WDPCP</i><br><i>TTC25</i> |
|             |  | RFX3    |    | Organs of laterality<br>Brain<br>Pancreas<br>Epidermis         | Left-right asymmetry defects<br>Hydrocephalus<br>Malformation of the corpus callosum<br>Perturbed hormone secretion | Truncated, dysfunctional motile cilia<br>Aberrant number of immotile cilia<br>Truncated immotile cilia | <i>Dync2li1</i><br><i>Dnah9</i><br><i>Dnah11</i>               |
|             |  | RFX4    |    | Brain<br>Testis  | Homozygous lethal<br>Reduction/absence of SCO<br>Patterning defects<br>Hydrocephalus                                | Truncated cilia  | <i>IFT172</i>  |
|             |  | RFX6    |    | Pancreas   | n/a   | n/a  | n/a  |
|             |  | RFX8    |    | Not known  | Not known   | Not known  | Not known  |
|             |  | RFX5    |    | Immune system  | n/a   | n/a  | n/a  |
|             |  | RFX7    |    | Not known  | Not known   | Not known  | Not known  |
|             |  | RFX9    |    | Not known  | Not known   | Not known  | Not known  |
| Flies       | <i>D. melanogaster</i>   | RFX     |    | Brain<br>Chordotonal and external sensory neurons              | Sensory behavioral defects  | Structurally abnormal cilia  | <i>nan</i><br><i>iav</i>                                       |
|             |  | RFX1    |    | Not known  | Not known   | Not known  | Not known  |
|             |  | RFX2    |  | Not known  | Not known   | Not known  | Not known  |
| Nematodes   | <i>C. elegans</i>  | DAF-19  |  | Ciliated sensory neurons                                       | Dauer formation<br>Dye filling and sensory behavioral defects   | Absence of all cilia   | Numerous   |
| Fungi       | <i>S. cerevisiae</i>   | CRT1    |  | Single-celled budding yeast                                    | n/a   | n/a  | n/a  |
|             | <i>S. pombe</i>  | SAK1    |  | Single-celled fission yeast                                    | n/a   | n/a  | n/a  |

**Figure 20.** The expression and function of RFX family transcription factors in various organisms.

Schematics of each protein with the highlighted conserved RFX protein domains: activation domain (blue); DNA-binding domain (green); domain B (red); domain C (purple); the dimerization domain (yellow). The RFX factors directly connected to ciliogenesis are highlighted in blue; those that have not been connected to ciliogenesis are highlighted in yellow; factors that have been loosely associated with ciliogenesis are highlighted in green. Vertebrate RFX factors are grouped according to phylogenetic studies of the DBD domain and the presence/absence of additional protein domains. ALMS1, Alstrom syndrome 1; Dnah, dynein, axonemal, heavy chain genes; Dync2li1, dynein cytoplasmic 2 light intermediate chain 1; iav, inactive; IFT, intraflagellar transport genes; n/a, not applicable; nan, nanchung; SCO, subcommissural organ; TFs, transcription factors; TTC25, tetratricopeptide repeat domain 25; WDPCP, WD repeat-containing planar cell polarity effector (Choksi et al, 2014).

Analogously to Rfx2, Rfx3 functions in motile and immotile cilia. Rfx3 activates the expression of crucial intraflagellar transport components and controls the expression of proteins specific to the basal bodies and the transition zone (Piasecki et al, 2010; Tan et al, 2013; Thomas et al, 2010). Moreover, Rfx3 was shown to regulate primary cilia growth in the embryonic node and the endocrine pancreas of mice (Bonnafe et al, 2004; Thomas et al, 2010).

Another member of Rfx family is Rfx4, highly expressed during the brain development, where it governs the primary cilia growth, and in the testis. Mice deficient for Rfx4 show defects in the dorsal-ventral patterning (Thomas et al, 2010; Ashique et al, 2009).

Interestingly, all known targets of Rfx 2,3 and 4 transcription factors in *C.elegans*, *Drosophila* and mice are involved in ciliogenesis. Among these are for example BBS proteins, some of the IFT proteins, as well as nephronophthisis proteins and rootletin. The last two are important components of the transition zone and the striated rootlet of basal bodies, respectively (Thomas et al, 2010; Yang et al, 2005).

On the other hand, members of the second subgroup of Rfx transcription factors, like Rfx5 and Rfx6, regulate genes of the HLA class and play a role in pancreatic development, respectively. Also, Rfx1 regulatory role is not associated with cilia (Choksi et al, 2014). Members of the Rfx subgroup, which do not control ciliogenesis, possess the same DNA binding domain, however they show different target specificities (Thomas et al, 2010).

Rfx transcription factors are functionally redundant, since loss of only one Rfx in mice does not lead to complete ciliary loss. This is especially true for Rfx 2-4 factors, which are able to form heterodimers (Thomas et al, 2010).

### **3.1.2. FoxJ1**

The FoxJ1 (also known as HFH-4) transcription factor belongs to the forkhead/winged-helix family. Members of the forkhead family have been found in vertebrates and many invertebrates. Evidences from diverse organisms, where



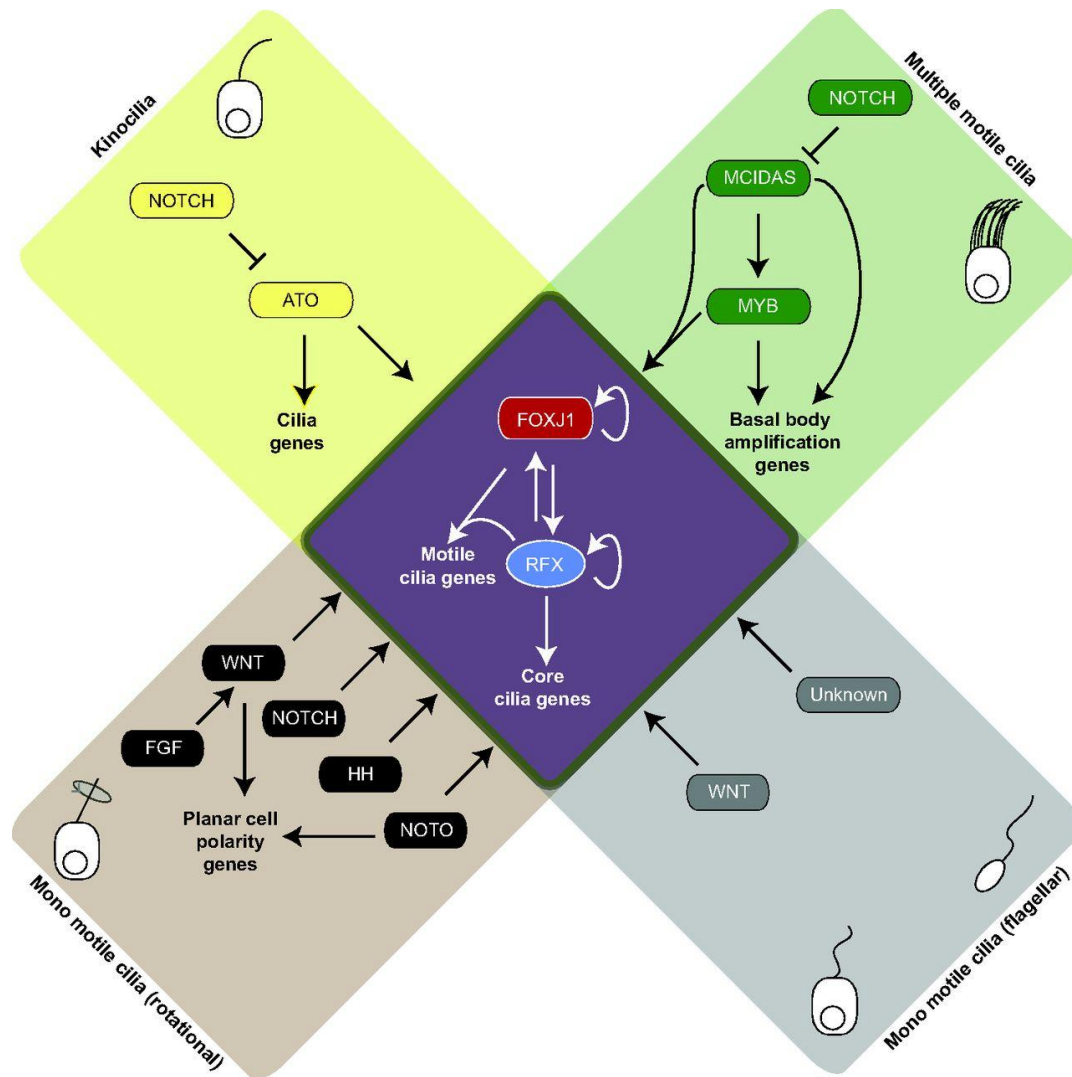
FoxJ1 is specifically expressed in tissues equipped with motile cilia, suggest a cilia-related function of FoxJ1 (Fig.21) (Murphy et al, 1997).

Indeed, Foxj1 controls the formation of motile cilia. For example, the FoxJ1 knockout mice exhibit hydrocephalus and left-right asymmetry defects, and also show lack of motile cilia in the nasal epithelium and ventricular cells, thus revealing motile cilia defects (Brody et al, 2000).

Furthermore, in *Xenopus* and zebrafish embryos, the ectopic expression of Foxj1 causes differentiation and growth of functional motile cilia in various tissues (Stubbs et al, 2008; Yu et al, 2008).

Moreover, in the absence of FoxJ1 the ezrin-mediated anchoring of basal bodies to apical plasma membrane is disrupted (Brody et al, 2000, Thomas et al, 2010, Gomperts et al, 2004). These data confirm the specific role of Foxj1 as a conserved master regulator of motile ciliogenesis, and particularly in the regulation of basal body docking (Choksi et al, 2014, Thomas et al, 2010, Brody et al, 2000).

Recent studies on Foxj1 allowed to identify many of its target genes. The cohort of genes regulated by Foxj1 includes some, which are known to be required for special aspects of motile cilia, but also genes more widely required for ciliogenesis, such as IFT proteins or tubulins (Choksi et al, 2014).



**Figure 21.** The regulatory logic of making cilia types that require the RFX/FOXJ1 module. The RFX/FOXJ1 transcriptional cassette is deployed by different signaling pathways and transcriptional modulators to generate ciliary diversity (Choksi et al, 2014).

### 3.1.3 Myb

A characteristic feature of MYB family is that some of its members are ubiquitously expressed and specifically required for the G1/S transition, while others show restricted expression. The myb transcription factor, which is involved in ciliogenesis is encoded by the myeloblastosis protooncogene Myb (c-Myb) (Tan et al,

2013). Until recently, Myb was known to regulate the cell cycle and progenitor cell proliferation in colon and brain (Ramsay et Gonda, 2008).

Currently, Myb was found to be expressed in the developing MCCs of vertebrate airways and frog larval skin. It was shown that the inactivation of Myb delays or inhibits the process of centriole amplification and also the expression of Foxj1 (Tan et al, 2014; Wang et al, 2013). The expression pattern of Myb was unchanged in Foxj1 null mutant, while the number of Myb-expressing cells was increased after treatment with the Notch inhibitor DAPT. Therefore, given that Myb is expressed in immature MCCs until basal bodies docking, it was proposed that Myb functions upstream of Foxj1 and downstream of the Notch signaling pathway (Fig.21) (Tan et al, 2013).

This discovery of Myb involvement in the centriole amplification of MCCs is controversial, since it was also shown that Myb promotes S phase and cell cycling. However, the apparently opposite roles of Myb were reconciled by introducing another type of cell cycle phase called S\*, during which centriole are multiplied, but DNA synthesis does not occur (Tan et al, 2013).

### **3.1.4 E2F**

E2F transcription factors are key activators and repressors of genes involved in the cell cycle progression. Recently, they have been also described as regulators of multiciliogenesis (Ma and al, 2014). Interestingly, their expression is under the control of miRNAs. For instance, the miR-449 miRNA binds to and inhibits the expression of E2f2 (Lize et al, 2011).

E2f4 and E2f5, two other members of the E2f family, regulate the process of centriole amplification. E2f4 or 5 (functionally redundant) together with CDC27B and Multicilin (described in next paragraph) during the acentriolar pathway of centriole amplification form a complex named EDM in multiciliated cells (MCCs). EDM complex activates genes required for centriole assembly (Ma et al, 2014).

### 3.2. Post-transcriptional level

Several classes of small non-coding RNAs play important roles in post-transcriptional gene regulation through destabilizing mRNAs or blocking their translation, and thus exerting a negative control on gene expression.

#### 3.2.1. Small non-coding RNAs: definition and biogenesis

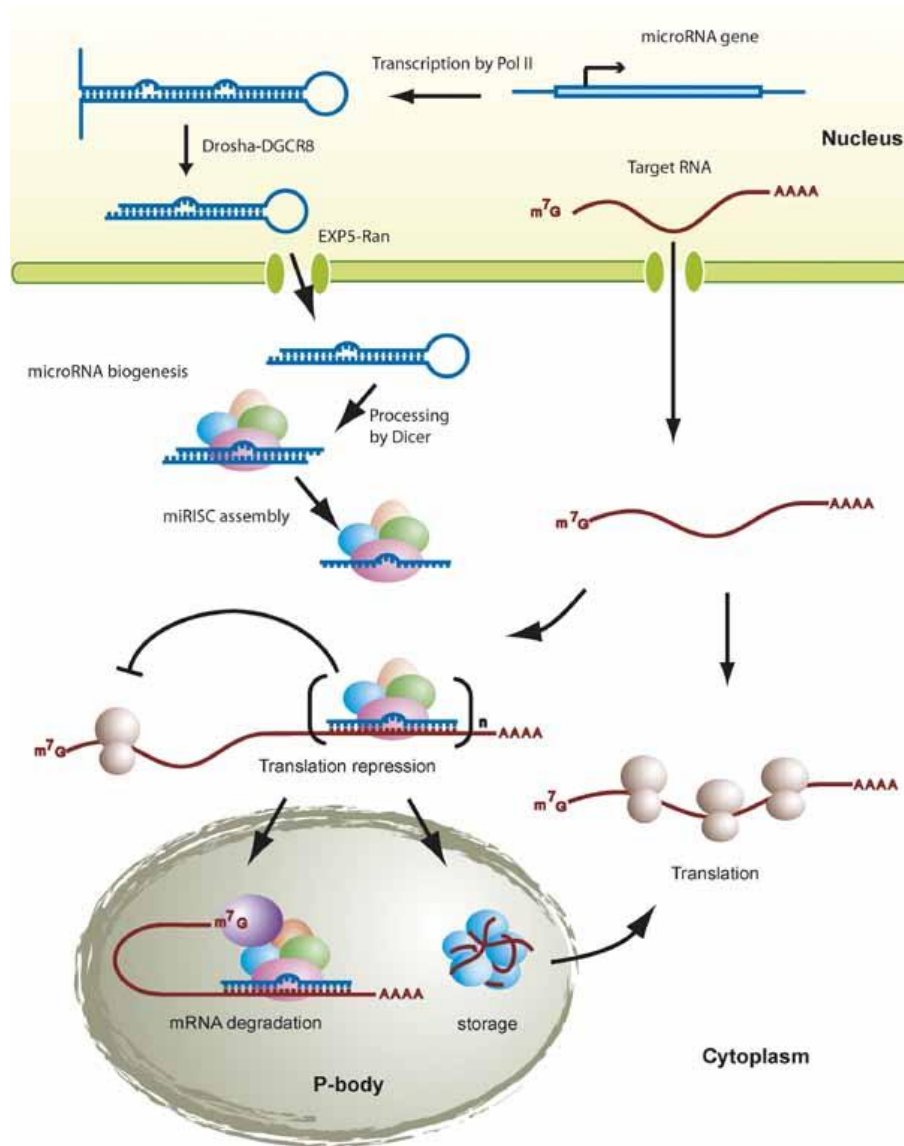
Post-transcriptional gene silencing is based on the activity of different classes of small non-coding RNAs, including microRNAs (miRNAs), small-interfering RNAs (siRNAs), PIWI-interacting RNAs (piRNAs), trans-acting siRNAs (tasiRNAs), small-scan RNAs (scnRNAs) and repeat-associated siRNAs (rasiRNA). The power of small, non-coding RNAs was first revealed by studies on *C.elegans* in 1998, when Fire and colleagues showed that RNAs are involved in the regulation of expression of other RNA transcripts as well as in the maintenance of transposon silencing in the germline genome (Fire et al, 1998). Small RNAs share some common features, such as the length (in average of 19-31 nucleotides) and function. They epigenetically silence the expression of target genes or mobile genetic elements in many evolutionary distant organisms (Chu and Rana, 2007).

One class of small non-coding RNA are microRNAs. They are 21-22 nucleotide long RNAs, present in animals as well as in plants, where they require different degrees of complementarity to their targets. In animals, miRNAs pair imperfectly to the 3' untranslated end (3'UTR) of their target mRNA, while in plants they need to be perfectly complementary to target mRNA (Filipowicz et al, 2005).

miRNAs are transcribed from dedicated genes, which are nested in the introns of non-coding or coding genes and in the exons of non-coding genes (Rodriguez et al, 2004, Chu and Rana, 2007). miRNAs are generated from hairpin-structure precursors and undergo maturation during a two-step process, which require the activity of two enzymes of the RNAase III family: Dicer and Drosha (Fig.21).

First, miRNA is transcribed by RNA polymerase II to pri-miRNA, which is characterized by a 5' capping structure and a 3' poly-A tail. Then, the pri-miRNA is cleaved by Drosha into a 70-nucleotide long pre-miRNA with 5' phosphate end and with a 2-nucleotide 3' overhang. This cleavage takes place in the nucleus, then pre-

miRNAs are transported to the cytoplasm. The transport from the nucleus to the cytoplasm occurs with the help of the nuclear export factor named Exportin-5 (Exp5) and the Ran GTP-binding protein. These proteins form a nuclear transport complex, which deliver pre-miRNA through the nuclear pore to the cytoplasm (Chu and Rana, 2007). In the cytoplasm, the Dicer RNAase III chops long double-stranded pre-miRNAs into ~22-nt duplexes of mature miRNA. Additionally, Dicer interacts with the RNA Binding Proteins (RBP). The Dicer-RBP connection helps miRNAs to associate with the RNA silencing Complex (RISC) required for miRNA activity. The RISC complex is composed of several different proteins. Argonautes (Ago) are the best-known family of RISC proteins, which directly associate with miRNA. For example in mammalian cells, four Ago proteins can be distinguished, but only one, called Ago2 has an endonuclease activity to cut RNA sequences, and thus forming the 5' end of the guide strand. Only one strand of miRNA with less stability at the 5' end is incorporated to RISC complex, while the second is eliminated (Fig.22).



**Figure 22.** The miRNA biogenesis and gene silencing activity (Chu et Rana, 2007).

### 3.2.1.1. Mechanisms of miRNA-mediated gene regulation

miRNAs guide strand bind mRNAs through a 2-8 nucleotide long region, called the “seed” sequence. Interestingly, individual miRNA can binds many (>100) targets. At the same time each individual mRNA target can interact with the seed sequences of many different miRNAs through its 3’UTR. Additionally, mRNA targets may potentially be regulated by binding to atypical or non-conserved sites of miRNA (Flynt et Lai, 2008). Computational analysis of the seed sequences of miRNA and the 3’UTR of mRNA targets showed that more than one-third of human protein-coding genes might be regulated by miRNAs (Lewis et al, 2005).

However, each of many targets of the same miRNA can respond differently to targeting, both quantitatively and qualitatively. In other words, it is still not clear to what extent a given target is repressed by a given miRNA. Therefore, miRNAs activity is classified based on their targets into three groups: “switch”, “tuning” and “neutral” targets. “Switch” targets are those, whose activity is turned off by miRNAs to undetectable levels. “Tuning” targets are those, whose activity is not completely suppressed and which remain functional to a certain extent in cells expressing the miRNA. Here, a miRNA can be even continuously co-expressed with its targets. “Neutral” targets are those for which the interaction with a given miRNA does not have any consequences (Flynt and Lai, 2008).

Usually, the interaction between miRNA and mRNA leads to target degradation or translation inhibition. The mRNA degradation takes place in the cytoplasm at specific sites called P-bodies, which contain proteins involved in mRNA remodeling, decapping, translational repression and 5' to 3' exonuclease activity (Valencia-Sanchez et al, 2006). Hence, P bodies serve for mRNA storage or degradation (Fig.22). Translation inhibition by miRNA occurs by two possible mechanisms through blocking protein synthesis at the initiation step or after its initiation (Chu and Rana, 2007).

#### **3.2.1.1. A miR-34**

It is important to note that some miRNAs can be structurally or functionally related to each other. An example are members from the well conserved vertebrate family of miRNA called miR-34 family. It comprises three genomic loci: miR-34a, miR-34b/c, and miR-449a/b/c. The last locus is called collectively miR-449. Members of miR-34 family show high sequence homology within the seed region important for their function (He et al, 2007; Song et al, 2013).

During studies on multiple tumor suppressor effects miR-34 was described as a p53 target (He et al, 2007, Chang et al, 2007, Song et al, 2014). It was shown that miR-34 mediates the function of p53 in the cell cycle arrest and promotes apoptosis in a wide range of tissues. Bona-fide targets of miR-34 are for example: the histone deacetylase SIRT1, cyclin-dependent kinases (CDK), cyclins and E2Fs. Therefore,

the inhibition of SIRT1 causes the accumulation of active p53. On the other hand, targeting cyclins and E2Fs leads to the inhibition of the E2F pathway and therefore to cell cycle arrest (Lize et al, 2011).

Nowadays, a growing amount of evidence confirms the role of miR-34 in the regulation of ciliogenesis. In mammals, miR-34 is known to be specifically enriched in organs containing motile cilia including lung, brain, testis and female reproductive tract (Song et al, 2014). Recently, it was shown that miR-34 together with miR-449 regulate basal bodies maturation and docking by the post-transcriptional repression of the centriolar protein Cp110 in mouse and frog multiciliated epithelium (Song et al, 2014).

More specifically, it was demonstrated that in zebrafish miR-34a is involved in neural development and miR-34c is required for spermatogenesis (Wang et al, 2013), while miR-34b is specifically enriched in kidney and olfactory placode MCCs, where it regulates kidney morphogenesis and olfactory organ development (Wang et al, 2013).

In zebrafish kidney one putative target of miR-34b involved in multiciliogenesis is *cmyb*. The interaction between miR-34 and *cmyb* regulates multiciliogenesis by controlling centriole amplification and basal body docking. Moreover, decreased levels of miR-34 lead to overexpression of centriole specific proteins, including Plk4 (Wang et al, 2013).

#### **3.2.1.1. B miR-449**

miR-449 is a member of the miR-34 family of miRNAs. Therefore, many similarities can be found between the members of this family including their high expression level in the organs equipped with cilia (Lize et al, 2011, Marcet et al, 2011).

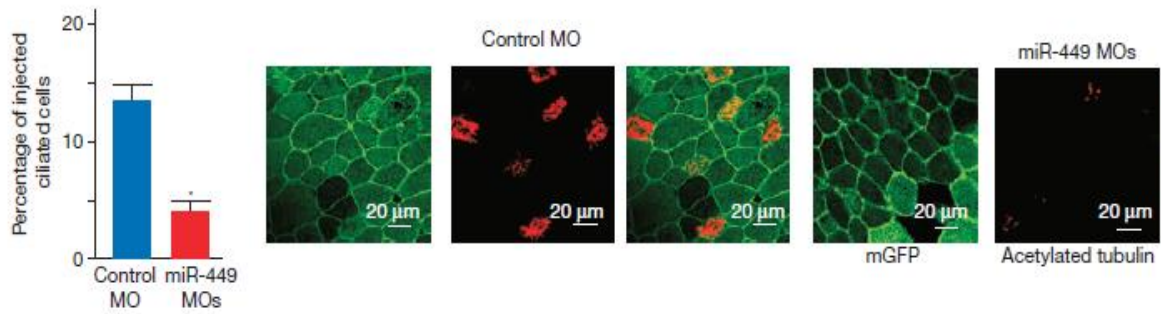
Originally the expression of miR-449 was described in the embryonic mouse brain (Redshaw et al, 2006, Lize et al, 2011). miR-449 is also expressed in human and murine testis (Lize et al, 2010), and is specifically increased in differentiated human and frog multiciliated cells (Marcet et al, 2011), which corroborates the involvement of miR-449 in mucociliary epithelium development (Fig.23).



The genomic location of miRNAs is likely to be related to their function. In *Xenopus*, the miR-449 cluster is located in a highly conserved region within the second intron of the CDC20B gene (Fig.23, 24). CDC20B is a homolog of CDC20, known to be an activator of the anaphase-promoting complex (APC) during mitosis (Fang et al, 1998). CDC20B was found to be expressed in frog mucociliary epithelium and up-regulated during MCCs differentiation (unpublished data). Therefore, a possible role of miR-449 and its host gene in specification of this tissue is expected.

Recently, the importance of miR-449 in human and frog multiciliated cells differentiation was demonstrated (Marcet et al, 2011). Therefore, it was shown that miR-449 binds to Notch and Delta1 and that their inhibition is a prerequisite to multiciliated cell terminal differentiation (Fig.23) (Marcet et al, 2011). Also, the involvement of miR-449 in cell fate determination was presented (Lize et al, 2010).

The regulation of miR-449 is unclear. One of the candidates to be the regulator of miR-449 is a transcription factor from the E2F family. Therefore, it was shown that miR-449, as a downstream effector of the S-phase promoting transcription factor E2F1, is down-regulated during apoptosis (Bou et al, 2011, Lize et al, 2011). However, miR-449 can also negatively regulate the E2F pathway through its targets: CDK2 and CDK6. This suggests the existence of a feedback loop between miR-449 and E2F transcription factors (Lize et al, 2010).



**Figure 23.** MiR-449 knockdown inhibits multiciliogenesis in *Xenopus laevis* embryonic skin. Percentage of injected cells that develop cilia in control vs miR-449 morphants. Cilia detection in tailbud stage embryos with an antibody against acetylated tubulin (cilia marker), injected cells were stained with anti-gfp antibody in green. In miR-449 morphants cells do not exhibit cilia staining (Marcet et al, 2011).

### 3.3 Regulatory proteins

The process of multiciliogenesis may be controlled by non-transcription factor-type regulatory proteins as well. The best-known protein regulators of multiciliogenesis are Multicilin and CCNO.

#### 3.3.1 Multicilin

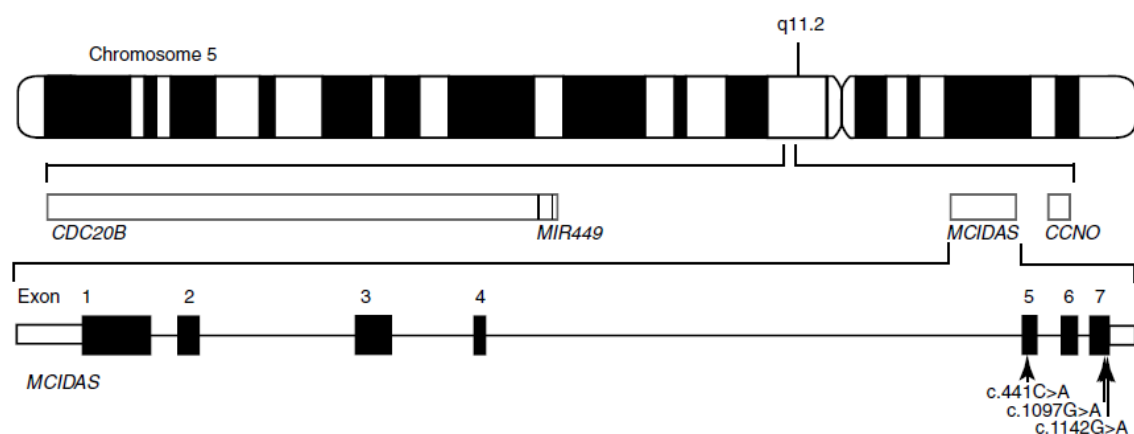
Multicilin (MCI) is a coiled-coil protein, which directly activates the expression of genes required for the generation of multiciliated cells. The multicilin gene is located within a genomic locus that is dedicated to multiciliated cell regulators. MCI is encoded by a gene called MCIDAS (Stubbs et al, 2012), flanked by CDC20B and CCNO (Fig.24). Recently, an involvement of a CCNO in the multiciliogenesis was characterized in mammals and amphibians (Wallmeier et al, 2013).

Multicilin plays a crucial role in the formation of multiple motile cilia. The MCI morpholino injection caused an early repression of MCCs differentiation by decreasing the number of centrioles in frog embryonic skin. Therefore, it was shown that MCI is necessary and sufficient to promote the differentiation of multiciliated cells in *Xenopus laevis* mucociliary epithelium (Fig.21) (Stubbs et al, 2012).

MCI is a scaffolding protein, which acts in multi-protein complex. MCI was demonstrated as regulatory protein sufficient to activate the expression of other MCC-specific genes mostly through binding to geminin, a protein known to inhibit the expression of embryonic genes. Stubbs and colleagues showed that the regulatory function of MCI relies on its ability to coordinately promote cell cycle exit and the deuterosome-mediated centriole assembly pathway (Stubbs et al, 2012).

Recently, it was suggested that E2F4 and/or E2F5 transcription factors might enhance the function of MCI during MCC differentiation (Ma et al, 2014).

It was also presented that MCI induced Myb expression in MCCs, therefore MCI is upstream of Myb transcription factor, however downstream of Notch (Fig.21) (Tanetal,2013).



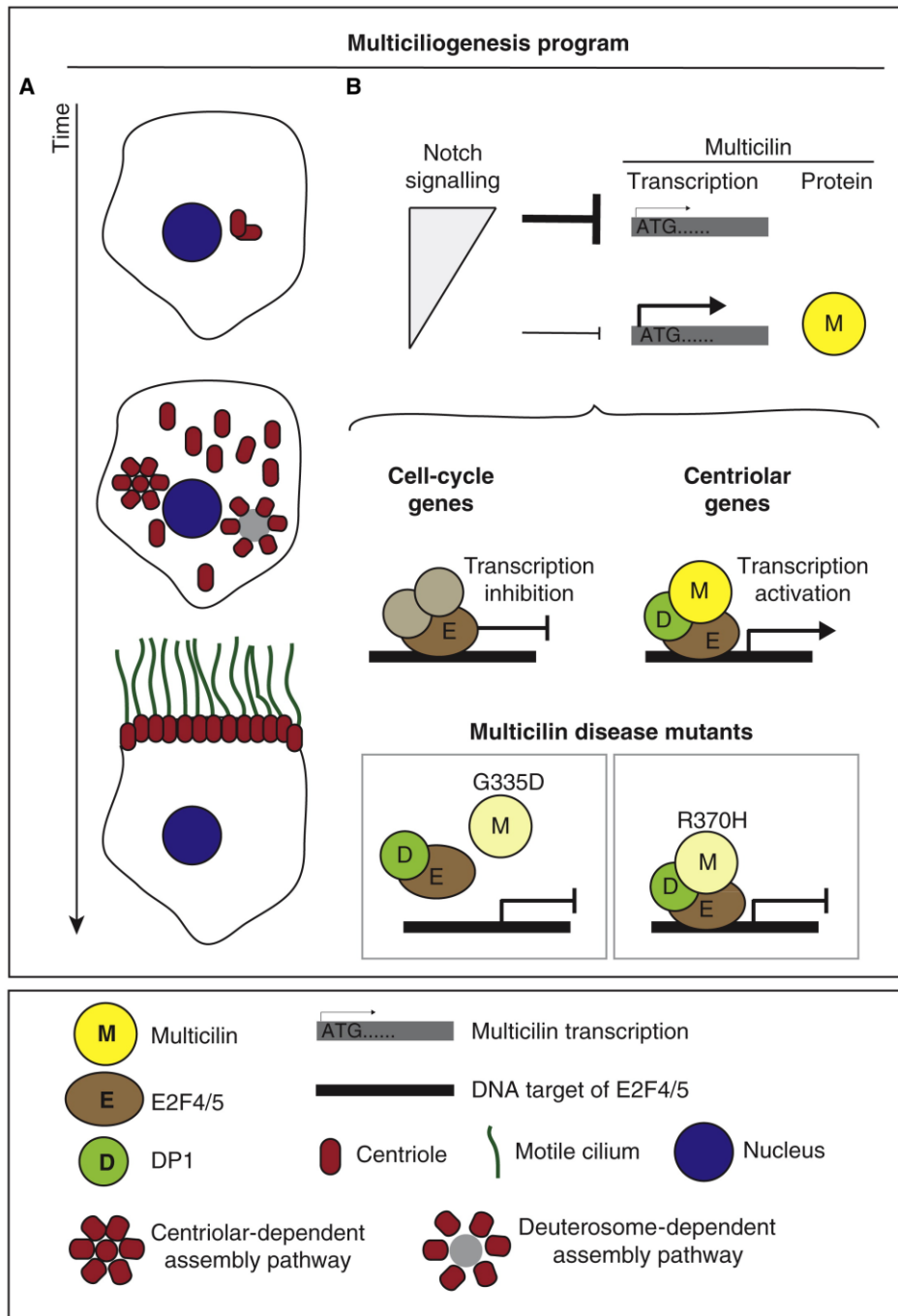
**Figure 24.** Schematic overview of chromosome 5, harboring the *CCNO*, *MCIDAS*, *CDC20B* and *miR-449* genes (Boon et al., 2014).

### 3.3.2. CCNO

The CCNO gene consists of three exons encoding a 1053 bp cDNA and a 350 amino-acid protein, called cyclin O. CCNO resides in the same genomic region where CDC20B is found. Moreover, the close neighbor of CCNO is MCIDAS, which encodes MCI (Fig.24) (Stubbs et al, 2012; Boon et al, 2014).

The expected function of CCNO was the regulation of the cell cycle and transcription. It was shown that in humans CCNO mutations cause a chronic airway disease characterized by progressive loss of respiratory function, while in *Xenopus laevis* embryonic skin the down-regulation of CCNO by morpholino injection caused a strong reduction of the mother centrioles (positively stained for CEP164), without affecting the cell fate. Moreover, the formation of MCCs was rescued in CCNO MO co-injected with a CCNO RNA (Wallmeier et al, 2013). It was proposed that CCNO acts downstream of MCI, since MCI expression failed to rescue the phenotype induced by CCNO MO injection.

It was concluded that CCNO acts on MCCs by promoting the mother centriole amplification and maturation via the deuterosome-dependent centriole assembly pathway (Wallmeier et al, 2013).

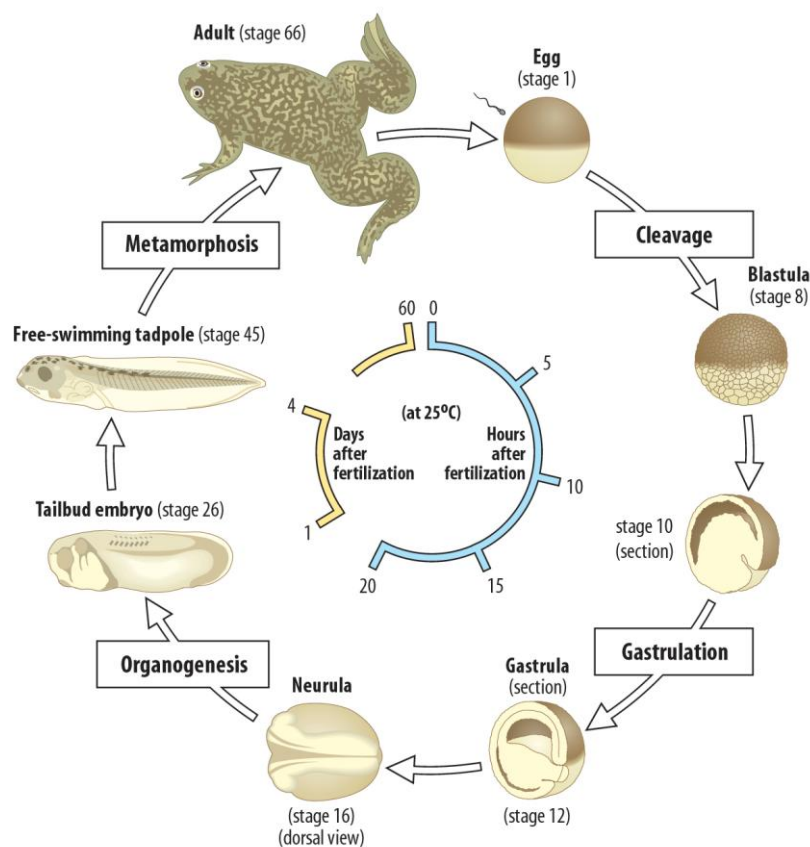


Current Biology

**Figure 24.** A) Schematic representation of an epithelial cell going through the process of multiciliogenesis. Centriole assembly occurs through both a centriole-dependent pathway and a deuterosome-dependent pathway. B) A decrease in Notch signaling results in transcriptional activation of multicilin. This favors the formation of the EDM complex (formed by multicilin, E2F4/5, and DP1), which activates the transcription of genes required for centriole assembly. At the same time, E2F4/5 and DP1 associate with regulators other than multicilin to inhibit the transcription of cell-cycle genes, thus ensuring cell-cycle exit. Mutations in multicilin impair transcriptional activation for different reasons: G335D cannot form the EDM complex, whereas R370H can form this complex but fails to activate transcription (Balestra et Gonczy, 2014).

#### 4. The embryonic epidermis of *Xenopus laevis* as a model system for studying the formation of mucociliary epithelia

*Xenopus laevis* is an excellent animal to study the vertebrate development. It is a robust animal, easy to rise in the laboratory. The production of eggs can be induced in females by simple hormone injection (Gonadotropin chorionique), and each spawn contains up to hundreds of eggs, which develop quite fast. The fertilization takes place externally (Fig.25), while the eggs and the embryos are of relatively large size ( $> 1\text{mm}$ ), which allows an easy observation and manipulation (Sive et al, 2000).



**Figure 25.** Basic steps of *Xenopus laevis* development.

The skin of amphibian embryos was among the first observed example of tissue generating a cilia-driven fluid flow. Because of its accessibility and amenability to live imaging and molecular manipulations the frog larval skin became a very attractive model to study.

Since *Xenopus laevis* genome has been sequenced many molecular and genetic tools can be applied. For example, the injection of morpholino into the skin for loss-of-function assays. Also, skin transplantation and the standard methods including immunohistochemistry, colorimetric and fluorescence *in situ* hybridization, confocal and transmission microscopy can be applied. Currently, the frog embryonic skin is commonly used to study the ciliated cell differentiation, radial intercalation, cilia polarity and ciliary beating (Werner et Mitchell, 2013), but also the cell-cell interaction within mucociliary epithelium (Dubaisi et Papalopulu, 2010).

However, like all model organisms, also *Xenopus laevis* has some disadvantages. Among these, its long generation time (1-2 years) and tetraploidy (Sive et al. 2000).

#### **4.1. The *Xenopus* mucociliary epithelium (MCE).**

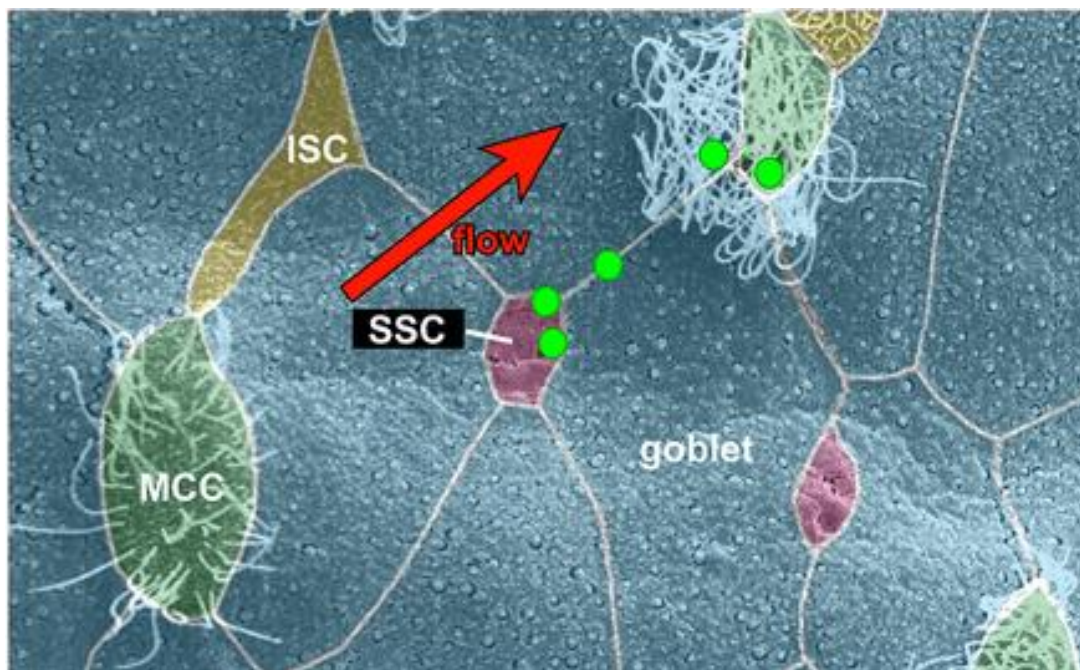
Epithelia along with muscle tissue, nervous tissue and connective tissue are the fourth basic types of animal tissue. The main function of the epithelial tissue is to protect the underlying tissues from harmful physical and biological factors. For example, the mucosal epithelia of the gut, the secretory epithelia of the kidney and the mucociliary epithelia of the lung play the same basic role, although their predominant functions are different. For example, human mucociliary epithelium is also essential for homeostasis of many organs, while the MCE of frogs is involved in respiration through the skin (Hayes et al, 2008; Werner et Mitchell, 2012).

Epithelial tissues can be classified by using two criteria. The morphology of their cells and the number of layers they are composed of. Therefore, we can distinguish the squamous, cuboidal, columnar, simple, stratified and transitional epithelium (van Lommel, 2002).

The frog embryonic epidermis shows histological and cytological similarities to the mucociliary epithelium, which covers the mammalian upper respiratory tract. The

resemblance is based on the presence of mucus-secreting and multiciliated cells (Billett and Gould, 1971; Dubaissi and Papalopulu, 2010). The mucociliary epithelium of *Xenopus laevis* embryos is an excellent model system for studying the molecular mechanisms of ciliogenesis as well as to explore the physiology and pathophysiology of human airways (Deblandre et al, 1999; Hayes et al, 2007).

The mature frog embryonic skin consists of two layers of ectodermal tissue (outer and inner), morphologically very different. The outer layer (also called superficial layer) contains four cell types: mucus-secreting (goblet) cells, multiciliated cells (MCCs), ionocytes (ISC) and small secretory cells (SSC) (Fig.26). The inner layer, also called sensorial layer is composed of basal cells. However, at the early stages of the ectoderm development the inner layer hosts the progenitors of almost all epidermal cell types, except for the goblet cells precursors (Walentek et al, 2014).



**Figure 26.** Model of the cell types presence in the mucociliary epithelium of the *Xenopus laevis* tadpole skin (Walentek et al, 2014)



#### **4.1.1 Structure and function**

##### **4.1.1 A Mucus-secreting cells**

Mucus secreting or goblet cells make up the majority of the mucociliary epithelium. Goblet cells develop in the outer layer, where after differentiation they become functional (Dubaisi et Papalopulu, 2010).

The goblet cells in the epidermis of amphibian embryos have been found in 1971 by Billett and Gould (Billett and Gould, 1971). The main function of these cells is the production of mucus, with a likely function of antibacterial barrier. However the chemical composition of this mucus is not well known. Also, no specific mucins have been detectable in the goblet cells secretory vesicles (Dubaisi et Papalopulu, 2010). However, it was shown that mucus contains a lectin called Xeel, which is involved in the recognition of pathogen-associated glycans (Nagata et al, 2003). In general, lectins mediate intracellular protein trafficking, innate immunity, cell adhesion and communication (Nagata et al, 2003).

Not much is known about how the secretory activity of the mucus-secreting cells is controlled (Cibois et al, 2014; Dubaisi et Papalopulu, 2010).

##### **4.1.1 B Multiciliated cells**

Another cell type in the *Xenopus laevis* mucociliary epithelium are Multiciliated Cells (MCCs), which originate from their progenitors in the inner epidermal layer at the early stages of the embryo development (late gastrula ~st.13). MCCs show a regularly spaced pattern, where two multiciliated cells never develop next to one another. Each MCC of *Xenopus* MCE carries 100-200 cilia at its apical surface (Stubbs et al, 2006; Werner et Mitchell, 2011; Cibois et al, 2014).

Interestingly, the MCC progenitors can be distinguished from progenitors of other cell types by simple  $\alpha$ -tubulin immunostaining.  $\alpha$ -tubulin is a major component of microtubules. On the other hand, mature MCCs can be distinguished from the other cells by immunostaining with acetylated-tubulin, a modified form of tubulin.

Interestingly, *Xenopus* MCCs exist in the mucociliary epithelium only for a short time period. In the late stages of development (st. 43), MCCs start to transdifferentiate into goblet cells and produce secretory vesicles (Kessel et al, 1974; Cibois et al, 2014). The mechanisms controlling this transition are completely unknown, but it is interesting to note that massive conversion of ciliated cells into goblet cells (mucous metaplasia) is a feature of some human respiratory diseases (Cibois et al, 2014; Curran and Cohn, 2010).

#### **4.1.1. C Ionocytes**

Ionocytes (ISC) are small, proton-secreting cells with a triangular shape present in *Xenopus* larval skin. Their presence and function were revealed four years ago by Dubaissi and Papalopulu (Dubaissi et Papalopulu, 2010). It was shown that ionocytes are distributed across the *Xenopus* MCE in an irregular pattern. Moreover, it has been described that ionocytes are closely associated with the MCCs. Most of the time direct contact with a single multiciliated cell is made by one or two ionocytes (Dubaissi et Papalopulu, 2010).

The regulation of ionic balance provided by ionocytes is required for the proper development of *Xenopus laevis* embryos. Accordingly, ionocytes strongly express ion channels and transporter such as: vacuolar proton pumps (v-ATPase), pendrin (slc26a4) and monocarboxylate transporter 4 (mct4). Also, the presence of ca12 transmembrane enzyme has been reported in the ISCs. Ca12 catalyzes the reversible hydration of the carbon-dioxide-releasing protons, while V-ATPase acidifies the local environment and intracellular vesicles. In some studies, it has been shown that the acidification by V-ATPase is necessary for the activation of signaling pathways, including Wnt, Notch and PCP (Vaccari et al, 2010).

The above-mentioned ionic channels, transporters and enzymes are used by ionocytes to control the osmotic balance and the pH of the mucociliary epithelium (Dubaissi et Papalopulu, 2010).

A loss-of-function assay showed that depletion of ionocytes results in the impairment of composition and function of the mucociliary epithelium. Therefore, ionocytes are involved in the proper development of the other cell types by controlling

the osmotic balance of the epithelial tissues. Moreover, it was suggested that the ionocytes participate in the regulation of the cilia growth and ciliary beating, and also in the secretion of mucus by goblet cells (Dubaisi et Papalopulu, 2010).

So far, no evidence of ionocytes existence in the human airway has been reported. However, frog ionocytes seem to be analogous to the ionocytes of transporting epithelia such as the mammalian kidney (Dubaisi et Papalopulu, 2010; Quigley et al, 2010).

#### **4.1.1.D Small secretory cells**

The small secretory cells (SSCs) are a recently discovered cell type of *Xenopus laevis* mucociliary epithelium. SSCs are scattered throughout the epidermis in a pattern similar to the ionocytes. However, they differentiate much later than the ionocytes, specifically at the early tadpole stages (Walentek et al, 2014).

The characteristic feature of the SSCs is the synthesis of serotonin within vesicle-like structures, which are then secreted and transported towards the MCCs. It was shown that blocking the synthesis of serotonin caused disruption of the ciliary beating and apical expansion of SSCs into the outer epidermal layer in MCE, while the SSC differentiation was not changed upon serotonin inhibition (Walentek et al, 2014; Dubaisi et al, 2014). Therefore, it was concluded that serotonin controls the production and secretion of the mucus, as well as the regulation of velocity of cilia-driven flow through its receptors, such as Htr3 (Walentek et al, 2014). It was also suggested that serotonin can regulate the molecular composition of secreted mucus (Walentek et al, 2014).

An additional function of SSCs is the protection of embryos from bacterial infection, since the SSCs secretory vesicles contain, besides serotonin, a highly glycosylated material constituted of several potential antimicrobial substances (Dubaisi et al, 2014). Therefore, three modalities of SSC dependent protection were proposed. First, production of the mucus layer composed of the glycoprotein otogelins, which are able to trap bacteria. Second, the secretion of anti-infective molecules such as antibacterial peptide (AMPs) and glycolipoproteins such as

vitellogenin and apolipoprotein B. Third, an indirect effect of SSCs on the neighboring cells (Walentek et al, 2014).

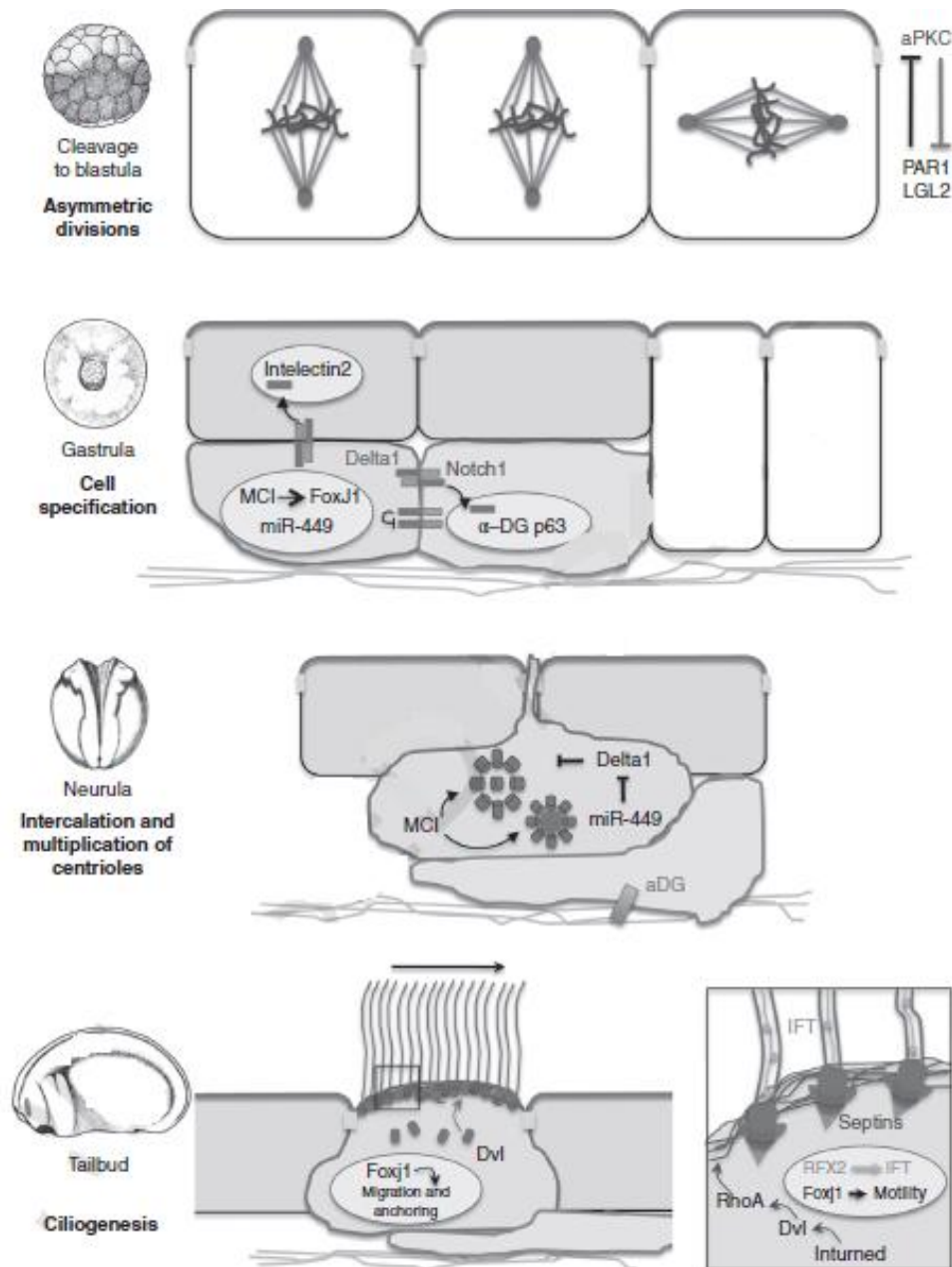
Since SSCs are newly discovered cell type, further investigations on their function, but also on their development are required.

#### **4.2. Multistep formation**

The process of *Xenopus* epidermis formation can be divided into 4 steps: layer segregation, cell fate specification, cell intercalation from the inner to outer layer and cell differentiation (Fig.27).

#### **4.2. A Layer segregation**

This step of mucociliary epithelium development occurs during cleavage and blastula stages. The formation of two distinct ectodermal cell layers results from asymmetric cell divisions. In the non-neural ectoderm these two layers are called inner or sensorial, and outer or superficial, respectively. The outer layer consists of large columnar cells, which are tightly adherent to each other, while the inner layer is built of smaller and loosely adherent cells (Deblandre et al, 1999).



**Figure 27.** The four steps of MCC biogenesis. Step 1 from cleavage to blastula stages, divisions along the apical-basal axis generate distinct daughter cells through asymmetric segregation of maternal determinants. Step 2 during gastrulation, MCC progenitors are born in the inner epidermal layer. They express Delta1, which activates the Notch1 receptor both in neighboring inner cells (express  $\alpha$ -DG and P63) and in outer cells (express the goblet cells marker Intelectin). MCC progenitors express FoxJ1, MCI and the microRNA miR-449. Step 3. During neurulation, the MCC progenitors undergo radial intercalation and centriole multiplication required to produce dozens of BBs necessary for ciliary growth. Step 4. At tailbud stages, ciliogenesis proceeds through the migration and anchoring of BBs at the apical cortex of the cell. This process is under the control of FoxJ1 and PCP components, such as Dvl (Cibois et al, 2014).

The superficial cells divide along the apical-basal axis leading to the formation of outer polarized cells, and inner non-polarized cells (Chalmers et al, 2003; Cibois et al, 2014). Accordingly, polarized cells from outer layer, which form a true epithelium with tight junctions, express atypical protein kinase C (aPKC), while an antagonist of aPKC called PAR1 is inherited by inner cells (Chalmers et al, 2003; Cibois et al, 2014).

Based on the results from functional assays it has been suggested that PAR1 is necessary and sufficient for the adoption of MCC fate, whereas aPKC has the opposite effect (Fig.26) (Ossipova et al, 2007).

## **4.2. B Cell fate specification**

Cell fate determination occurs during gastrulation and identifies the progenitors of MCCs, ISC and SSCs. Cell fate determination is linked to the Notch signaling pathway and lateral inhibition (Bray, 2006).

The Notch signaling pathway is highly conserved in the animal kingdom, where it controls the cell fate decisions in numerous contexts. The Notch signaling plays a pivotal role in development. Its misregulation or loss of function underline multiple human disorders from developmental diseases to cancer (Kopan et al, 2009).

The activation of Notch pathway occurs through binding of the transmembrane Notch receptor to one of its ligands, Delta or Serrate. This interaction results in releasing of the Notch intracellular domain, which translocates to the nucleus and activates the transcription of target genes. Interestingly, several lines of evidence show that the activation of Notch signaling yields negative responses on the cells differentiation program (Sprinzak et al, 2010).

The Notch receptor together with its ligands mediates a mechanism called lateral inhibition (Hayes et al, 1999). Lateral inhibition restricts the number of cells that choose the same fate. This mechanism is based on the activation of Notch receptor by the neighboring cells, which express the Delta ligand. Therefore, the progression of cells into the differentiated state is blocked (Hayes et al, 1999, Deblandre et al, 1999, Stubbs et al, 2006).

Moreover, in *Xenopus* epidermis, the Notch pathway activation is also important for the specification of inner epidermal cells. Among the genes activated by Notch in basal cells are  $\alpha$ -Dystroglycan ( $\alpha$ DG) and p63. The first one encodes a transmembrane protein, which plays a role in the skin morphogenesis by controlling the basement membrane formation and CCP intercalation (Sirour et al, 2011). The second gene encodes a transcription factor called p63, which is identified as target of Notch signaling in basal cells and required for epidermal development (Sirour et al, 2011). For example, in vertebrate stratified epithelia p63 controls the stem cell potential of basal cells (Rock et al, 2009).

It is expected that additional signaling pathways are involved in the cell fate choices. One of the candidates of cell fate modulator is the BMP pathway activated in the non-neural ectoderm after cell fate specification (Schohl and Fagotto, 2002).

The central role of Notch signaling in the cell specification allowed to identify key regulators of MCC, ionocyte and SSC cell fate. Currently, it is known that MCCs are under the control of transcription factors such as: Foxj1, Rfx, Myb and E2F4/5 (see Chapter 3). Moreover, our knowledge of multiciliated cell fate regulators is expanding rapidly (Stubbs et al, 2008; Choksi et al, 2014; Tan et al, 2013; Ma et al, 2014). The specification of ionocytes is controlled by the FOX family of transcription factors, specifically by the forkhead box protein I1e (foxi1e) (Dubaisi et Papalopulu, 2010). The specification of SSCs is also controlled by a forkhead family member called foxa1 (Dubaisi et al, 2014).

## **4.2. C Cell radial intercalation**

After cell specification the precursors of the MCCs, SSCs and ionocytes leave the inner layer to intercalate into the outer layer. This process is called cell radial intercalation and was revealed in *Xenopus* embryonic skin in 1992, when the progenitors of ciliated cells originated from the inner layer were labeled (at neurula stage) (Drysdale et Elinson, 1992). At that time it was shown that almost half of the intercalating cells correspond to ciliated cells precursors, while another half correspond to the ionocyte progenitors (Deblandre et al, 1999, Drysdale et Elinson, 1992).

Nowadays, it is known that the intercalation of CCP from the inner into the outer layer occurs in two steps (Stubbs et al, 2006; Chung et al, 2014). The first step starts when the intercalating cells emit protrusions (filopodia) to probe the gaps between outer layer cells, although, the tight junctions among outer layer cells remain intact. The second step causes the cells intercalation into vertices of three or four cells from the outer layer, thus intercalating cells reached the surface of epidermis (Stubbs et al, 2006).

Interestingly, CCPs intercalate individually, whereas INCs can emerge to the surface in small groups, of two or three cells. These differences can be explained by the fact that INCs can reside next to each other, but also that they are smaller than CCPs. It is also known that the CCPs intercalate before INCs (Stubbs et al, 2006).

Concomitantly with intercalation CCPs have to establish their regularly spaced pattern. Many lines of evidence suggest the presence of two mechanisms responsible for spaced pattern generation. The first mechanism is based on the lateral inhibition through Notch signaling pathway (Deblandre et al, 1999), while the second one is explained by the physical limitations to cell intercalation *per se* (Stubbs et al, 2006). This is due to the fact that CCs are only able to intercalate at the junction point (vertex) of at least three or four outer layer cells. These two mechanisms are likely to coexist in the *Xenopus* epidermis (Stubbs et al, 2006).

$\alpha$ -DG is one of very few known regulator of the intercalation, but the mechanism of  $\alpha$ -DG action remains unclear (Sirour et al, 2011). Another regulator of intercalation is Rab11, a member of the small GTPases family, involved in the vesicular trafficking. It was demonstrated that the MCC precursors deficient for Rab11 are trapped in the inner layer (Kim et al, 2012).

## **4.2. D Cell differentiation**

Cell differentiation takes place within the outer epidermal layer. Our current understanding of this step of mucociliary epithelium formation is incomplete. For example, the regulators of goblet cell activity and the chemical composition of the mucus as well as the precise function of ionocytes remain poorly described (Cibois et al, 2014). The focus has been put on differentiation of the MCCs, since these cells



are known to be related to human diseases. The process of MCCs differentiation through multiciliogenesis is described in the chapter 2.

## **5. Aim of the work: Identification and functional analysis of new miR-449 targets required for development of the *Xenopus* mucociliary epithelium**

The activity of the Kodjabachian laboratory at IBDM is aimed at better understanding the cellular and molecular mechanisms that control the organogenesis of the *Xenopus laevis* embryonic epidermal mucociliary epithelium.

Previous work from the laboratory has showed that the activity of the miR-449 microRNA is necessary for the proper formation of mucociliary epithelia in *Xenopus* and human, and in particular for the correct differentiation of the multiciliated cells. (Marcet et al., 2011). Our research is now focusing on the identification and functional characterization of miR-449 targets.

A first part of my doctoral work dealt with the identification and characterization of miR-449 targets involved in the formation of the so-called actin cap. A specific accumulation of actin is required for the anchoring of basal bodies underneath the apical membrane of multiciliated cells. This led me to focus my attention to two modulators of the small GTPase signaling, R-RAS and Arghdib. The results of this work are partially resumed in a manuscript of which I am joint first author and which is currently under revision in the journal 'Nature Communications', and partially presented as unpublished data in the Results and also in Discussion section.

During the last year of my thesis work, I also started the characterization of another putative target of miR-449, the secreted factor SCF, which appears to play a role in the process of MCC intercalation into the epidermal outer layer. These still unpublished data are resumed in the Results section.

## Results

## II. Results

### 6. Submitted data and additional information on R-Ras

#### R-Ras like family member - R-Ras

One of the putative targets of miR-449 is a small GTPase R-RAS. R-Ras involvement in the process of cytoskeleton reorganization has been already mentioned in the literature (for example Pan et al, 2007). This prompted us to study a possible role of R-Ras in the formation of the apical dense meshwork of actin required for basal body anchoring in MCCs.

The Ras proteins act as molecular switches, which cycle between guanine diphosphate (GDP) -bound inactive form and guanine triphosphate (GTP) -bound active form. GDP-bound Ras proteins become activated by interaction with members of structurally diverse classes of proteins termed guanine-nucleotide exchange factors (GEFs). The activity of GEFs causes the release of GDP by an allosteric change in two crucial regions of the GTPase termed, Switch1 and Switch2. GDP is then rapidly replaced by the more abundant GTP (Ehrhardt et al, 2002).

The Switch1 region is a part of so-called effector loop, where different proteins bind to Ras in its GTP-bound configuration. The hydrolysis of GTP to GDP form is under the control of GTPase activating proteins (GAPs), which bind to the GTP-bound Ras proteins at the Switch 2 region. GAPs act as negative regulators of Ras proteins by enhancing their low intrinsic GTPase activity and keeping them in an inactive GDP-bound state (Ehrhardt et al, 2002).

The Ras superfamily of small GTPases is divided into several subfamilies. One of the known subfamily is the classical Ras family, consisting of the Ras proteins (K-Ras, N-Ras, H-Ras), Rap proteins (Rap1a, Rab1b, Rap2a, Rap2b) R-Ras like proteins (R-Ras, R-Ras2 =TC21, M-Ras), Ra1 proteins (Ra1A, Ra1B) and Rheb protein (Bos, 1997).

The classical Ras family plays a pivotal role in cell differentiation and growth, however less is known about the functions of the other Ras subfamilies. Recently, scientific focus was shifted towards small, poorly known subfamily of R-Ras like proteins, which consists of R-Ras, TC21 and M-Ras.

One characteristic feature of R-Ras like subfamily is the ability to activate the extracellular regulated kinase/mitogen-activated protein kinase cascade (MAPK)

(Ohba et al, 2000). Therefore, all the members of this subfamily possess common GEFs, including the RasGEF exchange factor (Jeong et al, 2005). Additionally, they also share common GAPs such as: p120RasGAP, neurofibromin and effectors like: Raf, PI3-kinase, RalGDS (Jeong et al, 2005).

Another characteristic feature of R-Ras like proteins subfamily is the presence at their carboxy end of the so-called CaaX motif, where a cysteine is followed by two aliphatic residues, while X represents serine or methionine (Reuther and Der, 2000). The CaaX motif is characterized as a signal sequence, which promotes the association of Ras proteins with the plasma membrane. Additionally, the carboxyl-terminal signal undergoes post-translational modifications such as farnesylation, AAX proteolysis and carboxymethylation (Reuther and Der, 2000).

Interestingly, it has been indicated that the M-Ras carboxyl terminus differs from those of TC21 and R-Ras. The divergent carboxy-terminal sequences of R-Ras like proteins might govern Ras member-specific associations with different areas of the plasma membrane (Roy et al, 1999). Different trafficking of Ras proteins to the plasma membrane may explain functional distinctions among Ras proteins (Reuther and Der, 2000).

Moreover, R-Ras has a 26 amino acid extension at its N-terminus and exhibits 70% similarity to TC21. The R-Ras protein is also highly homologous to classical Ras with 55% of identity (Jeong et al, 2005).

To sum up, the R-Ras like subfamily consist a distinct family of GTPases. Its members show common, but also very specific structural features. Moreover, a homology can be found between the members of R-Ras like and classical Ras GTPases family. Therefore, they could be activated by the same extracellular stimuli and might interact with the same effectors, which suggests that they can also activate the same signaling pathways (Roy et al, 1999).

Moreover, the members of R-Ras like subfamily play different functions. Therefore, R-Ras protein plays a unique role in the integrin-mediated cell adhesion (Zhang et al, 1996). Although the mechanism of integrins activation is not clear, one of the possible explanation may be the existence of the R-Ras specific signal sequences involved in the association, such as the effector loop, the prenylation site and the proline-rich sequence (Zhang et al, 1996).

Another evidence, which supports the presence of a link between R-Ras and integrins has been found in the context of Notch signaling pathway. It was shown that

mammalian Notch activates integrins, but does not affect their expression. It was demonstrated that the  $\gamma$ -secretase-dependent cleavage and activation of Notch activates not only integrins, but also R-Ras (Hodkinson et al, 2007). Moreover, studies on Ras GTPases indicated that targeting of R-Ras to focal adhesions is critical for its ability to regulate integrins activation (Hodkinson et al, 2007).

Several lines of evidence pointed out the existence of a possible link between R-Ras and filamentous actin (Pan et al, 2007, Jeong et al, 2005). For example, it was indicated that R-Ras can interact with actin cross-linkers such as Filamin A. In turn, Filamin A plays a role for instance in epithelial cell shape control, actin cytoskeleton remodeling and primary cilia formation (Gawecka et al, 2010; Griffiths et al, 2011; Adams et al, 2012). Moreover, it was described, that Filamin A binds to F-actin. Recently, a connection between filamin A and integrins was also found (Zhou et al, 2009). Therefore, interaction between Filamin A and R-Ras could be an explanation for R-Ras involvement in the F-actin cytoskeleton reorganization.

R-Ras as small GTPase can also interact with and modulate the activity of other GTPases, for example RhoA. One of many roles of RhoA is the regulation of cytoskeleton and actin reorganization. For example, Pan and colleagues showed that the formation of apical actin web-like structure in the primary cultures of mouse airway epithelial cells depends on Rho-GTPase activity (Pan et al, 2007). Therefore, it is expected that as RhoA, R-Ras is also potentially involved in the regulation of actin cytoskeleton.

## **\* Manuscript**

### **miR-449 controls apical actin network formation during multiciliogenesis through small GTPase signaling**

Benoît Chevalier<sup>1, 2, \*</sup>, Anna Adamiok<sup>3, \*</sup>, Olivier Mercey<sup>1, 2</sup>, Laure-Emmanuelle Zaragosi<sup>1, 2</sup>,

Andrea Pasini<sup>3</sup>, Laurent Kodjabachian<sup>3</sup>, Pascal Barbry<sup>1, 2, †, §</sup>, Brice Marcet<sup>1, 2, †, §</sup>

<sup>1</sup> CNRS-IPMC, UMR-7275, Sophia-Antipolis, France.

<sup>2</sup> University of Nice-Sophia-Antipolis (UNS), Sophia-Antipolis, France.

<sup>3</sup> Aix-Marseille Université, CNRS, UMR7288, Institut de Biologie du Développement de Marseille (IBDM), Marseille, France.

\* These authors contributed equally

§ Co-senior authors

† Correspondence should be addressed to Brice Marcet and Pascal Barbry:

[marcet@ipmc.cnrs.fr](mailto:marcet@ipmc.cnrs.fr), [barbry@ipmc.cnrs.fr](mailto:barbry@ipmc.cnrs.fr); IPMC-CNRS/UNS, UMR-7275, 660 Route

des Lucioles, 06560 Sophia-Antipolis, Valbonne, France.

Phone : 00-33-(0)4-93-95-77-93

Fax : 00-33-(0)4-93-95-77-94

Number of words (max 5000) (except Materials & Methods 3000 words max, References 70 and legends :350 words/fig) 10 figures max :

## Abstract

Multiciliated cells (MCCs), found throughout the metazoan kingdom, contribute to multiple biological processes. Recently, we demonstrated that microRNAs of the miR-449 family control vertebrate MCCs differentiation by repressing the Notch pathway. Here, we report that the apical actin cytoskeleton reorganization, a prerequisite for basal bodies anchoring and cilia elongation, is also controlled by miR-449. Using human airway primary cultures and *Xenopus* embryonic epidermis we show that miR-449 silencing inhibits RhoA activity and apical actin web formation in MCCs. We identify transcripts coding for the small GTPase R-Ras as miR-449 validated targets. Apical actin reorganization and multiciliogenesis were impaired when the *RRAS* mRNA was protected from miR-449 binding. Multiciliogenesis was rescued when the translation of protected *RRAS* transcripts was prevented. Altogether, our data demonstrate that miR-449 acts at several distinct steps of multiciliogenesis in vertebrates, and identify R-Ras as a new player in apical actin reorganization.



## Introduction

Multiciliated cells (MCCs), characterized by the presence of multiple motile cilia at their apical surface, have been described in many vertebrates<sup>1-3</sup>. Coordinated ciliary beating allows efficient fluid movement and is required for physiological processes such as elimination of mucus from the respiratory tract, circulation of the cerebrospinal fluid, or migration of the embryo in the fallopian tubes<sup>1</sup>. The physiological importance of MCCs is highlighted by the ever growing number of human disorders associated with defects of the motile cilia<sup>1, 2, 4, 5</sup>. Multiciliogenesis, which occurs during normal development and during regeneration of damaged tissues, can be studied in experimental setups, such as primary cultures of human airway epithelium<sup>6</sup> and *Xenopus* embryonic epidermis<sup>7</sup>. Several stereotypical steps are observed: (i) exit from the cell cycle of MCC precursors, (ii) massive postmitotic multiplication of centrioles (centriologenes), (iii) reorganization of the apical actin cytoskeleton into a dense cortical meshwork of actin, (iv) migration of the newly synthesized centrioles toward the apical pole of the cell, where they anchor to the actin meshwork, and mature into ciliary organizing centers known as basal bodies (v) elongation of one cilium from each basal body<sup>8-15</sup>. Recently, key regulators of multiciliogenesis have been identified, including the FOXJ1, RFX (regulatory factor X) and MYB transcription factors as well as the geminin-related nuclear protein multicilin<sup>16-23</sup>. The reorganization of the apical actin cytoskeleton is an early event of multiciliogenesis which involves an activation of the small GTPase RhoA in a FOXJ1-dependent manner<sup>15, 17, 18, 24</sup>. Recent work has highlighted the importance of the interaction between Rho GTPase signaling and the planar cell polarity pathway to control the assembly of apical actin filaments, as well as the docking and the planar polarization of basal bodies<sup>25, 26</sup>. Proteins of the ezrin-radixin-moesin (ERM) family, which link actin to the cell membrane, require RhoA-dependent phosphorylation to interact

with cortical actin<sup>27-31</sup>. Both ezrin and its interacting protein EBP50 are specifically localized at the apical membrane of airway MCCs, through a FOXJ1-dependent mechanism<sup>15, 17, 32, 33</sup>. The activity of Rho GTPases and their action on actin cytoskeletal dynamics can be modulated by interactions with other GTPases, such as the Ras family member R-Ras<sup>34-39</sup> or with Rho guanine nucleotide exchange factors, Rho GTPase-activating proteins and Rho GDP-dissociation inhibitors<sup>40, 41</sup>.

Because the elaboration of functional motile cilia is exquisitely sensitive to the reorganization of the actin cytoskeleton, we reasoned that miR-449, a family of three microRNAs (miR-449a, miR-449b and miR-449c) that we recently established as a conserved regulator of multiciliogenesis<sup>9</sup>, may control one or more molecules associated with actin dynamics. MicroRNAs (miRNAs or miRs) are a class of small single-stranded and non-coding regulatory RNAs that control many biological processes by repressing gene expression at a post-transcriptional level<sup>42, 43</sup>. Abnormal miRNA activity has been associated with several human pathologies including airway diseases<sup>44</sup>. We previously demonstrated that miR-449 promotes centriole multiplication and multiciliogenesis, through the direct repression of Notch1 and its ligand Delta-like 1<sup>9</sup>. However, miRNAs can target multiple transcripts and thereby modulate several pathways, including those interfering with Rho GTPase signaling<sup>45, 46</sup>. We now show that miR-449 activity is also required for the establishment of the apical actin cytoskeleton, through the repression of the small GTPase R-Ras. MiR-449 can thus be considered as a global control system of multiciliogenesis that governs several distinct steps of this complex physiological process.

## Results & Discussion

### Apical actin cytoskeleton reorganization during multiciliogenesis

Apical actin cytoskeleton formation was examined at several time-points during differentiation of primary cultures of human airway epithelial cells (HAECs) grown at an air-liquid interface (ALI) and in *Xenopus* embryonic epidermis <sup>9</sup>. Formation of the apical meshwork of filamentous actin (F-actin) was monitored directly by staining with fluorescent phalloidin and indirectly by immunostaining with anti-ezrin or anti-phospho-ERM antibodies. In human and *Xenopus*, the acetylated-tubulin positive MCCs displayed a strong enrichment of apical F-actin, which was associated with submembranous *puncta* of ezrin (human: Fig. 1a; *Xenopus*: Fig. 1d). In HAECs, basal bodies, positive for  $\gamma$ -tubulin labeling, were embedded within an apical F-actin and ezrin meshwork (Fig. 1b). In HAECs, this meshwork was already detected several days before basal bodies docking (data not show). Reorganization of actin filaments involves cofilin, a ubiquitous G-actin binding factor <sup>47</sup>. Only unphosphorylated cofilin can bind actin to promote its polymerization/depolymerization and phosphorylation-dependent cofilin inactivation is essential for cytoskeletal reorganization <sup>47</sup>. In human airway epithelium, the level of phosphorylated cofilin-1 and ezrin increased when multiciliogenesis proceeded (Fig. 1c). In parallel, we noticed an increased expression of the ERM binding protein EBP50 (Fig. 1c), an adapter protein localized at the apical region of MCCs and required for the maintenance of active ERM proteins at the apical membranes of polarized epithelia <sup>15, 33</sup>. These observations are consistent with the formation of an apical actin web in both models of MCCs.

### **miR-449 controls apical actin cytoskeleton reorganization in vertebrate MCCs.**

After having shown that miR-449 silencing prevented centriole multiplication and ciliogenesis in human and frog MCCs <sup>9</sup>, we wondered whether they could also interfere with the formation of the apical actin network. To invalidate miR-449 activity, we transfected HAECs with a cholesterol-conjugated antagomiR directed against miR-449a/b (AntagomiR-449a/b) and assessed MCCs differentiation. We also knocked down miR-449 in *Xenopus* MCCs by injecting a cocktail of morpholino-modified antisense oligonucleotides against miR-449a/b/c into prospective epidermis at the 8-cell stage. Such a miR-449 silencing does not affect cell viability in HAECs and frog embryos <sup>9</sup>. MiR-449 knockdown suppressed multiciliogenesis and apical actin web formation in both HAECs and *Xenopus* embryonic epidermis (Fig. 2, a-d). In HAECs, miR-449 silencing affected both multiciliogenesis and the apical actin meshwork, as revealed by a decrease of  $51 \pm 3.5\%$  in the number of MCCs and of  $33 \pm 7\%$  in the number of ezrin-positive cells (Fig. 2, a-b). In *Xenopus* epidermal MCCs injected with miR-449 morpholinos at stage 20, F-actin and motile cilia staining were severely reduced: the number of MCCs lowered to  $18 \pm 13\%$ , and the number of apical actin cap-positive cells lowered to  $9 \pm 8\%$  (Fig. 2, c-d). Thus, miR-449 interferes with MCC apical actin meshwork formation in both models. The impact of miR-449 on the actin cytoskeleton was further investigated by looking at stress fibers, which are thick and relatively stable actin filaments present in non-motile cells <sup>48, 49</sup>. Since proliferating A549 epithelial cells contain stress fibers, but are devoid of miR-449, we were able to test the impact of miR-449 over-expression on the architecture of stress fibers in this model. MiR-449 over-expression led to an increase in stress fibers formation (Fig. 3a). Western blot analysis revealed an increased ERM phosphorylation in miR-449-transfected proliferating primary HAECs (Fig. 3b). These results are consistent with the regulatory role played by phospho-ERM during actin

cytoskeleton dynamics<sup>47, 50</sup>. MiR-449 can thus contribute to actin cytoskeleton remodeling in several independent models.

### **miR-449 stimulates RhoA GTPase activity**

RhoA-activated actin remodeling appears as a central regulatory event required for multiciliogenesis and airway epithelium differentiation<sup>15, 51</sup>. To assess the functional impact of miR-449 on RhoA activity, proliferating HAECs were transfected with miR-449 and differentiating HAECs were treated with the antagomiR-449. In both cases, the activity of RhoA was measured in a pull-down assay with Rhotekin, a protein that stoichiometrically interacts with GTP-bound Rho. As a positive control, proliferating HAECs were also incubated with calpeptin (Rho activator I, from Cytoskeleton, Denver, CO 80223, USA). In proliferating primary HAECs, miR-449 overexpression caused an increase of about 50% of the level of active RhoA-GTP, similar to the effect of calpeptin (Fig. 3c). In differentiating HAECs, miR-449 silencing triggered the opposite effect, *i.e.* a significant decrease in RhoA activity (Fig. 3c). These data indicate that miR-449 can modulate the RhoA pathway during multiciliogenesis in HAECs.

### **R-Ras is a direct target of miR449**

To determine the molecular mechanisms by which miR-449 control apical actin cytoskeleton reorganization, we looked for miR-449 mRNA targets that could regulate this process. We defined a putative miR-449 target among transcripts that were both repressed during MCC differentiation and following over-expression of miR-449 (GEO, GSE22147)<sup>9</sup>. We analyzed the differentiation of HAECs at four time points and on three independent donors (where Pr, Po, EC, LC represent the proliferating step at day 0, the polarization step at day 7, the early

multiciliogenesis step at day 14 and the late multiciliogenesis step at day 21, respectively). Day number corresponds to the number of days after setting up the cells at an air-liquid interface (ALI). MiR-449-transfections were performed in proliferating HAECs from five independent donors. Several miRNA target prediction tools were then used to identify putative targets among down-regulated transcripts <sup>52</sup>. A similar approach has previously allowed us to identify and characterize cell cycle-related genes and *DLL1/NOTCH1* transcripts as *bona fide* miR-449 targets involved in the terminal differentiation of MCC precursors <sup>9</sup>. We report now another important miR-449 target, *RRAS*, which belongs to the small GTPase signaling system involved in the Rho pathway and is involved in actin cytoskeleton remodeling <sup>38</sup>. Interestingly, a recent gene expression profiling study performed in mouse trachea indicated that the level of expression of *RRAS* transcripts was higher in non-ciliated cells than in ciliated cells <sup>53</sup> (GSE42500). *RRAS* encodes the R-Ras protein, a member of a superfamily of small GTPases related to Ras <sup>54</sup>.

*RRAS* was significantly expressed in primary cultures of HAECs (Fig. 4a). Levels of both *RRAS* transcript and R-Ras protein slightly decreased at the onset of MCC differentiation and thereafter (Fig. 4a, b). The reduction of *RRAS* level at the beginning of MCC differentiation is concomitant with the increase of miR-449 (Fig. 4a-c). The same situation was observed in explanted epidermis of *Xenopus* embryo, where *rras* expression was detected at neurula stage 16, dramatically increased between stages 17 and 20, and subsequently dropped (Fig. 4d). These stages encompass the differentiation of MCCs and the collapse of *rras* expression between stages 20 and 23 mirrors the increase in epidermal miR-449 expression (Fig. 4e).

The expression of R-Ras was analyzed at a cellular resolution in HAECs. Immunofluorescence experiments revealed that the expression of R-Ras was higher in non-ciliated CD151+ basal cells <sup>9, 55</sup> than in acetylated-tubulin positive MCCs (Fig. 5a). In *Xenopus* epidermis, real-time PCR and fluorescent *in situ* hybridization failed to reveal *rras*

expression at stage 13, prior to the onset of MCC differentiation. At stages 16 and 19, *rras* was mostly expressed by inner epidermal layer cells negative for the MCC marker *alpha-tubulin* (Fig. 5b). Altogether, these data show that R-Ras expression is mainly excluded from the miR449-expressing MCC precursors during most of the multiciliogenesis process in both species. In order to directly establish the human *RRAS* transcript as a direct target of miR449, we used a dual luciferase reporter assay in HEK293 cells. MiR-449 expression strongly reduced the relative luciferase activity of a chimeric construct containing the wild-type 3'-UTR of *RRAS*. This effect was abolished by mutations in the putative miR-449 binding sites (Fig. 5c). Four miR-449 "seed" sequences were detected in the *RRAS* 3'-UTR (Fig. S1). Mutation of each individual sequence only partially blocked the effect of miR-449 overexpression, whereas combining mutations of all four sites led to a full reversion of the miR-449 repressive effect (Fig. 5c). Among the four miR-449 binding sites in the 3'-UTR of *RRAS*, the strongest reversion was observed for the most 3' site, which also corresponds to the only one conserved between human and *Xenopus* (Fig. 5c and S1). Finally, overexpression of miR-449 in proliferating HAECs strongly reduced the levels of the transcript (Fig. 5d) and the protein (Fig 5e-f). These results thus establish R-Ras as a *bona fide* target of miR-449, and suggest its possible involvement during the process of HAEC differentiation. We then focused our attention on the functional impact of miR-449-mediated repression of *RRAS* in MCCs.

### **Repression of R-Ras by miR-449 is necessary for apical actin reorganization and multiciliogenesis**

We designed target protection assays in which cholesterol-conjugated modified oligonucleotides (in HAECs) or morpholino oligonucleotides (in frog epidermis) can compete with the binding of miR-449 on the sites identified within the human and *Xenopus* 3'-UTRs

of *RRAS*. In human cells, the *RRAS* protector oligonucleotide effectively blocked the action of ectopic miR-449 on *RRAS* 3'-UTR in luciferase assays (Fig. 6a). Importantly, the *RRAS* protector oligonucleotide was able to increase endogenous R-Ras protein level in both species (Fig. 6b-d), suggesting that miR-449 directly contributes to *RRAS* down-regulation in MCCs. In *Xenopus* explanted epidermis, morpholino-mediated inhibition of miR-449 activity or morpholino-mediated protection of the unique miR-449 binding site in *rras* 3'UTR both led to an increase of *rras* transcript or protein levels whereas the opposite effect was induced using morpholino-mediated inhibition of *rras* (Fig. 6d,e,f). These assays indicated that *RRAS* transcripts were specifically targeted by miR-449 in MCCs in both models. Incidentally, both models also express low levels of *RRAS2*, a *RRAS*-related gene. However, variations in *RRAS2* expression remained small during MCC differentiation and in response to miR-449 overexpression in HAECs (data not shown, see GEO, GSE22147). In *Xenopus*, *RRAS2* mRNA was detected at very low levels in epidermal explants, and was not altered by alterations of miR-449 (Fig. 6d,e).

In human (Fig. 7a,c), as well as in *Xenopus* (Fig. 7b,d), we noticed a strong reduction in both the number of MCCs and the apical actin meshwork formation in response to protection of the *RRAS* transcript from miR-449. On the contrary to HAECs where the identification of cells truly transfected with the protector oligonucleotide was not possible, the visualization of morpholino-injected cells was possible using fluorescent tracer in *Xenopus* embryonic epidermis. These observations are consistent with an effect limited to miR-449 positive MCCs. Importantly, we show in *Xenopus* epidermis that actin cap formation and multiciliogenesis was rescued when a morpholino designed to block R-Ras translation was co-injected with the *rras* protector morpholino (Fig. 7b,d). This assay confirmed that the maintenance of low levels of R-Ras activity within MCC precursors was essential for apical actin cap formation and multiciliogenesis.



Ironically, *RRAS* silencing using siRNAs or morpholinos had no significant impact on RhoA activity itself (Fig. S1), despite it was self-sufficient to affect apical actin meshwork and multiciliogenesis in both species (Fig. 7a, 7eb-d). This is probably due to the fact that *RRAS* silencing in non-ciliated cells may indirectly impair MCC differentiation in a Rho-independent manner, as previously observed in *Xenopus* in another context <sup>56</sup>. An alternative but not exclusive explanation could be that *RRAS* activity within MCC precursors must be kept low, but not totally suppressed. An experimental limitation of the human model is that *RRAS* silencing has to be performed before the onset of multiciliogenesis, and it remains possible that *RRAS* activity is indeed required at earlier steps of MCC differentiation. Later on, repression of *RRAS* by miR-449 becomes important for apical actin network assembly and multiciliogenesis in human and frog MCCs.

It has been shown that R-Ras activity was increased by Notch pathway activation. Since miR-449 repressed Notch signaling during vertebrate multiciliogenesis <sup>9</sup>, one could hypothesize that in addition to the direct inhibition of *RRAS* transcripts by miR-449, R-Ras activity might also be inhibited through miR-449-induced Delta-Notch repression.

In line with the large increase of RhoA that we observed in response to miR-449 expression, it is also noteworthy that besides its specific action on R-Ras, miR-449 may also alter several molecules related to actin dynamics, as previously reported elsewhere for miR-129-3p in another context <sup>57</sup>.

In conclusion, the data presented here show that miR-449 favors the assembly of an apical actin cytoskeleton during MCCs differentiation, thus uncovering a further level of control of the process of multiciliogenesis by miR-449. This study illustrates how a single microRNA family can possibly integrate complex cellular processes through the control of multiple targets belonging to several different signaling pathways.

## **Materials & Methods**

### **Subjects/tissue samples**

Inferior turbinates or nasal polyps were from patients who underwent surgical intervention for nasal obstruction or septoplasty (kindly provided by Pr Castillo, Pasteur Hospital, Nice, France or by Epithelix Sàrl, Genova, Switzerland). The use of human tissues was authorized by the bioethical law 94-654 of the French Public Health Code after written consent from the patients.

### **Isolation and culture of human airway epithelial cells**

Primary HAEC cultures were performed according to <sup>9</sup>.

### ***Xenopus* injections**

Eggs obtained from NASCO females were fertilized in vitro, dejellied, cultured and injected as described <sup>9</sup>. cRNAs were generated with the Ambion mMessage mMachine® kit (Life Technologies). pCS105/mGFP-CAAX (a gift from C. Chang, University of Alabama at Birmingham, USA) was linearized with AseI and cRNA was synthesized with Sp6 polymerase as previously described <sup>9</sup>. All injections were done at least twice.

### **Immunocytochemistry**

**Human** : Fresh cultures of ALI-D21 (LC) HAECs sections were used for detection of acetylated-tubulin, ezrin, actin (phalloidin), and nuclei as described in <sup>9</sup>. Cells were fixed (4% paraformaldehyde, 15 min, 4°C), rinsed (PBS-glycine 0.1M, 10 min) and permeabilized (0.1% Triton X-100, 5 min). Only for centrin-2 immunostaining, cells were fixed with methanol

(10min, -20°C). Fixed cells were blocked 1h in 3% BSA and incubated for 1h at room temperature with primary antibodies or overnight at 4°C with the following antibodies. Then, cells were incubated for 1h with appropriate secondary antibodies (Alexa Fluor®, 1:500, Invitrogen), nuclei were stained with DAPI (300 nM, Invitrogen) and when indicated F-Actin were stained with Alexa Fluor® 594 Phalloidin (1U/staining). Stained cells were mounted with ProLong® Gold antifade reagents (Invitrogen, Life technologies) and examined with Leica SP5 confocal imaging system, Olympus FV10i.

***Xenopus*** : For F-actin staining embryos were fixed in 4% formaldehyde/PBT 1h at 4°C and stained with phalloidin-Alexa Fluor 555 (Invitrogen, 1:40) for 4 hours at room temperature. For immunostaining, embryos were fixed in MEMFA (0.5M MOPS, pH7.4, 100mM EGTA, 1mM MgSO<sub>4</sub>, 3.7% Formaldehyde). Whole-mount embryos or sections were blocked in 15% goat serum. The following primary antibodies were used: mouse anti-acetylated-tubulin (Sigma, 1:500, Sigma), chicken anti-GFP (Aves, 1:500). After washing in PBT, sections or whole-mount embryos were incubated with the appropriate secondary antibody: anti-chicken Alexa Fluor 488 (1:500, Invitrogen), anti-mouse Alexa Fluor 555 (1:500, Invitrogen) or anti-mouse Alexa Fluor 647 (all from Invitrogen, 1:500). Epidermis fragments were peeled from embryos at stages 20, 25 and mounted on a glass coverslip with fluoromount (Diagnostic BioSystem).

### **Western Blot and small GTPases activity measurement**

**Human** : Primary HAECs cells were harvested by scraping in Ripa lysis Buffer (Thermo Scientific Pierce), cleared by centrifugation. Protein concentration was determined using the BCA assay (Thermo Fisher Scientific) and equivalent amounts of protein were resolved on SDS polyacrylamide gels using Novex® NuPAGE® SDS-PAGE Gel System following manufacturer's instructions. Proteins were transferred to PVDF membranes and analyzed by

immunoblotting with appropriate primary antibodies and HRP-conjugated secondary antibodies (1/5000, Dako). Immunoreactive bands were detected using immobilon ECL kit (Merck Millipore) on LAS-3000 imager (Fujifilm).

*Xenopus* : MO-ATG-*rras*-injected, MO-Po-*rras*-injected or control neurula stage (st.19) *Xenopus laevis* embryos were lysed in Halt Protease Inhibitor Single Use Cocktail (Thermo Scientific), the lysate was cleared by centrifugation, protein concentration was determined by NanoDrop reading and identical amounts of protein for each condition were resolved on 12% SDS polyacrylamide gel using the Hoefer Gel Caster system. Proteins were transferred to PVDF membrane and analyzed by immunoblotting with anti-rabbit R-Ras (1/300, Antibody Verify) or anti-mouse- $\alpha$ -tubulin (1/2000, Sigma Aldrich) primary antibody and HRP-conjugated secondary antibodies (1/2000, Jackson). Immunoreactive bands were detected using Pierce ECL2 kit (Thermo Scientific) on Amersham Hyperfilm (GE Healthcare).

### **Small GTPases activity assay**

The activation of RhoA and Rac1, 2, 3 were evaluated by the GST pulldown with recombinant proteins GST-Rhotekin-RBD (Merck Millipore) and PAK-1 PBD (Merck Millipore), respectively.

HAECs were seeded on type-I collagen-coated surface, miRNA mimics and siRNA were transfected for 72h. Cells were lysed in cell lysis buffer (50mM Tris pH 7.5, 10mM MgCl<sub>2</sub>, 0.5M NaCl, and 2% Igepal) containing a proteinase inhibitor cocktail, lysate were cleared by centrifugation and immediately quantified using BCA assay kit. Approximately 400  $\mu$ g of total proteins were incubated with the GST fusion protein at 4°C for 30 min. Supernatants were then incubated with Pierce Glutathione Magnetic Beads for 30 min at 4°C, and washed 3 times with wash buffer (25 mM Tris pH 7.5, 30 mM MgCl<sub>2</sub>, 40 mM NaCl) using magnetic

rack. Samples and pull down were resuspend in loading buffer and bloted using Novex® NuPAGE® SDS-PAGE Gel System following manufacturer's instructions.

### **Total RNA extraction**

**Human** : Automated total RNA extraction were performed using QIAcube and miRNeasy kit from Qiagen according manufacturer's instructions. Total RNAs were quantified using NanoDrop 1000 Spectrophotometer (Thermo Scientific) and integrity of samples (RIN > 8) were evaluated using RNA nano-chips and Agilent 2100 Bioanalyzer Instrument (Agilent Technologies).

**Xenopus** : Total RNAs were isolated from animal caps dissected at stages 10 to 11 and cultured in MBS (880mM NaCl, 10mM KCl, 8.2mM MgSO<sub>4</sub>, 24mM NaHCO<sub>3</sub>, 100mM Hepes pH7.4, 4.1mM CaCl<sub>2</sub>, 3.3mM Ca(NO<sub>3</sub>)<sub>2</sub>). Twenty explants for each sample (stages 14 or 25) were collected for RNA extraction. Total RNAs were isolated using the RNAeasy mini kit (Qiagen) according to the manufacturer's instructions and quantified using NanoDrop Spectrophotometer. cDNAs were synthesized using iScript Reverse Transcription Supermix (BioRad).

### **Quantitative RT-PCR**

**Human** : Real-time PCR was performed using TaqMan® Gene Expression Assay and TaqMan® MicroRNA Assay (Life technologies) on a Lightcycler 480 (Roche) according to manufacturer's instructions. Expression levels of mature microRNAs and RNA messenger were calculated using the 2-deltaCT method, using respectively RNU44 and UBC as endogenous controls.

**Xenopus** : Primers were designed using Primer-BLAST Software. PCR reactions were carried out using SYBRGreen on a CFX Biorad qPCR cycler. All experiments were repeated at least

twice on separate injections and the RT-qPCR was performed in triplicate. The relative expression of *RRAS* was normalized to the expression of the housekeeping gene *ornithine decarboxylase* (ODC). The RT-qPCR *RRAS* primers are as follows: Forward: 5'-gtaaccaaagaggaagcgctca-3'; Reverse: 5'-ggatgacacaagggaactttt-3'.

### **MiR-449 silencing and target protection experiments**

**Human** : 3'- cholesterol linked 2'-*O*-Methyl miR-449a/b antisense oligonucleotide (antagomiR), 5'-*c<sub>s</sub>u<sub>s</sub>c<sub>s</sub>uucaacacugccacau<sub>s</sub>u<sub>s</sub>u*-Chol-3' and *RRAS* protector oligonucleotide 5'-*c<sub>s</sub>g<sub>s</sub>u<sub>s</sub>uggcagugacauuuuuu<sub>s</sub>u<sub>s</sub>u*-Chol-3' (phosphorothioate bonds are indicated by subscript 's') were purchased from Eurogentec (Seraing, Belgique). miR-449 antagomiR targets *Homo sapiens* miR-449a (full match) and miR-449b with one mismatch. The *RRAS* protector is a complementary antisense oligonucleotide targeting the conserved miR-449 binding site of the human *RRAS* 3'-UTR. Negative control was the Clear-miR(tm) (5'-*c<sub>s</sub>a<sub>s</sub>u<sub>s</sub>cgucgaucguagcg<sub>s</sub>c<sub>s</sub>a*-Chol-3') from Eurogentec. AntagomiR and protectors were used as previously described <sup>9</sup>.

**Xenopus** : Morpholino antisense oligonucleotides (MOs): MO against miR-449 (GeneTools, LLC): miR-449a MO, 5'-*accagctaacattacactgcct*-3'; miR-449b MO, 5'-*gccagctaaaactacactgcct*-3'; miR-449c MO, 5'-*acagccagctagcaagtgcactgcc*-3'; MO control, 5'-*tgcacgtttcaatacagaccgt*-3'. A mixture of 10 ng of each miR-449 MO was injected in one animal-ventral blastomere at the 8-cell stage. Protector MO directed against miR-449-binding sites in *rras* 3'-UTR: 5'-*gttggaatgtaggtgcaattcggt*-3'. Protector MO (5.7 or 7.5 ng) was injected in one animal-ventral blastomere at the 8-cell stage. Morpholino oligonucleotide blocking the translation of *rras*: 5'-*gctccttggaactcatagtcgctgc*-3'. 15 or 25 ng of *rras* translation MO was injected in one animal-ventral blastomere at the 8-cell stage.

### **Ectopic expression of microRNAs/siRNAs**

Cells were grown to 30 % confluency in proliferation medium on plastic, glass coverslip or on transwell® filters. Cells were then transfected with synthetic negative control miRNA (miR-Neg, Ambion) or synthetic miR-449a/b miRNAs (Ambion) (10 nM final concentration). Total RNAs or proteins were extracted, or immunostaining performed, from 24h to 72h later. For siRNA experiments in differentiating HAECs, cells were then transfected with a siRNA against the human *RRAS* transcript or a negative control SiRNA (Stealth RNAi<sup>TM</sup> SiRNAs, Life Technologies) (20 nM final concentration) using Lipofectamine RNAi Max Reagent (Invitrogen) in OPTIMEM (Invitrogen) according manufacturer's instructions. The next day, an additional transfection was performed using the same procedure, before HAEC differentiation was induced in ALI the third day. Finally, HAECs were harvested for western blot analyses or processed for immunofluorescence experiments after 7, 14 and 21 days of culture in ALI.

### **Plasmid constructs and Luciferase measurements**

Sequence from the wild-type or mutants 3'-UTR of *RRAS* were synthesized (gBlocks® Gene Fragments, Integrated DNA Technologies) and cloned into psiCheck2 vector (Promega). For mutated 3'-UTRs, three bases of each seed region were changed by complementary bases. PiCheck2 constructions were co-transfected with synthetic microRNAs mimics (Ambion, Applied Biosystems) with or without antagomiRs or antisense protectors into HEK293T cells, and luciferase activity was measured using the dual reporter luciferase assay kit (Promega), according to the manufacturer's protocol.

## List of Antibodies used

| Sp.                         | Target             | Réf./clone | Manufacturer                   | Dilution                |
|-----------------------------|--------------------|------------|--------------------------------|-------------------------|
| Ms                          | Acetylated-Tubulin | 6-11B-1    | Sigma-Aldrich                  | 1/1000                  |
| Ms                          | $\gamma$ -Tubulin  | GTU-88     | Sigma-Aldrich                  | 1/1000                  |
| Ms                          | CD151              | 14A2.H1    | BD biosciences                 | 1/100                   |
| Rb                          | R-Ras              | C-19       | Santa Cruz Biotechnology, Inc. | 1/1000 (WB), 1/400 (IF) |
| Rb                          | Ezrin              | 07-130     | Merck Millipore                | 1/1000 (WB), 1/100 (IF) |
| Rb                          | P-ERM              | 41A3       | Cell Signaling Technology      | 1/1000 (WB), 1/100 (IF) |
| gt                          | actin              | I-19       | Santa Cruz Biotechnology, Inc. | 1/5000                  |
| gt                          | Hsp60              |            | Santa Cruz Biotechnology, Inc. | 1/5000                  |
| Rb                          | RhoA               | 67B9       | Cell Signaling Technology      | 1/1000                  |
| Rb                          | P-Cofilin 1        | (hSer3)-R  | Santa Cruz Biotechnology, Inc. | 1/500                   |
| Rb                          | Cofilin            | 3312       | Cell Signaling Technology      | 1/1000                  |
| HRP conjugate anti-Ms/Rb/Gt |                    |            | Dako                           | Lot Dependant           |

## *In situ* hybridization on *Xenopus* embryos

Whole-mount *in situ* hybridization was done as described previously<sup>58</sup>. *RRAS* Digoxigenin-labelled sense and antisense riboprobes (Anna/Andrea please add clone number and provider) and fluorescein-labelled antisense  $\alpha$ -tubulin riboprobe (Deblandre et al. 1999) were generated from linearized plasmids using RNA-labeling mix (Roche). Locked Nucleic Acid (LNA) antisense probe against the mature form of miR-449a was described previously<sup>9</sup>. For fluorescent *in situ* hybridization (FISH) on sections, embryos were fixed in MEMFA 2h at room temperature or overnight at 4°C, stored in methanol at least 24h at -20°C, rehydrated and washed in triethanolamine (0.1M)/acetic anhydrid. Embryos were then transfered in



successive sucrose washes from 5% to 30% sucrose in PBT. They were then embedded in O.C.T Compound (VWR Chemicals Prolabo), flash frozen and 12µm thick sections were prepared with a CM3050S Leica cryostat. Slides were kept at -80°C at least overnight before FISH. FISH was carried out using Tyramide Signal Amplification – TSA TM Plus Cyanine 3/Fluorescein System (PerkinElmer). Before hybridation, and after Proteinase K digestion (3min at 2µg/ml), endogenous peroxydase activity was blocked in a bath of H<sub>2</sub>O<sub>2</sub> 3% in PBS for 20 min. Sections were hybridized with a mixture of Digoxigenin- and Fluorescein-labelled probes 40 ng each) overnight at 60°C. Following washes (2 times with 2% SSC / 0.1% Chaps at 60°C ; 2 times with 0.2% SSC / 0.1% Chaps at 37°C), the Digoxigenin-labelled probe was revealed first through incubation with a mouse anti-DIG antibody conjugated to horseradish peroxidase (POD) (Roche, 1:500), followed by incubation in Cy3 fluorophore amplification reagent (1/50 in the TSA diluent during 10 min). This reaction was then blocked in a bath of 2% H<sub>2</sub>O<sub>2</sub> during 20 min. Next, the fluorescein-labelled probe was revealed with a mouse anti-fluorescein POD-conjugated antibody (Roche, 1:500), followed by incubation in Cy5 fluorophore amplification reagent (1/50 in the TSA diluent during 10 min). This second reaction was blocked in a bath of 2% H<sub>2</sub>O<sub>2</sub> during 20 min. Following double FISH, immunostaining with anti-GFP antibody was performed, and slides were processed for confocal imaging.

### **Confocal microscopy**

**Human** : Images were acquired using the Fv10i confocal imaging system (Olympus) with 60X oil immersion objective.

**Xenopus** : Flat-mounted epidermal explants were examined with a Zeiss LSM 780 confocal microscope.

Three-colour confocal z-series images were acquired using sequential laser excitation, converted into single plane projection and analyzed using ImageJ software.

## **ACKNOWLEDGEMENTS**

This work was supported by CNRS, Région PACA, CG06 and by grants from ANR (MERCi, COMMIT, MITHRA), Vaincre la Mucoviscidose, FRM (DEQ20130326464), ARC and INCa. We thank V. Magnone, G. Rios, S. Fourré, K. and LeBrigand from the IBISA Functional Genomics Platform, Sophia-Antipolis, for help with transcriptome analyses and bioinformatics, F. Brau and J. Cazareth, for cellular imaging, R. Waldmann and B. Mari for helpful discussions, F. Aguila for artwork. This work is the object of a CNRS patent N°09/03723.

## **Abbreviations List**

Multiciliated cells (MCCs); ezrin-radixin-moesin (ERM); Rho GDP-dissociation inhibitors (RhoGDIs); MicroRNAs (miRNAs or miR); miR-449a, miR-449b and miR-449c ( miR-449); human airway epithelial cells (HAECs); air-liquid interface (ALI); filamentous actin (F-actin); Morpholino(s) (MOs); protector antisense (Po); Proliferating step (Pr) ; polarization step (Po); early ciliogenesis step (EC); late ciliogenesis step (LC)

## **Author contributions**

B.M. & P.B. are the Principal Investigators (IPMC), initiated, designed and managed the entire project. L.K. is the Principal Investigator (IBDML) of the *Xenopus* section. B.M., L.K. and P.B. planned experiments, analysed and interpreted data and wrote the paper. B.C., L-E.Z and O.M. carried out cell culture, cellular and molecular biology, biochemistry and cellular imaging in human, A.A. carried out *Xenopus* experiments.

## Legends

### Figure 1

**Apical actin cytoskeleton in vertebrate MCCs.** (a) ALI-day 28 HAECs were stained for ezrin (using anti-ezrin antibody in green in panels a1, a5), F-actin (using phalloidin in red in panels a2, a6) and cilia (using anti-acetylated tubulin antibody in magenta in panels a3, a7). Nuclei were stained with DAPI (blue in panel a6). Panels a5-8 are orthogonal views (z slices) of a1-4. In acetylated tubulin-positive MCCs (white arrowheads), F-actin is apically enriched (a2, a6) and colocalizes with ezrin (a1, a5 and a4, a8). (b)  $\gamma$ -tubulin-positive basal bodies (magenta in panels b3, b4) colocalize with ezrin (b1, b4) and apical F-actin (b2, b4). (c) Dynamics of the phosphorylation state of ezrin or ERM and cofilin1 and of EBP50 expression during HAEC differentiation are indicative of actin remodeling (Pr: proliferating HAECs; Po: polarization stage, ALI days 5-10; EC: early ciliogenesis, ALI days 14-20; LC: late ciliogenesis, from ALI days 21). (d) In the epidermis of stage 25 *Xenopus* embryos, F-Actin (using phalloidin in red in panel d1) is apically enriched in acetylated tubulin-positive MCCs (magenta in panel d2-d3).

### Figure 2

**MiR-449 knockdown inhibits apical actin remodeling in MCCs and stimulates RhoA activity.** (a) Differentiating HAECs were chronically treated with control antagomiR (Antago-Neg; panels a1-a4) or anti-miR-449a/b (Antago-449; panels a5-a8) and stained for F-actin (panels a1, a5), ezrin (panels a2, a6) and acetylated-tubulin (panels a3, a7), at ALI day 21. MiR-449 inhibition affects F-actin apical enrichment (a5), ezrin apical localization (a6) and multiciliogenesis (a7). (b) The histogram indicates the relative rate of multiciliated cells

and apical ezrin positive cells per field in each experimental condition (20 fields per condition in triplicate). Data are means  $\pm$  s.d. from 9 and 3 donors for MCCs and ezrin positive cells, respectively (\*\*\*,  $p < 0.001$ , Student's t-test). (c) 8 cell-stage *Xenopus* embryos were injected in the epidermis precursor blastomeres with a mixture of synthetic mRNA coding for membrane-bound GFP (GFP-CAAX) and control morpholinos (CTR-MO; panels c2-c4) or morpholinos against miR-449 (449-MOs; panels c6-c8) then stained at stage 20 for F-actin (panels c1, c5, c9) and motile cilia using acetylated-tubulin antibody (panels c3, c7). GFP fluorescence visualizes the injected clone (panels c2, c6). Staining of F-actin and motile cilia in non-injected embryos are represented in panels c9, c10 and c11. Knockdown of miR-449 affects F-actin apical enrichment (c5) and multiciliogenesis (c7). (d) The histogram indicates the percentage of injected cells (positive for GFP fluorescence) that develop motile cilia or apical actin cap in controls (Stage 24+25 :  $n = 5$  fields/583 injected cells) and in miR-449 morphants (Stage 24+25 :  $n = 8$  fields/625 injected cells; P value  $_{st.24+25} = 0.0087$ , Mann-Whitney test with two-tailed P value).

### Figure 3

**miR-449 affects the formation of actin stress fibers, the phosphorylation state of ERM and the RhoA activity.**(a) Immunostaining of human alveolar A549 epithelial cells were grown on glass coverslips for 72h, then transfected with synthetic control negative miRNA (miR-Neg) or synthetic miR-449a (miR-449a) for 48h and stained for F-Actin (phalloidin in red) and nuclei (DAPI in blue). Ectopic expression of miR-449a mimics leads to the formation of thick bundles of actin. (b) MiR-449 overexpression in proliferating HAECs for 72h stimulates the phosphorylation of ERM. Phosphorylated protein levels were normalized with non-phosphorylated ERM and with an antibody against HSP60 as a loading control. Normalized fold changes are indicated upon the corresponding bands. Experiments were

representative of three donors. (c) Proliferating HAECs were transfected for 72h with miR-Neg or miR-449a then incubated for 2h with the RhoA Activator. RhoA activation was measured in a GST-Rhotekin pull-down assay. HAECs at ALI day 7 were treated for 72h with antago-449 or antago-Neg, and RhoA activation was measured. The histogram indicates the relative RhoA activation in each experimental condition compared to the control set to 100%. Data represent the mean and s.d of 3 independent experiments (\*\*\*,  $p < 0.001$ ; \*\*,  $p < 0.01$ , \*  $p < 0.05$ , not significant (n.s), Student's t-test).

#### **Figure 4**

**Expression of R-Ras during vertebrate multiciliogenesis.** (a) Expression levels of *RRAS* transcripts during HAEC differentiation. Transcripts levels were normalized with *UBC* transcript as an internal control (Pr: proliferating HAECs; Po: polarization stage, ALI days 5-10; EC: early ciliogenesis, ALI days 14-20; LC: late ciliogenesis, from ALI days 21). (b) Expression levels of R-Ras protein during HAEC differentiation.  $\beta$ -actin was used as a loading control. (c) Relative abundance of miR-449a in differentiating HAECs. MicroRNA levels were normalized with *run44* as an internal control. (d) Real-time RT-PCR of *rras* transcripts in *Xenopus* epidermis indicates that *rras* expression increases between stages 9 to 19 and is then strongly down-regulated from stage 19 to 25. Transcript levels of *RRAS* were normalized against *Odc* transcript. (e) Transcript levels of *RRAS* decrease concomitantly with the induction of miR-449 expression. Transcript levels of *RRAS* were normalized against *Odc* transcript as an internal control, and miR-449 expression was normalized with U6 as an internal control. Error bars denotes standard deviation from three independent experiments.

## Figure 5

**Expression of R-Ras is controlled by MiR-449.** (a) Cytospins of dissociated differentiated HAECs (panels 1-3) were labeled to identify the specific cell type localization of R-Ras protein. R-Ras labeling (green; panels 2-3) was enriched in CD151-positive basal cells (red; panels 1-2), and mainly excluded from MCCs positive for acetylated-tubulin (magenta; arrowheads in panels 3). Nuclei are stained with dapi (blue; panels 1-3). (b) Fluorescent *in situ* hybridization on sections of *Xenopus* embryonic epidermis at stages 16 and 19 reveals that the *rras* mRNA (green; panels b1, 2) is largely excluded from MCC precursors labelled by the  $\alpha$ -tubulin mRNA (red; panels b1, 2). (c) Specific interaction between miR-449a/b and the 3'-UTRs of *RRAS* mRNAs was confirmed using luciferase reporter assay on constructs carrying either the wild-type or mutants 3'-UTR-binding site for miR-449. All experiments were done in triplicate; values were normalized with the internal Renilla luciferase control. (d) Real-time RT-PCR reveals a strong reduction in *RRAS* transcript levels following miR-449 but not miR-Neg overexpression for 24h or 48h in proliferating HAECs. Transcript levels were normalized against the *UBC* gene. Data represent the mean and s.d. of at least 3 independent experiments (\*\*\*,  $p < 0.001$ , Student's t-test) (e) The expression levels of R-Ras protein decrease after miR-449 overexpression in proliferating HAECs for 72h.  $\beta$ -actin is used as an internal control. (f) Quantification of R-Ras protein level in response to miR-449 overexpression. Data are means  $\pm$  s.d. from at least three independent experiments (\*\*\*,  $P < 0.001$ , \*\*,  $P < 0.01$ ; not significant (n.s), Student's t-test).

## Figure 6

**The target protection of *RRAS* specifically prevents the action of miR-449.** (a) Antago-449a/b and miR-449::*RRAS* protector oligonucleotides specifically prevent miR-449 binding on *RRAS* 3'-UTR. miR-449a transfection in HEK293 cells strongly reduced relative luciferase

activity of wild-type 3'-UTR chimeric constructs of *RRAS*. This effect was strongly blocked by antago-449a/b or miR-449::*RRAS* protector co-transfection, whereas it was not significantly affected by co-transfection with negative controls (antago-Neg or protector-Neg). Values were normalized to the internal *Renilla* Luciferase control. (b) Modulation of R-Ras protein level induced by miR-449::*RRAS* protection (PO-*RRAS*) in HAECs in comparison to treatment by negative control (PO-Neg). Protein levels were normalized with an antibody against HSP60 as an internal control. R-Ras protein level was increased by miR-449::*RRAS* protection, indicating the specificity of PO-*RRAS* and that *RRAS* is a true miR-449 target in human. Experiments were representative of three donors. (c) Modulation of R-Ras protein level induced by silencing of *RRAS* by SiRNA Si-*RRAS* in HAECs in comparison to treatment by negative control (Si-Neg). Protein levels were normalized with an antibody against HSP60 as an internal control. R-Ras protein level was strongly decreased by Si-*RRAS*, indicating the specificity of the SiRNA against *RRAS*. (d, e,) Real-time RT-PCR expression of *rras* (e) or *rras2* (f) in *Xenopus* embryos injected with MO-Neg, MO-PO-*rras*, or 449-MOs. Contrary to *rras*, *rras2* expression is very low and is not affected in either 449-MOs or MO-PO-*rras*, indicating that only *rras* is a true miR-449 target in *Xenopus*. Transcripts levels were normalized against *Odc* transcript as an internal control. Error bars denotes standard deviation from three independent experiments. (f) Protecting *rras* mRNA against interaction with miR449 results in increased levels of R-Ras protein. R-Ras levels in embryos injected with the protector morpholino MO-Po-*rras* are about 20% higher than in control non-injected embryos. By comparison, blocking *rras* translation by injection of MO-ATG-*rras* leads to an 80% decrease in the amount of R-Ras. Embryos were injected at 1 cell stage and lysed at stage 19. Signal intensity was measured with ImageJ, using  $\alpha$ -tubulin as an internal control.

## Figure 7

**Inhibiting the interaction between *RRAS* mRNA and miR-449 affects multiciliogenesis and apical actin cytoskeleton reorganization.** (a) Differentiating HAECs were chronically treated with negative antagomiR/Protector (Antago-Neg/Po-Neg), anti-miR-449a/b (Antago-449) or with an oligonucleotide protecting the miR-449 binding site on *RRAS* (Po-*RRAS*). Alternatively, HAECs were transfected at seeding time with a negative siRNA (Si-Neg) or a siRNA against *RRAS* (Si-*RRAS*). Motile cilia are stained with anti-acetylated-tubulin antibody (magenta) and F-actin with phalloidin (red). Protecting the *RRAS* mRNA from interaction with miR-449 leads to a decrease in MCC differentiation similar to that observed after inhibition of miR-449 activity. A decrease in the number of MCCs is also observed following inhibition of *RRAS* with Si-*RRAS*. (b) 8 cell-stage *Xenopus* embryos were injected in the epidermis precursor blastomeres with a mixture of synthetic mRNA coding for membrane-bound GFP (GFP-CAAX) and CTR-MO (CTR-Neg), 449-MOs, a morpholino protecting *rras* against binding by miR-449 (MO-Po-*rras*) or a morpholino blocking the translation of *rras* (MO-ATG *rras*). GFP-CAAX (green) labels the injected cells, MCCs are stained with an anti acetylated tubulin antibody (red). Protecting the *rras* mRNA from interaction with miR-449 results in a loss of MCCs. This phenotype is rescued when the translation of the protected *rras* mRNA is blocked by coinjection of MO ATG *rras*. (c) The histogram indicates the number of human MCCs per field in each experimental condition (20 fields per condition in triplicate). Data are means  $\pm$  s.d. from 2 donors. (d) The histogram indicates the percentage of injected cells (positive for mGFP) that develop proper motile cilia in *Xenopus*. CTR-Neg, n=10 embryos/413 injected cells; MO-PO-*rras*, n=8 embryos/350 injected cells; MO-ATG *rras*, n=8 embryos/290 injected cells; MO-PO-*rras* + MO-ATG *rras* n=9 embryos/395 injected cells (\*\*\*, P=0.009 and P<0.0001, and \*\*, P=0.0016, Mann-Whitney test).



## Figure S1

(a) MiR-449 binding sites located in the 3'-UTR of *Homo sapiens* (hsa) or *Xenopus laevis* (xla) *RRAS* mRNA were identified *in silico* using “microcible” miRNA target prediction tool available on our laboratory website ([www.microrray.fr](http://www.microrray.fr)). (b) Modulation of R-Ras protein level in proliferating HAECs transfected with miR-449 or Si-*RRAS* for 72h. Protein levels were normalized against  $\beta$ -Actin as an internal control and normalized fold changes are indicated beneath the corresponding bands. Experiments were representative of three donors. (c) RhoA activation was measured in proliferating HAECs using pull-down with GST-Rhotekin-RBD. miR-Neg, miR-449a, Si-Neg or Si-*RRAS* were transfected for 72h. The histogram indicates the relative RhoA activation in each experimental condition normalized to the control set to 100%. Data represent the mean and s.d of at least 3 independent experiments (\*\*,  $p < 0.01$ , Student's t-test).

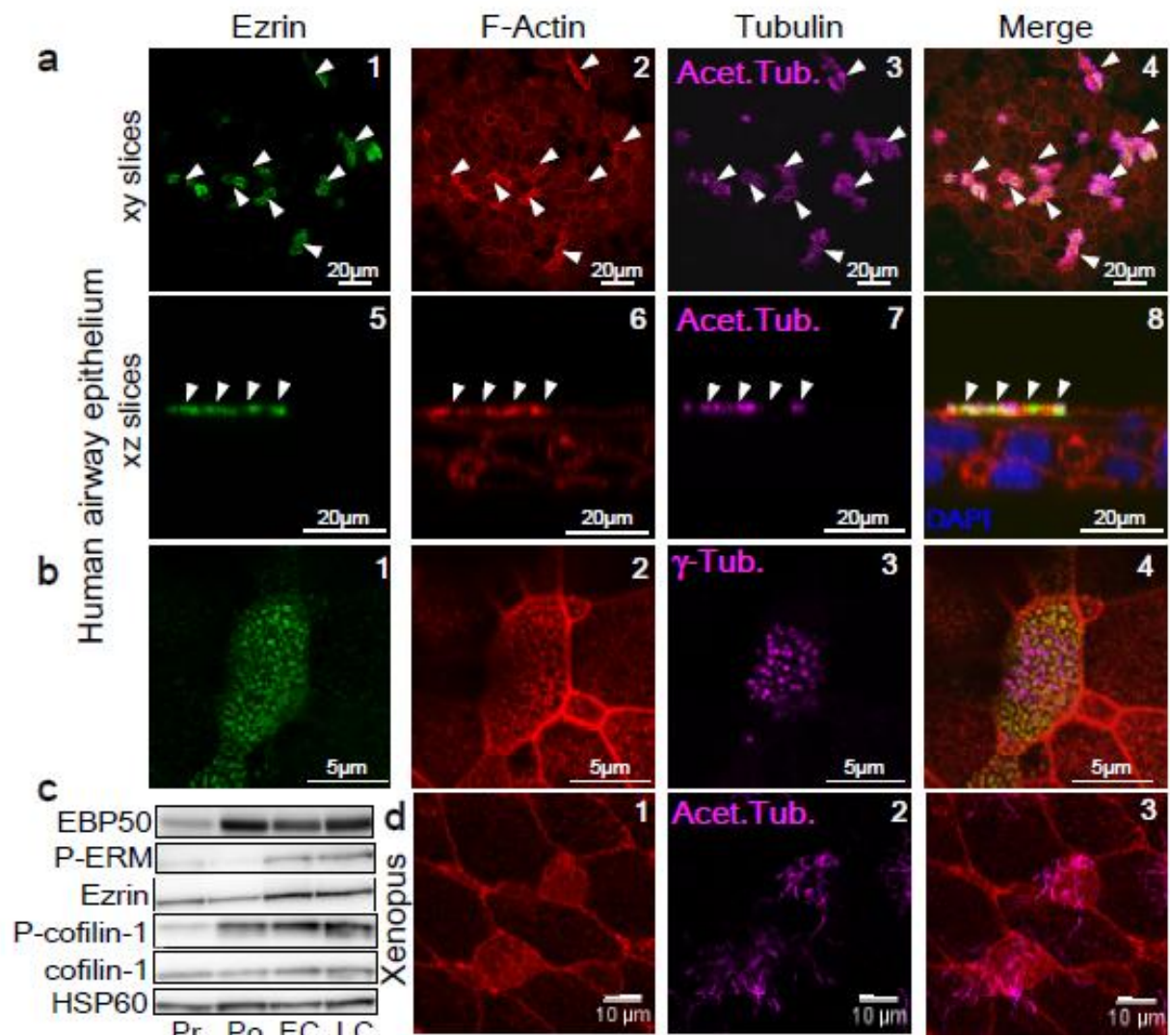


Figure1  
Chevalier & Adamiok et al.,

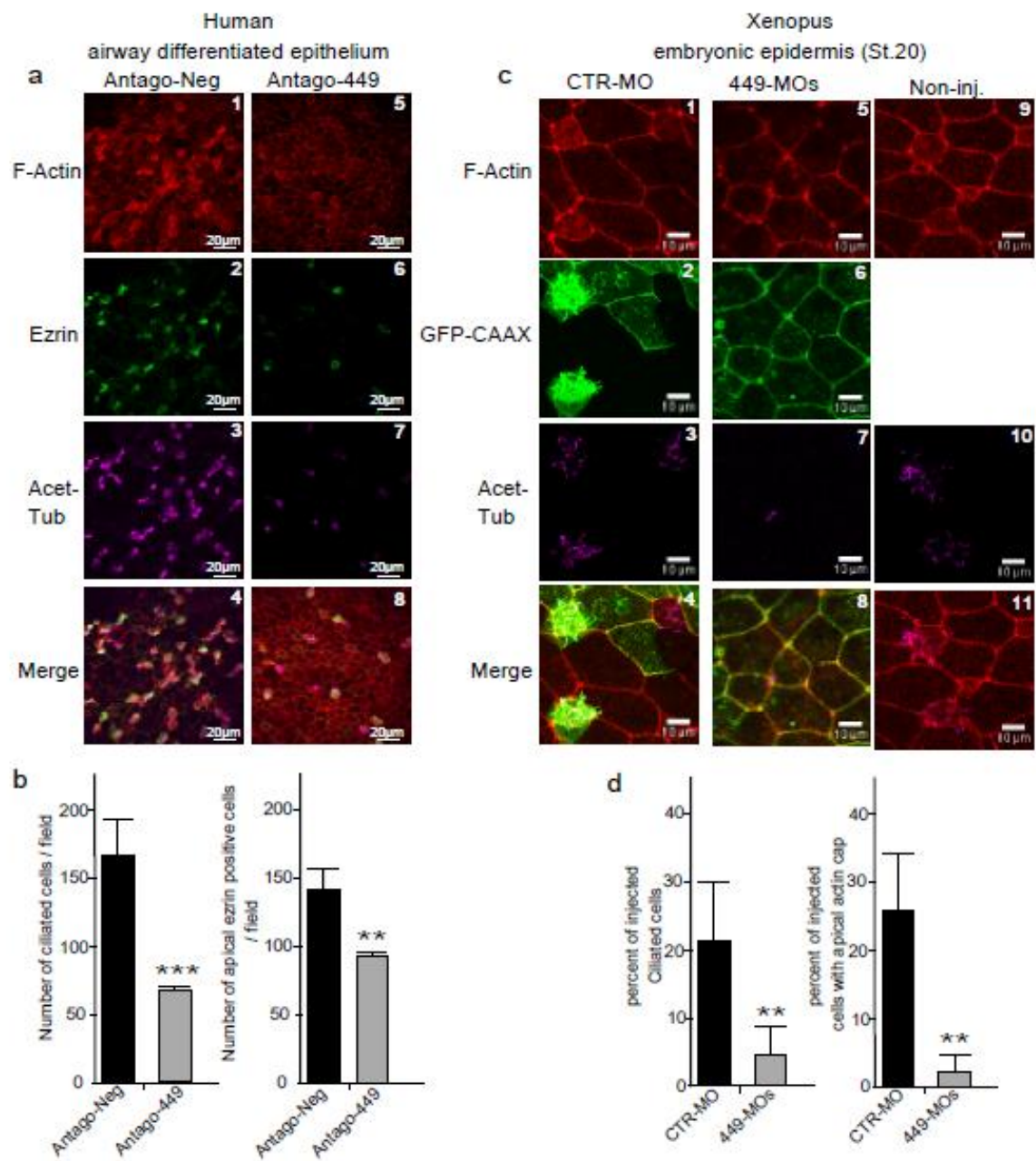


Figure 2  
Chevalier & Adamiok et al.,

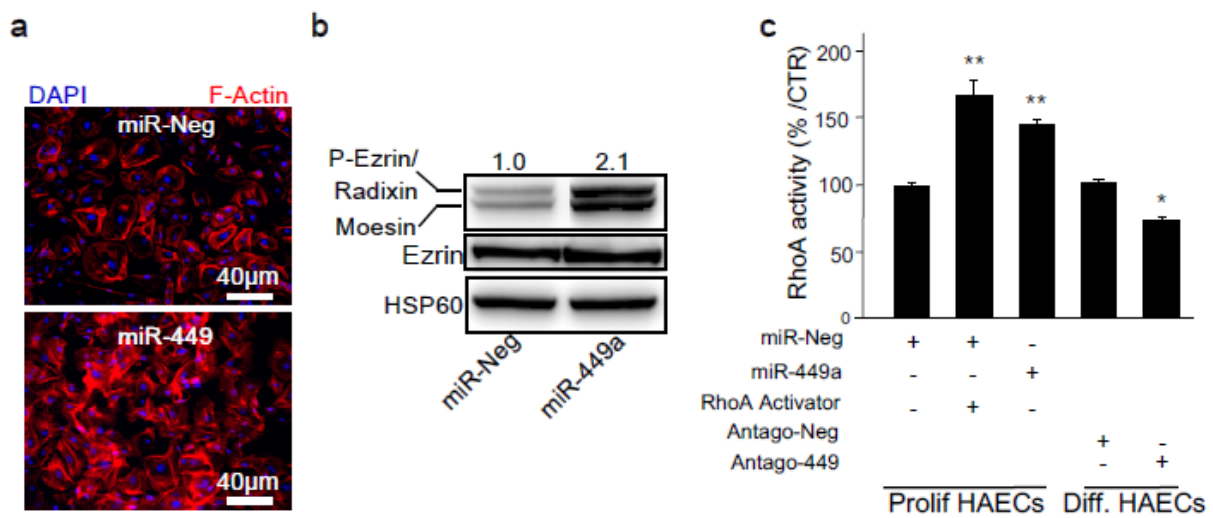


Figure 3  
Chevalier & Adamiok et al.,

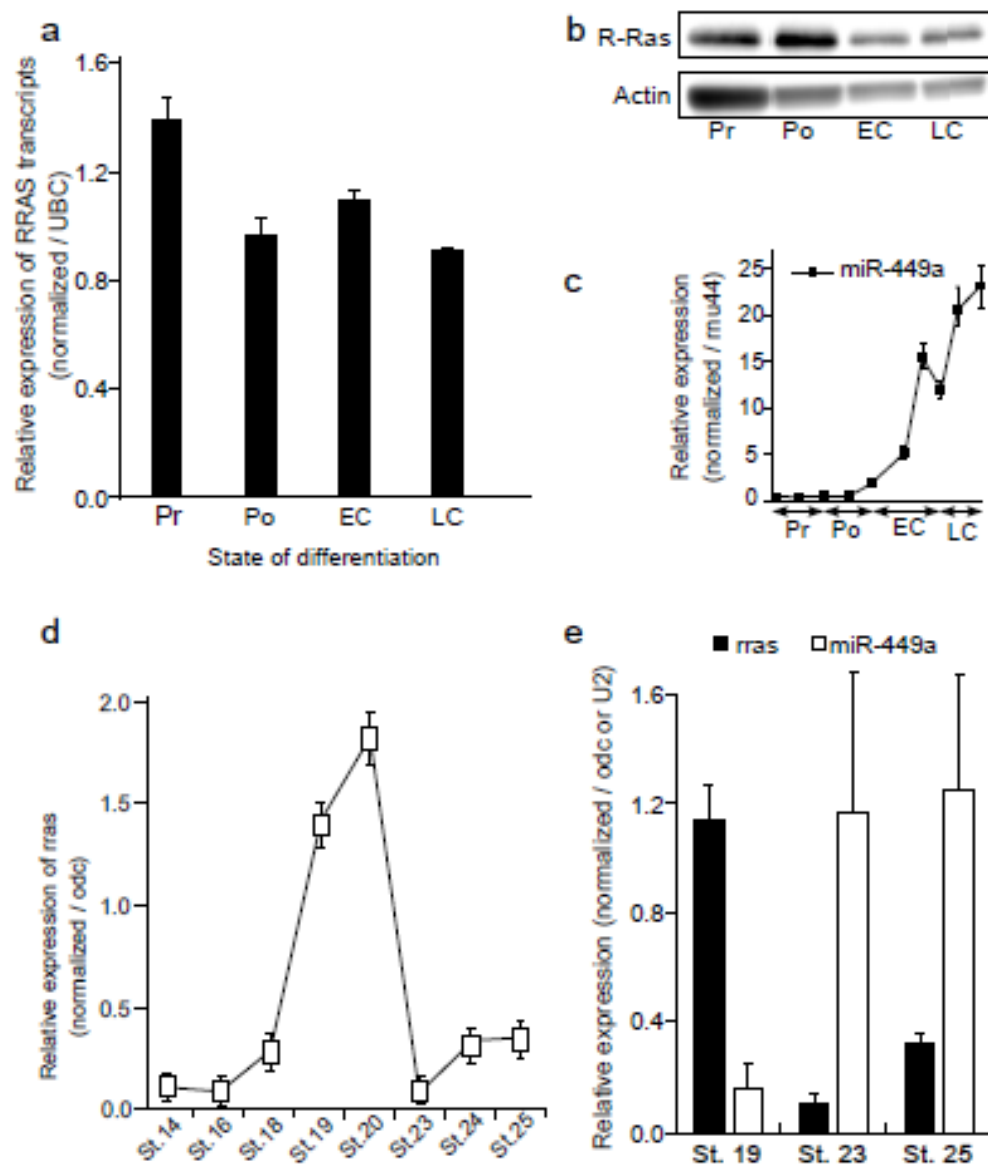


Figure 4  
Chevalier & Adamiok et al.,

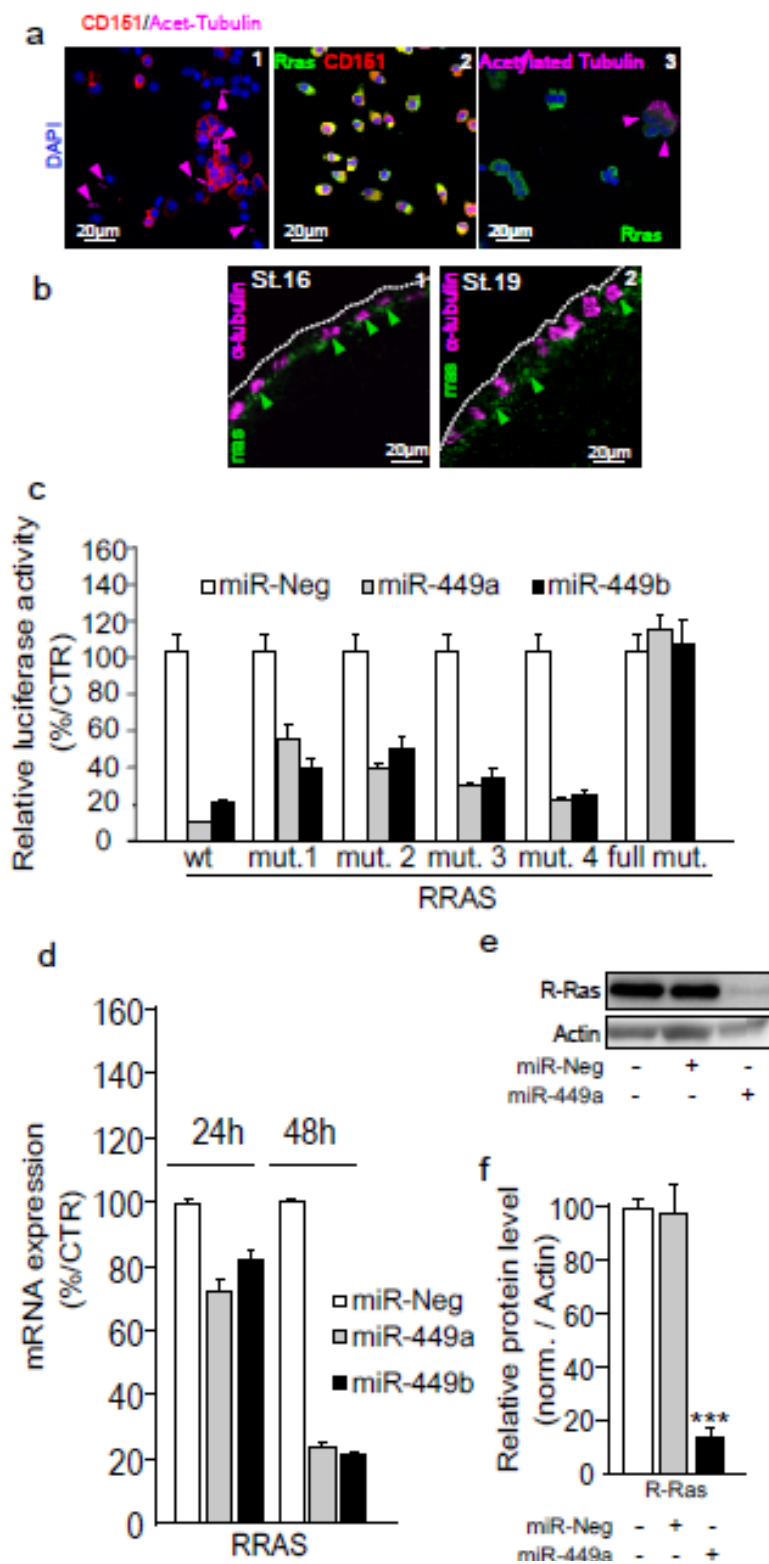


Figure 5  
Chevalier & Adamiok et al.,

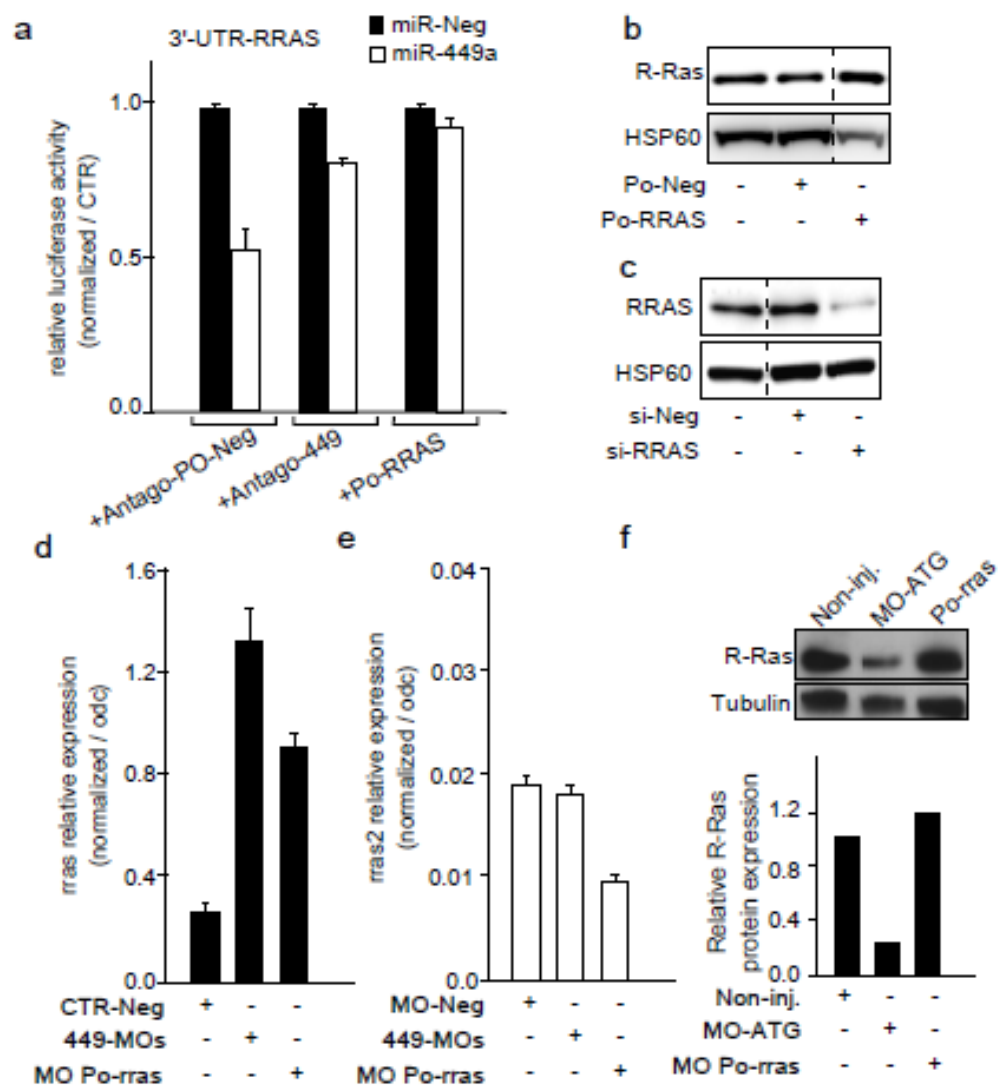


Figure 6  
Chevalier & Adamiok et al.,



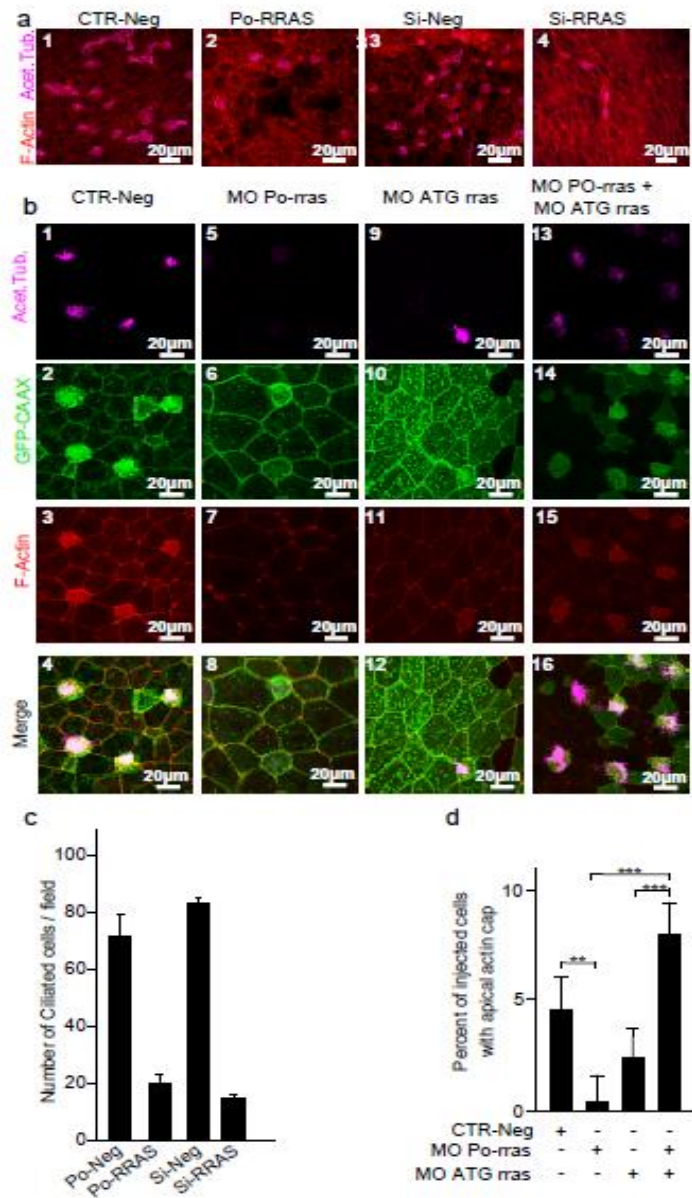


Figure 7  
Chevalier & Adamiok et al.,



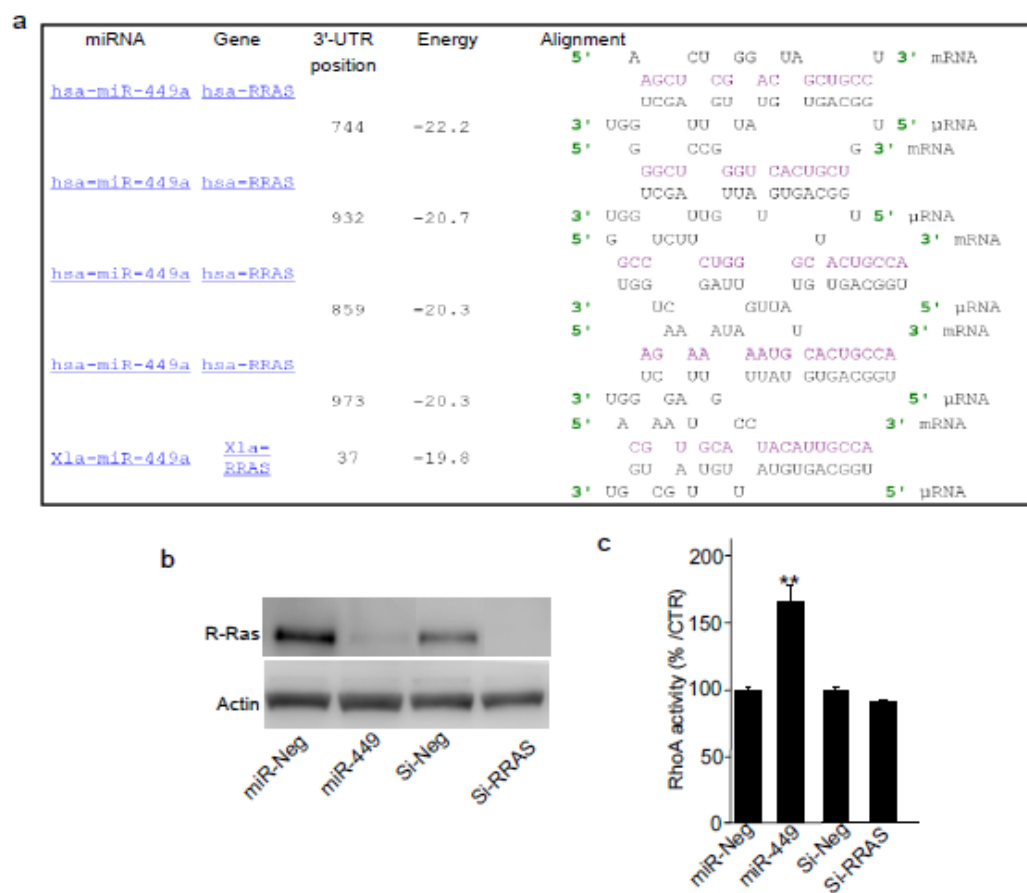
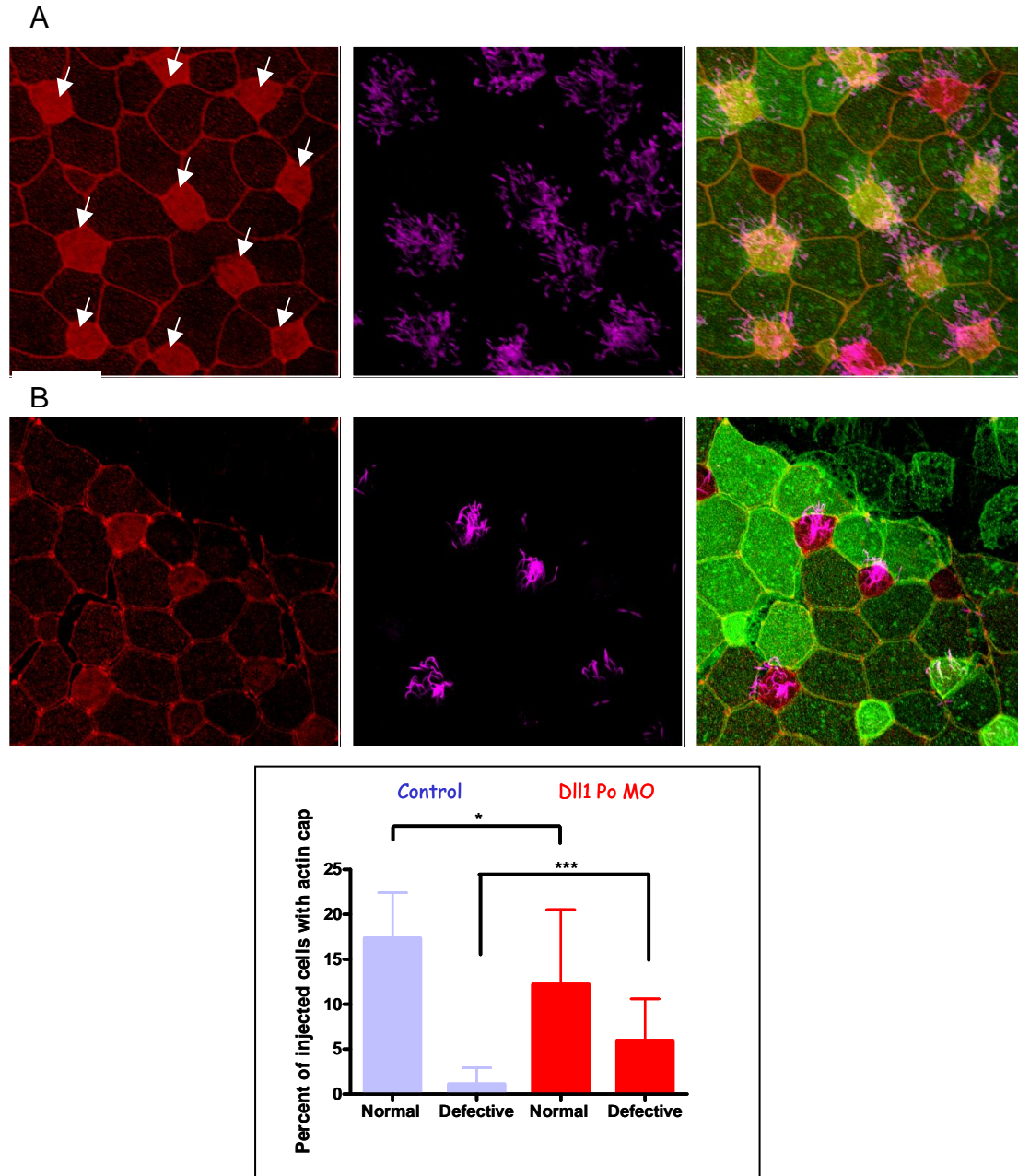


Figure S1  
Chevalier & Adamiok et al.,

**Unpublished data**

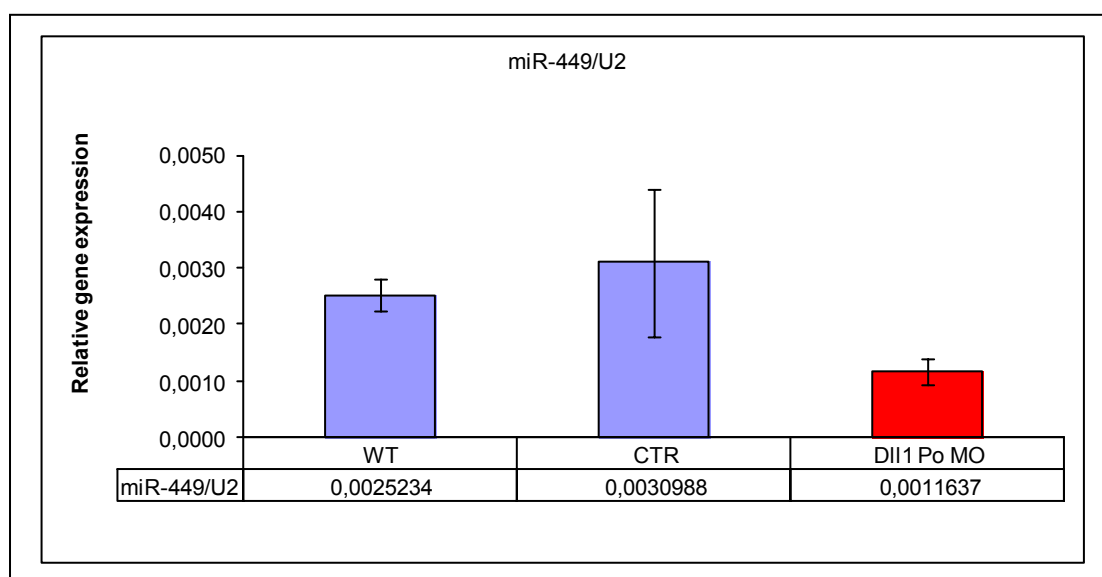
\* Additional data on Delta1  
(to be included in new version of manuscript)



**Figure S2.** Actin cap formation in control (A) and Delta1 Protector MO (B). The Delta1 protection from miR-449 binding caused disruptions in F-actin cytoskeleton reorganization in *Xenopus laevis* MCCs (embryos at stage 25). Histochemistry with phalloidin in red, acetylated-tubulin in magenta and membrane GFP in green. The graph shows the quantification of MCCs with normal and defective actin cap in control and morphants embryos.

The involvement of Delta1 a bona fide target of miR-449 in actin cap formation was tested by performing immunostaining with phalloidin (marker of F-actin) and acetylated-tubulin (marker of cilia) on embryos injected with Delta1 protector morpholino. These data showed that Delta1 controls the F-actin cytoskeleton reorganization in the MCCs of frog mucociliary epithelium (Fig. S2).

Moreover, we revealed the presence of a feedback loop between miR-449 and Delta1 by performing qRT-PCR on explanted ectoderm upon injection with Delta1 protector morpholino (Table S1).



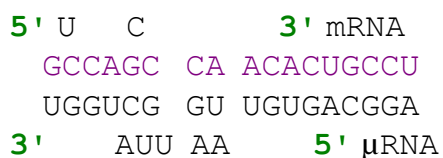
**Table S1.** miR-449 down-regulation upon Delta1 Protector MO injection in explanted ectoderm at stage 19.

## 7. Unpublished data on Rho- A GDP dissociation inhibitor beta (Arhgdib).

### 7.1. Arhgdib, a putative miR-449 target

The role of GTPases in the reorganization of the ciliated cells apical actin cytoskeleton has been already demonstrated (Pan et al, 2007). Therefore it was reasonable to search among the putative targets of miR-449 those, which could be the regulators of Rho-GTPases activity, such as GDP dissociation inhibitors (GDIs), GTP activating proteins (GAPs) and GTP exchange factors (GEFs). The first candidate was ArhdiB.

The target prediction software called Mediante/MicroCible (IPMC Sophia Antipolis website: <http://www.microarray.fr>) revealed the presence of a putative miR449 binding site in the 3' UTR of human and *Xenopus* Arhgdib (Fig. I). We expected that Arhgdib, a known regulator of Rho (Ota et al, 2004), could be a good candidate to be an actin cytoskeleton modulator in MCCs.



**Figure I.** miR-449a seed region matching to the Arhgdib 3'UTR mRNA.

Arhgdib is a member of the RhoGDI2 family of Rho inhibitors (Olofsson, 1999). So far, three Rho- GDIs have been described, called Rho-GDI1, Rho-GDI2 (RhoGDIβ, D4-GDI or Ly-GD) and Rho-GDI3. However, only Rho-GDI1 and 2 participate in the regulation of GDP-GTP cycle and the membrane association/dissociation cycle of Rho proteins (Olofsson, 1999). These inhibitors interact with the GDP bound inactive forms of Rho GTPases, thus preventing the binding of guanine nucleotide exchange factors to Rho. Hence, Arhgdib controls the Rho protein activity and localization. The spatiotemporal recruitment of RhoGTPases

to their targets must be tightly controlled, and RhoGDIs are involved in Rho GTPases translocation between the membrane and the cytoplasm as well as in Rho GTPases anchoring to the membrane (Olofsson et al, 1999).

Most of the studies on Arhgdib focused on its involvement in the hematopoiesis and cancer metastasis (Ota et al, 2004). However, it was also presented that RhoGDIs are involved in Rho GTPases translocation between the membrane and the cytoplasm (Olofsson et al, 1999). It was assumed, that RhoGDIs participate in Rho GTPase anchoring to the membrane.

The Rho-GTPases signaling pathway is related to many cellular processes, such as, cytoskeleton organization, cell adhesion, cells migration and survival, transcriptional regulation or vesicle trafficking (Ota et al, 2004, Pan et al, 2007), thereby it is expected that RhoGDIs play important roles in these processes, which in turn are related to the complex process of cilia formation.

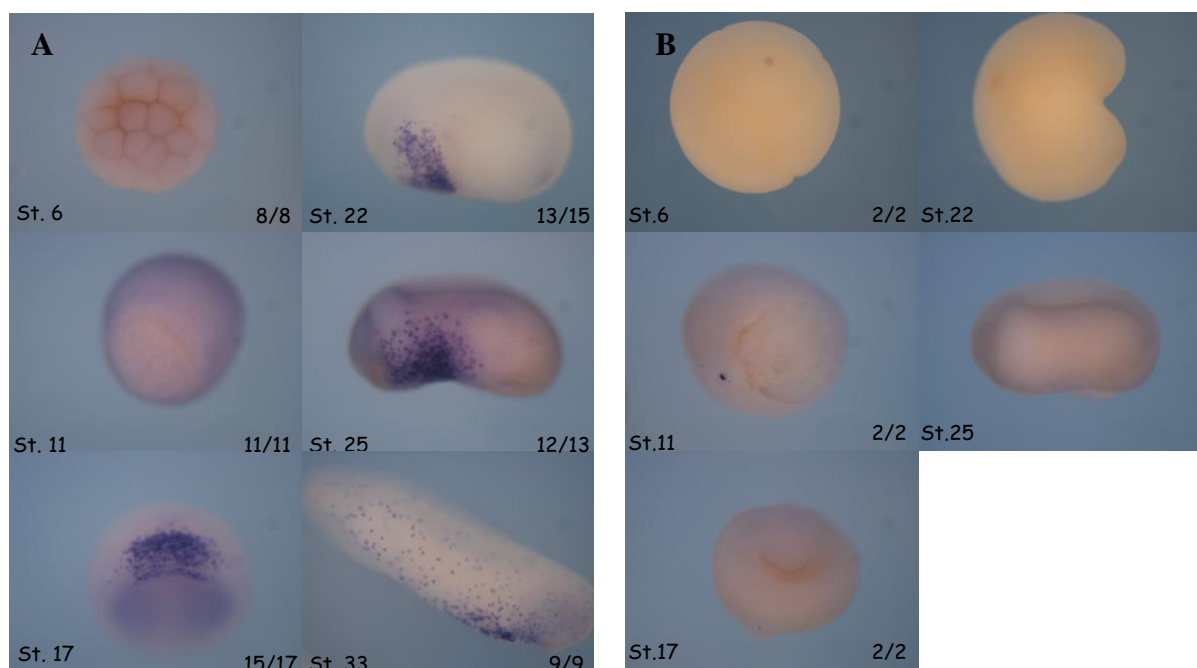
We therefore decided to explore more in detail the possible role of Arhgdib in *Xenopus* MCC development. For this, we started by analyzing its expression pattern.

## **7.2. Spatiotemporal expression of Arhgdib in whole-mount embryos.**

We performed *in situ* hybridizations with an Arhgdib digoxigenin-UTP labelled RNA probe between the cleavage and late tailbud stages (6 to 33) of *Xenopus laevis* development.

The expression pattern of Arhgdib changes during the course of embryo development (Fig.II). At early stages, between cleavage and gastrulation, Arhgdib RNA is not detectable. However, after stage 11 and before stage 17 Arhgdib starts to be apparent in the ventral mesoderm. From stage 17, the expression is high although, at stage 22, it is restricted to the Ventral Blood Island (VBI), located in the ventral mesoderm between the liver anlagen, the proctodeum and the dorsolateral plate. The high level of Arhgdib is visible at stage 25 (tailbud), when it seems to be present in the migrating hematopoietic cells, but also in the AGM (aorta-gonads-mesonephros) region. At stage 33 (late tailbud) Arhgdib expression shows a “salt and pepper” pattern, being present in scattered cells evenly distributed along the embryo (Fig. II). However, this expression remains restricted to hematopoietic cells.

Additionally, a sense Arhgdib RNA probe was used as a negative control. *In situ* with both probes, antisense and sense were performed in parallel. As expected the sense probe failed to detect any specific signal (Fig.IIB).



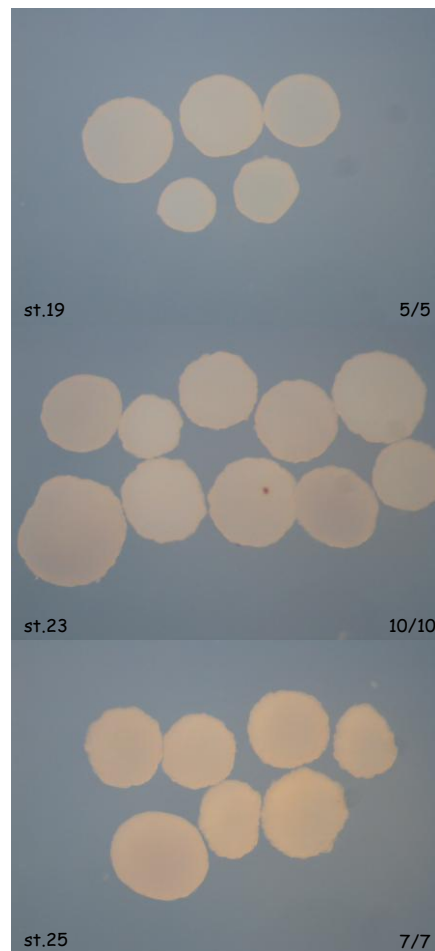
**Figure II.** Spatiotemporal expression pattern of Arhgdib RNA in *Xenopus laevis* embryos by using *In situ* hybridization at different stages of development (6, 11, 17, 22, 25 and 33). A) ISH with Arhgdib antisense probe, B) ISH with Arhgdib sense probe. Concentration of both probes: 100ng/ $\mu$ l.

### 7.3. Spatiotemporal expression of Arhgdib in explanted ectoderm

Since, the evidence for expression of Arhgdib in the ectoderm was not clear, we decided to perform *In situ* hybridization on ectoderm explants (animal caps). The histochemistry as well as *in situ* hybridization performed on explanted ectoderm give an ectoderm-specific staining, when compared to whole-mount embryos.

The same RNA probe used for Arhgdib *in situ* hybridization on whole-mount embryos was used for ISH on explanted ectoderm. However, here Arhgdib expression is not detectable at any of analysed stages (Fig. III). Therefore, we concluded that Arhgdib expression is absent from the ectoderm in *Xenopus laevis* embryos from cleavage to late tailbud stages, the time of development during which

multiciliogenesis occurs. Consequently, we decided not to continue the functional analysis of this gene.



**Figure III.** Spatiotemporal expression pattern of Arhgd1B RNA in *Xenopus laevis* explanted ectoderm by using *In situ* hybridization at different stages of the embryogenesis.



## 8. Unpublished, preliminary data on Steel a KIT ligand

### 8.1. Steel - a putative miR-449 target

Two different target prediction softwares including: Target Scan (Tab. I) and Mediante/MicroCible (designed by IPCM Sophia Antipolis) showed a miR-34/449 binding site at 3'UTR of Steel1 mRNA (Fig.IV).

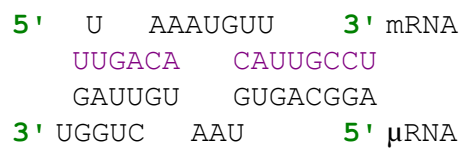
Additionally, we noticed that the Steel target site for miR-34/449 is widely conserved among the vertebrates, for example it exists in the goat, rat, mouse and human genomes.

**TargetScanHuman**  
Prediction of microRNA targets  
Release 6.2: June 2012

**Frog I miR-34ac/34bc-5p/449abc/449c-5p**  
85 conserved targets, with a total of 89 conserved sites and 12 poorly conserved sites.  
Table sorted by total context score [Sort table by aggregate P<sub>CT</sub>]  
Genes with only poorly conserved sites are not shown [View top predicted targets, irrespective of site conservation]  
The table shows at most one transcript per gene, selected for having the highest aggregate P<sub>CT</sub> (or the one with the longest 3' UTR, in case of a tie).  
[Show all transcripts]

| Human ortholog of target gene | Representative transcript | Gene name  | Conserved sites |      |         | Poorly conserved sites |      |         | Representative miRNA | Total context score | Aggregate P <sub>CT</sub> |
|-------------------------------|---------------------------|--|-----------------|------|---------|------------------------|------|---------|----------------------|---------------------|---------------------------|
|                               |                           |  | total           | 8mer | 7mer-m8 | total                  | 8mer | 7mer-m8 |                      |                     |                           |
| PALM2                         | NM_001067293              | paladinin 2  | 1               | 1    | 0       | 1                      | 1    | 0       | xt-miR-34a           | -0.88               | 0.64                      |
| NAV3                          | NM_014503                 | neuron navigator 3   | 2               | 1    | 1       | 1                      | 3    | 0       | xt-miR-34a           | -0.79               | 0.96                      |
| FOXN3                         | NM_001065471              | forkhead box N3  | 1               | 0    | 0       | 3                      | 3    | 1       | xt-miR-449           | -0.71               | 0.68                      |
| PRGRC2                        | NM_008520                 | progesterone receptor membrane component 2   | 1               | 0    | 0       | 1                      | 1    | 0       | xt-miR-449           | -0.64               | 0.67                      |
| PDGFRA                        | NM_006506                 | platelet-derived growth factor receptor, alpha polypeptide   | 2               | 0    | 1       | 1                      | 0    | 0       | xt-miR-34a           | -0.57               | 0.90                      |
| ZNF281                        | NM_016462                 | zinc finger protein 281  | 1               | 1    | 0       | 0                      | 3    | 0       | xt-miR-34a           | -0.55               | 0.87                      |
| FOXP1                         | NM_032662                 | forkhead box P1  | 2               | 0    | 2       | 0                      | 0    | 0       | xt-miR-34a           | -0.53               | 0.91                      |
| FOXQ                          | NM_032660                 | forkhead box Q   | 1               | 1    | 0       | 0                      | 0    | 0       | xt-miR-34a           | -0.53               | 0.82                      |
| PLAG1                         | NM_001114634              | pleiomorphic adenoma gene 1  | 1               | 1    | 0       | 0                      | 3    | 0       | xt-miR-34a           | -0.52               | 0.81                      |
| ZIC5                          | NM_033152                 | Zic family member 5  | 1               | 1    | 0       | 0                      | 3    | 0       | xt-miR-34a           | -0.52               | 0.85                      |
| CDK8                          | NM_001145336              | cyclin-dependent kinase 8  | 1               | 1    | 0       | 0                      | 3    | 0       | xt-miR-449           | -0.52               | 0.72                      |
| PPFIA1                        | NM_008525                 | protein tyrosine phosphatase, receptor type, I polypeptide (PTP1F), interacting protein (tipin), alpha 1 | 1               | 1    | 0       | 0                      | 3    | 0       | xt-miR-34a           | -0.51               | 0.64                      |
| KITLG                         | NM_008589                 | KIT ligand   | 1               | 1    | 0       | 0                      | 3    | 0       | xt-miR-34a           | -0.49               | 0.14                      |
| RGS17                         | NM_012419                 | regulator of G-protein signaling 17  | 1               | 1    | 0       | 0                      | 3    | 0       | xt-miR-34a           | -0.49               | 0.61                      |

**Table I.** A shortened list of predicted targets of miR-34/449 family of microRNAs in *Xenopus* obtained from the Target Scan. KIT ligand is also present.



**Figure IV.** miR-449a seed region matching to 3'UTR of *Xenopus* Steel1 mRNA. Data obtained from Mediante/MicroCible software.

The Steel gene (also known as SCF or Kitl) encodes a secreted glycoprotein acting as a ligand for a type III transmembrane tyrosine kinase of the PDGFR family, called KIT (Ashman, 1999). The interaction between steel ligand and its receptor c-kit occurs through a KIT extracellular region, which contains multiple immunoglobulin-like domains. Upon ligand binding the KIT receptor undergoes dimerization and autophosphorylation on some intracellular tyrosine residues. Phosphorylated tyrosine residues serve as docking sites for numerous signal transduction molecules. Therefore, activated KIT is able to interact with many, different components of signal transduction pathways, including JAK/STAT, Src, PI3K, Ras-Raf-MAPK and PLC (Ogawa et al, 1993; Ronnstrand, 2004).

The Steel/KIT signaling has been widely studied in cancer. Where, c-kit loss of function caused defects in pigmentation, reduced fertility and anemia (Ashman, 1999).

Also, some evidences on involvement of Steel/KIT signaling in *Xenopus* development can be found in the literature. Notably, *Xenopus* Steel is expressed in epidermis at early stages of development until stage 37, while the KIT receptor was found to be expressed by scattered epidermal cells (Goldman et al, 2006; Martin et Harland, 2004). Interestingly, *Xenopus* c-kit is among the genes up-regulated after overexpression of MULTICILIN, a protein required in multiciliogenesis (Stubbs et al, 2013), while in mouse c-kit was found enriched in purified MCCs (Hoh et al, 2012).

These observations, together with data obtained in our laboratory and showing that *Xenopus* KIT is indeed expressed by MCCs and that interfering with its function resulted in anomalies of the MCC distribution (A. Pasini, unpublished results)

prompted us to further analyze the possible role of the Steel/KIT pathway and of its likely regulation by miR449 in MCC and MCE development.

## **8.2. Spatiotemporal expression of *Xenopus* Steel1 and Steel2 in whole-mount embryos**

The expression pattern of Steel in *Xenopus laevis* embryos has been published by Martin and Harland, however we wanted to better analyze it. In their publication the expression of two *Xenopus laevis* Steel homologues: Xsl-1 and Xsl-2 have been investigated (Martin et Harland, 2004). Xsl-1 and Xsl-2 expression patterns overlap especially during early development, while later during tailbud stage they diverge significantly.

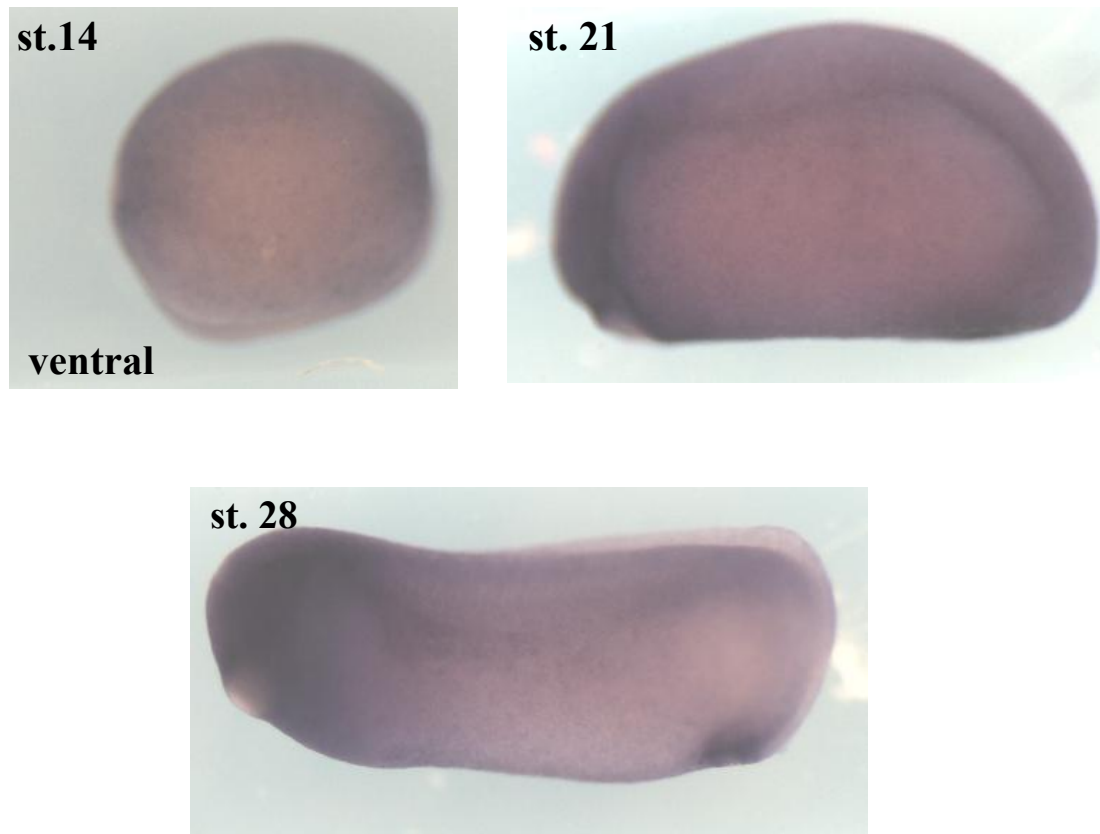
Therefore, to examine the presence of KIT ligand in *Xenopus laevis* embryonic skin we performed an *in situ* hybridization on the whole-mount embryos at different stages of the development (including stages 14, 21 and 28) (Fig. V).

The expression of XlSteel1 starts to be detectable at the beginning of neurulation, between stages 12 and 14, in the outer layer of non-neural ectoderm and in the inner ectodermal layer between the cement gland and neural plate. At stage 28 a high level of XlSteel1 expression is detectable in the forming proctodeum, a region of high ciliary density. At this stage XlSteel1 is also specifically expressed in the pronephrons, neural tube, gill arches and superficial region of the somite (Martin et Harland, 2004). The expression of Steel1 is maintained in the epidermis of *Xenopus laevis* embryos until stage 37. Interestingly, Steel1 is not detectable in the cement gland region at all analyzed stages (Fig.VI).

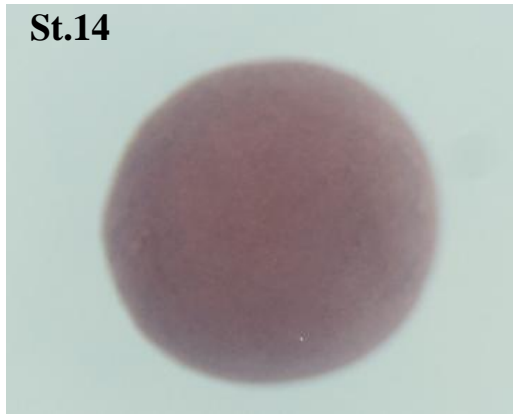
The expression of XlSteel2 is similar to XlSteel1 especially at early stages, until tadpole stages. Later, XlSteel2 is expressed in the ganglion and facial nerve projecting to visceral arch3, the mandibular arch, and the cleft of anterior somites. At stage 28 high expression of XlSteel2 is also apparent in proctodeum (Fig.VII) (Martin et Harland, 2004).

Altogether, our data supported Steel1 and Steel2 specific expression in the ectoderm of *Xenopus laevis* embryos (Fig. VI and VII, data from dr.Andrea Pasini).

However, we focused mostly on Steel1, since a miR-449 binding site has been found only in the 3'UTR of Steel1.



**Figure V.** Expression of *Xenopus laevis* Steel1 RNA by performing *in situ* hybridization on whole-mount embryos at different stages of development (stage 14, 21 and 28). Steel1 digoxigenin-UTP RNA probe was used in the concentration 100ng/ $\mu$ l.

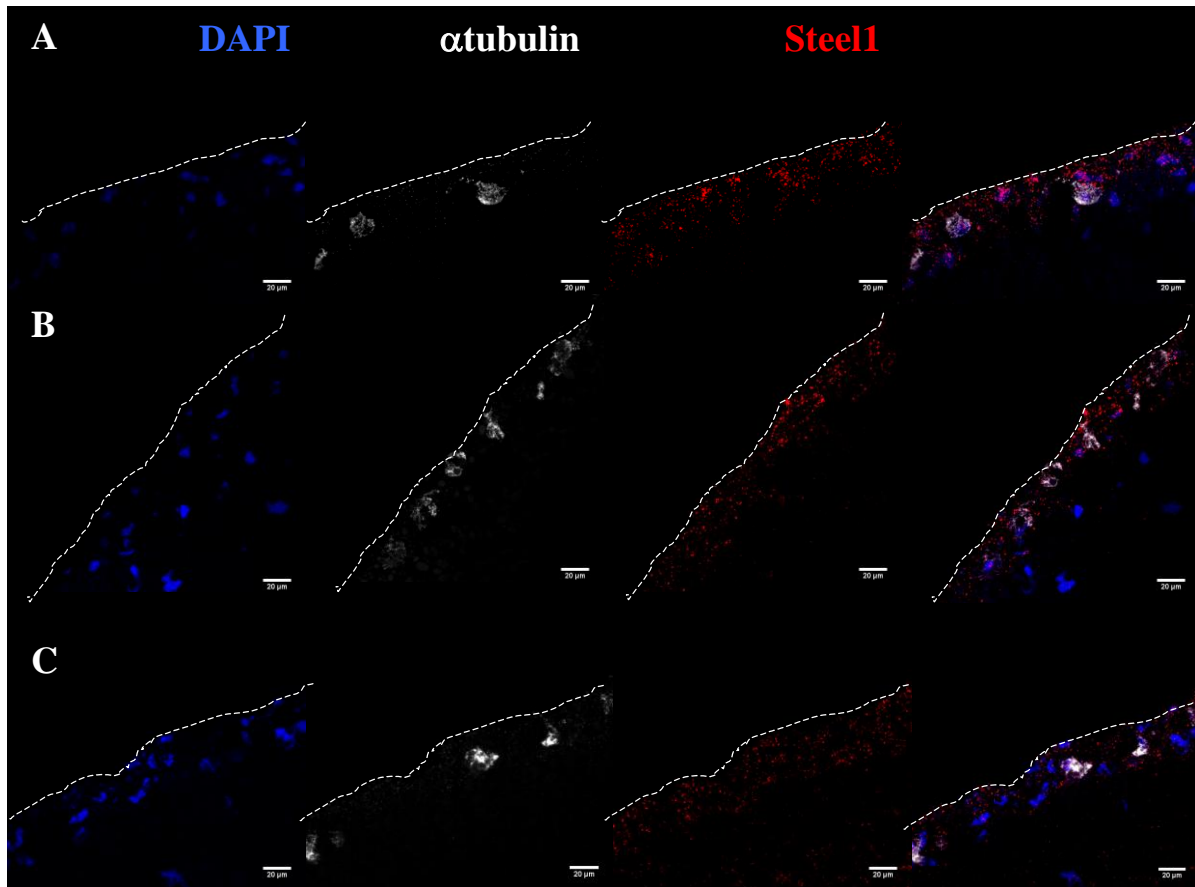


**Figure VI.** Expression of *Xenopus laevis* Steel2 RNA by performing an *in situ* hybridization on whole-mount embryos at different stages of development (stage 14, 21 and 28). Steel2 digoxigenin-UTP RNA probe was used in the concentration 100ng/ $\mu$ l.

### **8.3. Spatiotemporal expression of Steel1 RNA by using double fluorescent *In situ* hybridization (FISH) on sectioned embryos**

Next we wanted to determine the precise cell type of the *Xenopus* mucociliary epithelium where Steel1 is expressed. For that we used double fluorescent *in situ* hybridization on the sectioned embryos at early (Fig. VII) and late stages of development (Fig. VIII). Since we focus our work on the process of motile cilia formation, thus for double in fluorescent *in situ* hybridization we used  $\alpha$ tubulin RNA probe (marker of MCCs progenitors) together with Steel1 probe.

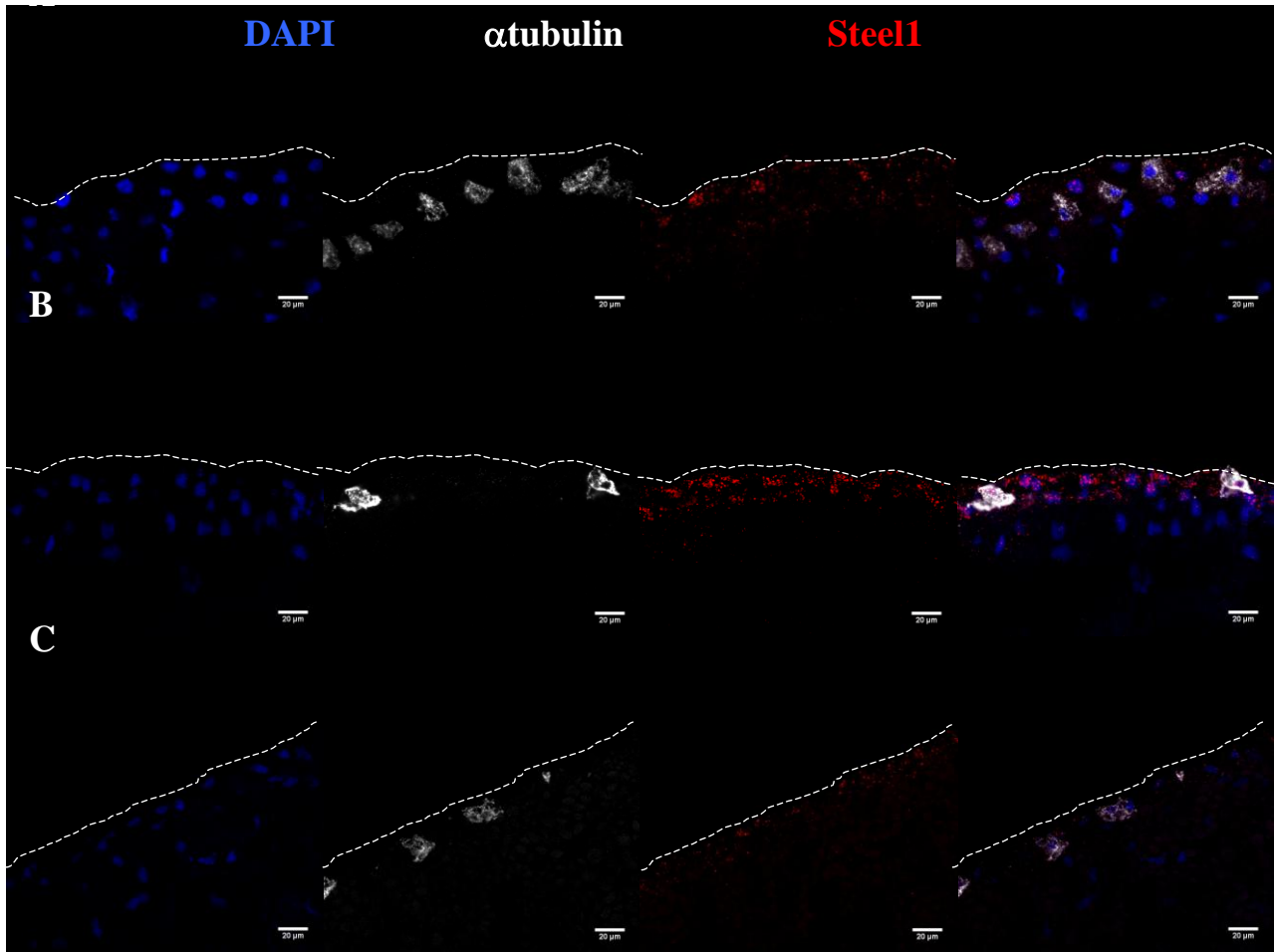
We noticed that Steel1 RNA at early stages (13, 15 and 16) of development is mostly present in the outer layer of ectoderm. It is also apparent in inner ectodermal layer, however at a lower level. At these stages the precursors of ciliated cells are just starting to intercalate into the outer layer and are still mostly found in the inner layer (Fig.VII).



**Figure VII.** Spatiotemporal expression of c-kit ligand Steel1 in non-injected embryos. Fluorescent *in situ* hybridization was performed on sectioned embryos at different developmental stages 13 (A), 15 (B) and 16 (C). DAPI stained the nucleus in blue. Double FISH:  $\alpha$ tubulin RNA probe in grey shows MCCPs, Steel1 RNA probe in red shows Steel1 positive cells.

At late stages (16, 18 and 20) Steel1 RNA is still mainly expressed in outer ectodermal layer, although the expression level at stage 20 is decreased. Interestingly, there's very little overlap between Steel1 and the alpha-tubulin signal, showing that Steel1 tends to be expressed at very low level in the prospective MCCs (Fig.VIII).

This is consistent with the hypothesis that Steel1 is a target of miR-449 and it suggests that Steel1 expression has to be spatially tightly controlled.

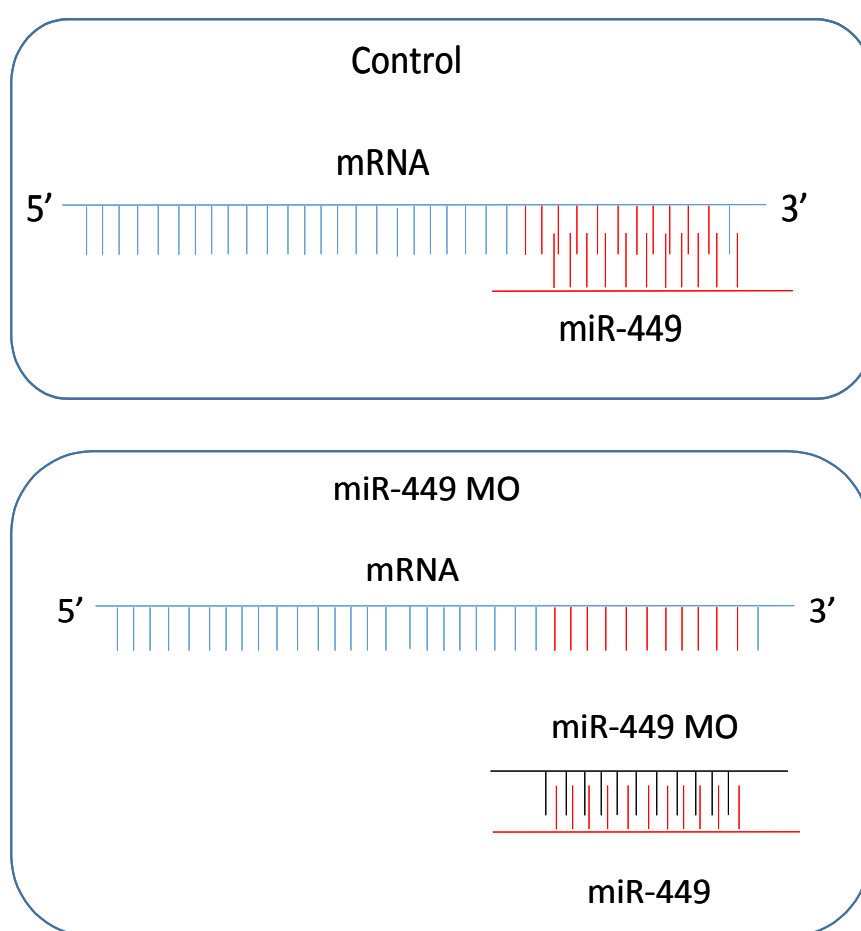


**Figure VIII.** Spatiotemporal expression of Steel1 in non-injected embryos. Fluorescent *in situ* hybridization was performed on sectioned embryos at different developmental stages 18 (A), 19 (B) and 24 (C). DAPI stained the nucleus in blue. Double FISH:  $\alpha$ tubulin RNA probe in grey shows MCCPs, Steel1 RNA probe in red shows Steel1 positive cells.



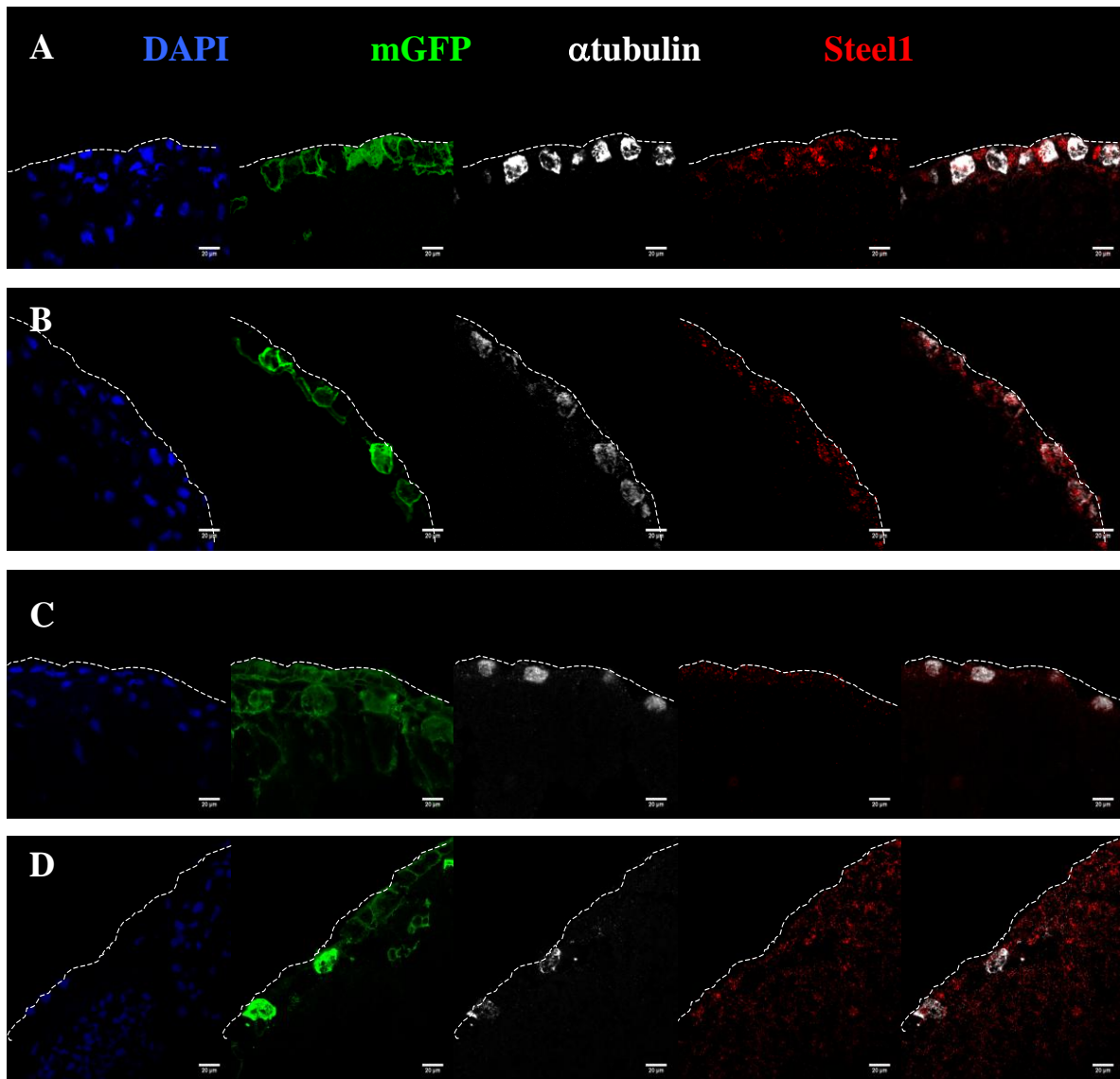
#### 8.4. Spatiotemporal expression of Steel1 RNA following miR-449a inactivation

As a first step to confirm that miR449 controls the expression of *Xenopus* Steel1, we compared the distribution of Steel1 mRNA at different stages of development (st.19 and 24) in control embryos (Fig.IX A, C) and embryos injected with morpholinos against miR-449a (miR-449a morphants) together with membrane GFP mRNA (Fig.IX B,D), these morpholinos bind to the seed region of miR-449a and prevent interaction of miR-449 with all of its mRNA targets. In other words, suppression of miR-449 activity causes indirect up-regulation of the mRNA targets (Scheme 1).



**Scheme I.** Mechanism of action of morpholinos blocking the activity of miRNA by taking example from miR-449. miR-449 MO bind to the seed region of miR-449 and prevent its binding to 3'UTR of all its target mRNAs.

As it was done previously for wild type embryos, double in fluorescent *in situ* hybridization with  $\alpha$ tubulin and Steel1 RNA probe was performed also in morphants. Immunostaining with antiGFP antibody was used to track the injected cells. In the control embryos the expression of Steel1 is strong in the outer ectodermal layer but not overlapping with the  $\alpha$ tubulin signal. On the other hand, in the miR-449a morphants Steel1 is detectable in the cells positive for the multiciliated cell progenitor (MCCPs) marker  $\alpha$ tubulin (Fig.IX). Additionally, Steel1 expression is increased in the outer and inner layer of ectoderm (Fig. IX D).

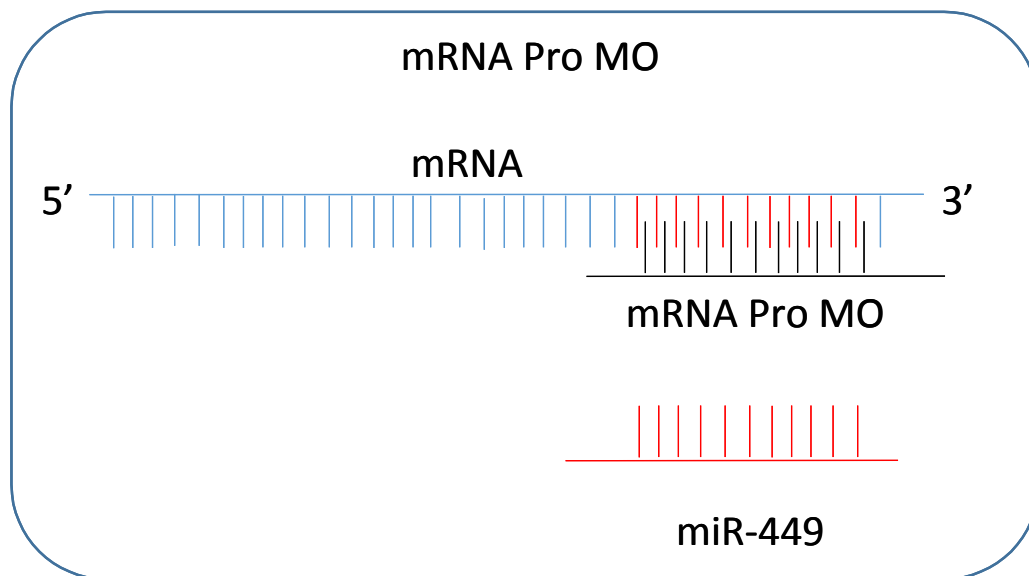


**Figure IX.** Spatiotemporal expression of Steel1 in control embryos (A and C) and miR-449 morphants (B and D). Fluorescent *in situ* hybridization was performed on sectioned embryos at different developmental stages 19 and 24. DAPI stained the nuclei in blue, GFP stained the injected cells in

green. Double FISH:  $\alpha$ tubulin RNA probe in grey shows MCCPs, Steel1 RNA probe in red shows Steel1 positive cells.

### **8.5. Using "protector morpholinos" to specifically and selectively inhibit the interaction between miR-449a and Steel1**

The previously used miR-449 MOs are suitable for deciphering the role of miR-449 and its targets in MCE development. However, this approach disrupts the interaction between miR-449 and all its targets. We designed specific morpholinos, which protect Steel1 from miR-449 binding (Steel1 Po MO). These antisense oligonucleotides specifically block the miR-449 binding site on the Steel1 3'UTR and thus free Steel1 mRNA from the inhibitory effect of miR449. Accordingly, these morpholinos indirectly up-regulate Steel1 by protecting it from miR-449 binding. Protector morpholinos are more specific, because they target not only the "seed" sequence (which is identical or extremely similar on all the targets), but also a bit of the flanking regions, which are specific to each target mRNA (Scheme II).



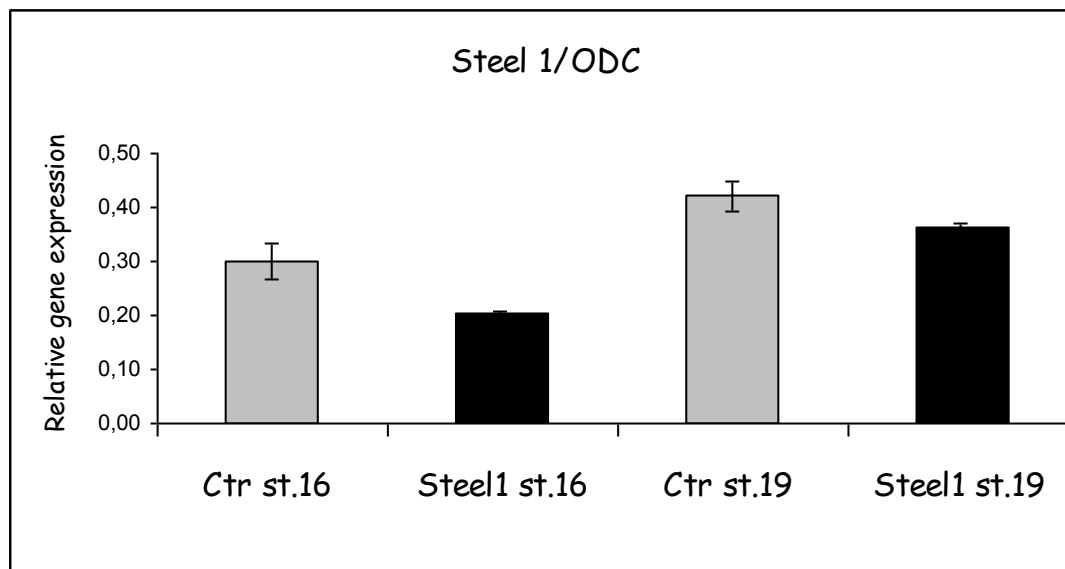
**Scheme II.** Mechanism of 3'UTR mRNA protection from microRNAs (for example miR-449) binding. The protector Morpholinos (mRNA Pro MO) bind to miR-449 binding site at 3'UTR of target mRNA and flanking region of particular mRNA.

First, we verified the activity of the designed protector morpholinos by performing RT-qPCR on explanted ectoderm at stages 16 and 19 from control and Steel1 Po morphants (Fig.X). As a control we used morpholinos, specifically binding to a region on the Steel1 3'UTR, which did not reveal consensus binding sites for any miRNAs (according to the Mediante/microcible software).

RT-qPCR with Steel1 specific primers fails to detect any significant increase in the levels of Steel1 mRNA after Steel1 Po injection (Fig.X). This experiment was repeated three times. One possibility is that miR-449 affects the rate of translation of a given mRNA, rather than its stability. If this was the case for miR449 on the Steel1 mRNA, the effect of the Steel1 Po would be detectable only with an anti-Steel antibody. Currently, we are looking for antiSteel antibodies that could cross-react with the Xenopus Steel1.

Another possibility is that the relative increase in the Steel1 signal is too low to be detected by RT-qPCR. This could be due to the fact that the protector morpholino increases Steel1 expression in MCC, however the number of MCC is too small for the variation to be significant.

Therefore, it is necessary to have a look at the cellular level, hence in fluorescent *in situ* hybridization on section was performed.

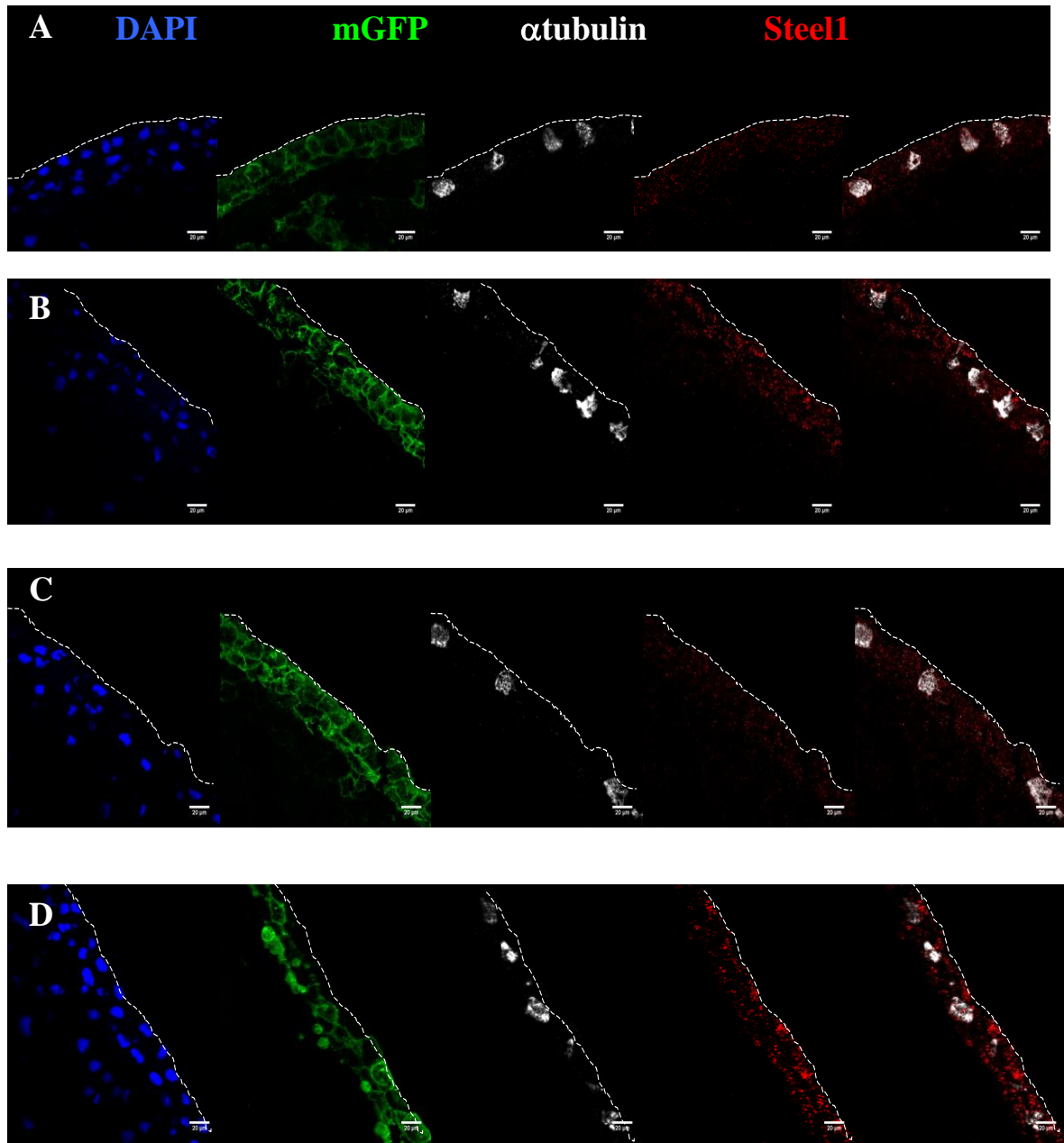


**Figure X.** Steel1 RT-qPCR on explanted ectoderm from control (grey) and Steel1 Po morphants (black) embryos at late neurula stage (st. 16 and 19). ODC was used as a reference gene. 8-cell-stage *Xenopus* embryos were injected in the epidermis precursor blastomeres with control morpholinos or morpholinos against Steel1 Po MO (60ng/ $\mu$ l). RNA was extracted from embryos at stages 16 and 19.

## 8.6. Spatiotemporal expression of Steel1 following Steel1 Po injection

To verify if the pattern of expression of Steel1 changes upon Steel1 protection from miR-449, we performed double fluorescent *in situ* hybridization for Steel1 and  $\alpha$ tubulin in sections from control and morphant embryos (Fig.XI).

Injection in the frogs epidermis precursor blastomeres of a Steel1 protector morpholino, results in Steel1 up-regulation in  $\alpha$ tubulin positive cells (Fig. XI). These results were consistent with those obtained upon injection with miR-449 morpholinos. Interestingly, Steel1 expression is affected mainly in the stages of development corresponding to the cell radial intercalation from inner into the outer ectodermal layer (Fig.XI). This is compatible with our hypothesis that the Steel/Kit signal plays a role in the process of MCC intercalation and that the control of Steel1 expression in MCCs by miR-449 expression is required for their proper intercalation and distribution.

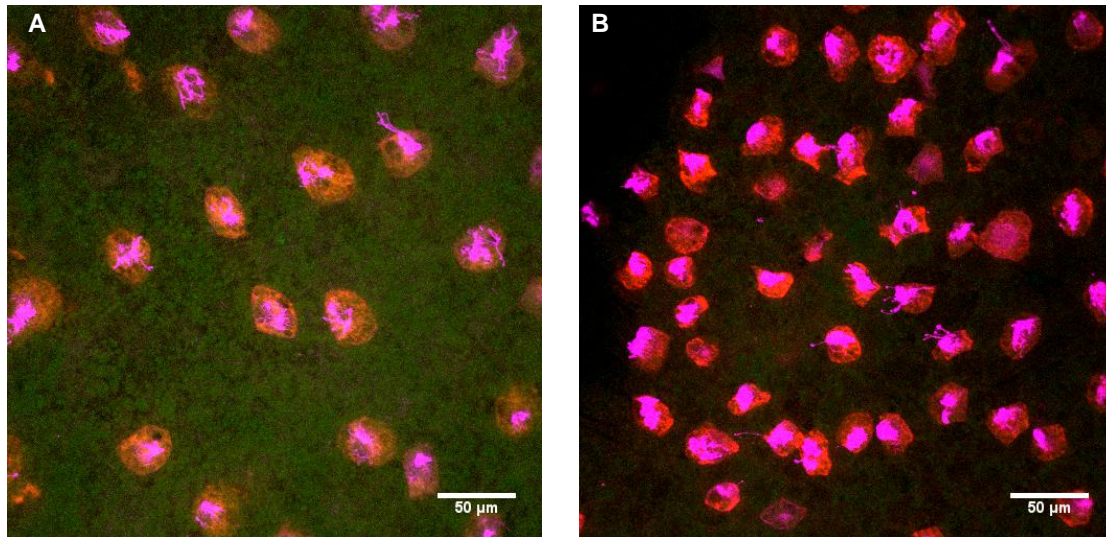


**Figure XI.** Spatiotemporal expression of Steel1 in control embryos (A and C) and Steel1 Po morphants (B and D). Fluorescent *in situ* hybridization was performed on sectioned embryos at different developmental stages 19 and 24. DAPI stained the nucleus in blue, GFP stained the injected cells in green. Double FISH:  $\alpha$ tubulin RNA probe in grey shows MCCPs, Steel1 RNA probe in red shows Steel1 positive cells.

### **8.7. Effect of Steel1 protection from miR-449 binding on MCCPs distribution and intercalation**

We attempted to better understand the involvement of Steel1 in mucociliary epithelium development, by looking at the MCCPs distribution within MCE after disruption of the miR449 control on Steel1 expression. Therefore, we performed  $\alpha$ tubulin (marker of MCCPs) *in situ* hybridization on whole-mount embryos injected with Steel1 Po morpholinos. We used embryos at late stage (st.25), when cilia are fully generated. When compare to control embryos, the Steel1 Po MO injected embryos show impairment in the MCCPs distribution within the embryonic skin (Fig.XII). The morphants exhibit defect in  $\alpha$ tubulin positive cells emergence into the outer layer. Moreover, the MCCPs in the Steel1 Po MO tend to be smaller, which could be explained by their possible arrest in the inner epidermal layer (Fig.XII).

These data shown that tightly controlled Steel1 expression is required for the proper cell development in *Xenopus laevis* mucociliary epithelium.

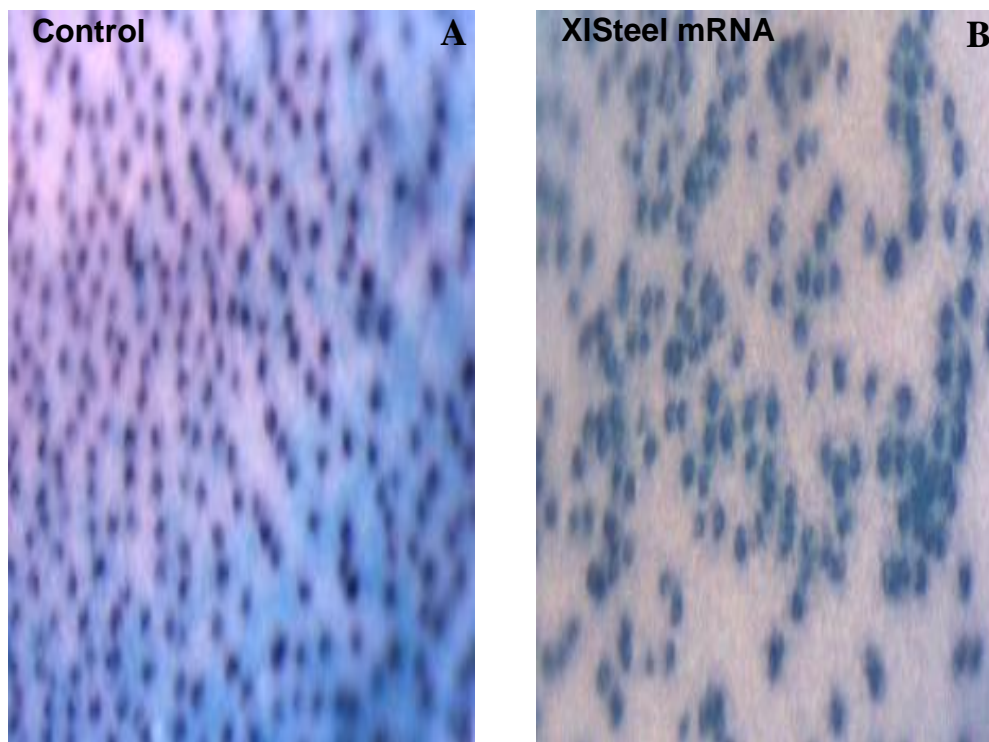


**Figure XII.** Distribution of MCCPs ( $\alpha$ tubulin positive) and MCCs (A,B) within the *Xenopus laevis* embryonic skin at stage 25, in the control embryos (A) and Steel1 PO MO (B). A) Control embryos show normal distribution and intercalation of MCCPs. B) The Steel1 Po MO show impaired distribution of MCCPs. They tend to be smaller and their number is increased when compared to MCCPs from control embryos. Concentration of  $\alpha$ tubulin RNA probe: 40ng/ $\mu$ l. Histochemistry with acetylated-tubulin (A, B) in magenta.

### 8.8. Effect on the Steel1 overexpression on MCCPs distribution and intercalation

In addition to an indirect up-regulation of Steel1 by its protection from miR-449 binding we performed the microinjection of Steel1 mRNA to directly overexpressed Steel1. Accordingly,  $\alpha$ tubulin whole-mount ISH was performed on stage 26 control and Steel mRNA injected embryos. When compared to control embryos, the overexpression of Steel1 affects the distribution and intercalation of MCC progenitors. The MCCPs are associated with each other and lost their spaced pattern of distribution in frog MCE (Fig. XIII).



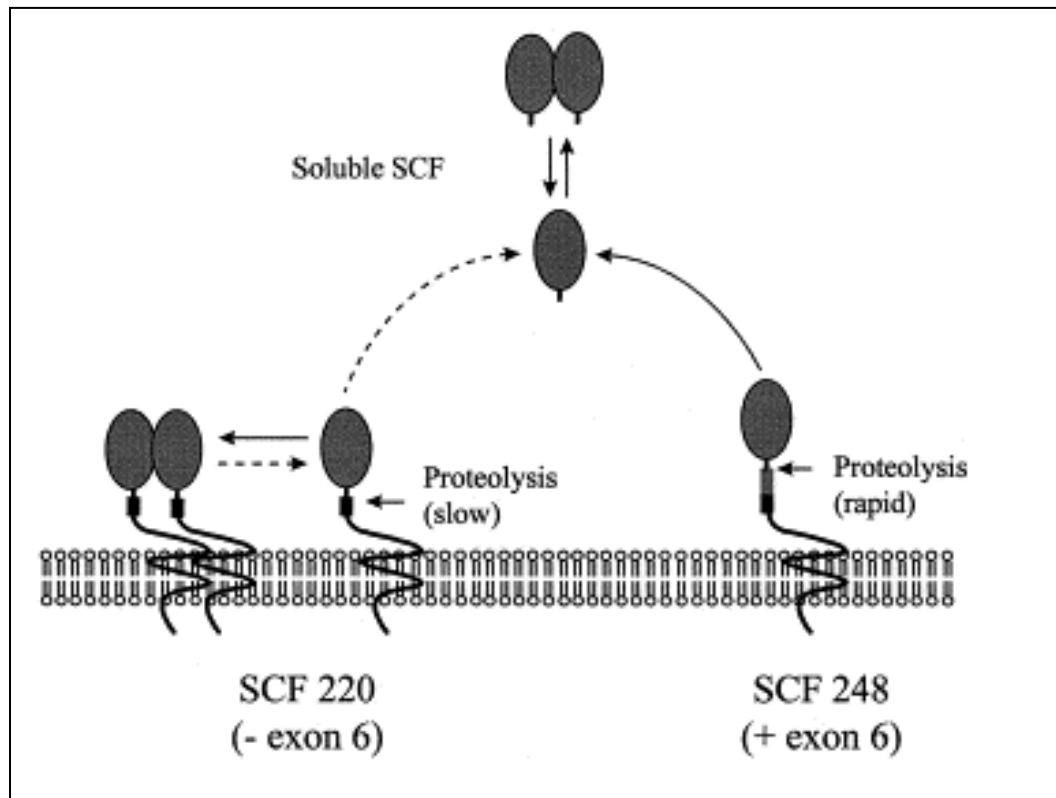


**Figure XIII.** Distribution of MCCPs ( $\alpha$ tubulin positive) within the *Xenopus laevis* embryonic skin at stage 26, in the control (A) and Steel1 mRNA injected embryos (B). A) Control embryos show normal distribution and intercalation of MCCPs. B) Steel1 mRNA injected embryos show impaired distribution and intercalation of MCCPs. The MCCPs tend to be bigger and emerge apical surface in the “clusters” composed of 2 or more MCCPs. Concentration of  $\alpha$ tubulin RNA probe: 40ng/ $\mu$ l.

### 8.9. Elucidating the existence of soluble or membrane bound forms of Steel1 in *Xenopus laevis* embryos.

The mammalian Steel protein can be present under two forms, membrane-bound or soluble. The difference between these two forms is related to the presence or absence of a proteolytic cleavage site for ADAM proteases, located within an amino acid stretch encoded by exon 6. Upon synthesis, both proteins are inserted in the plasma membrane, but the longest isoform, containing the protease consensus site, is successively cleaved to a soluble form, while a shorter isoform, obtained by

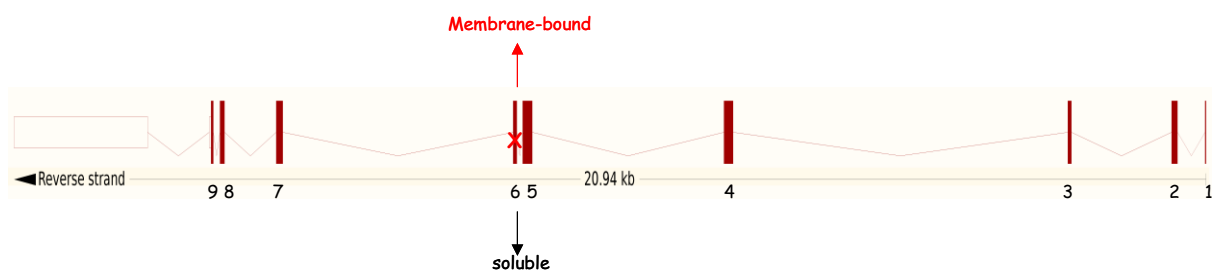
splicing of the exon 6 and therefore lacking the ADAM cleavage site, remains anchored at the membrane (Fig. XIV) (Ashman, 1999). Moreover, this isoform often forms dimers (Ashman, 1999; Ronnstrand, 2004).



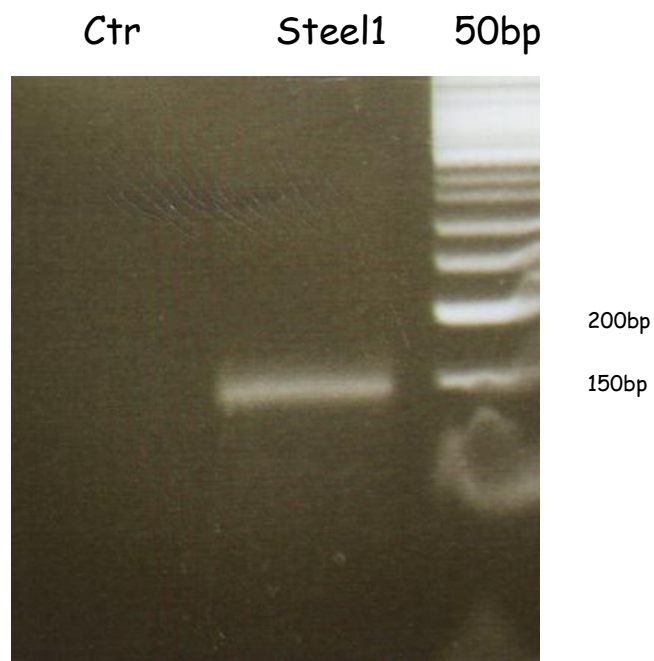
**Figure XIV.** Generation of different forms of SCF. Alternate mRNA splicing resulting in deletion or inclusion of exon 6 leads to the production of two transmembrane forms of SCF (220 or 248 amino acids long). Rapid proteolytic cleavage of SCF 248 gives rise to soluble SCF which can form dimers in solution. A secondary cleavage site, encoded by exon 7, leads to slow release of soluble SCF from SCF 220. Membrane bound SCF forms dimers which appear to be important for function (Ashman, 1999).

The two isoforms of Steel can interact with the KIT receptor, but exhibit different abilities to transmit signals. The membrane-bound isoform causes more sustained activation of KIT, while the soluble isoform leads to rapid and transient activation of KIT as well as its fast degradation. Moreover, membrane-bound ligand leads to more persistent activation of KIT and induces Erk1/2 and p38 mitogen-activated protein kinase (MAPK), as compared to the soluble form (Ronnstrand, 2004).

In *Xenopus*, both the Steel1 and the Steel2 genes present an exon 6, therefore both proteins could in theory be present in membrane-bound and soluble forms. To determine which form of Steel1 is present in the epidermis of *Xenopus laevis* embryos, we designed primers, matching to the flanking regions of the exon 6. The RT-PCR on cDNA synthesized from frog ectoderm explants at stage 16 with these primers only revealed the presence of the exon 6-containing isoform (Fig. XV and XVI). However, the aa stretch encoded by exon 6 does not contain a clear consensus site for ADAM cleavage. It is therefore possible that XlSteel1 is present as a membrane-bound, exon 6-carrying form, similar to what has been suggested for zebrafish Steel (Yao et Ge, 2010).



**Figure XV.** Schematic illustration of the transcript region of *Xenopus laevis* Steel1 with indicated exons in the red and introns in between. Steel1 transcript consists of 10 exons and 9 coding exons. Data obtained from the Ensemble Genome Browser.



**Figure XVI.** Image of RT-PCR product amplify with Steel1 specific primers on *Xenopus laevis* cDNA from whole-mount embryos stage16. The 50bp ladder indicates a small band corresponding to the size of exon 6.

### **III. Materials and methods**

Relative to the Steel analysis

#### **RT-qPCR**

The primers were designed using Primer-BLAST Software. PCR reactions were carried out using SYBRGreen on a CFX Biorad qPCR cycler. All experiments were repeated at least twice on separate injections and the qRT-PCR was performed in triplicate. The relative expression of STEEL1 was normalized to the expression of the housekeeping gene ODC. The qRT-PCR STEEL1 primers are as follows:

Forward:

5' GCACTGGCCTGCTTAGTCAT 3'

Reverse:

5' GCAACTGCCGACAAGCTATC 3'

RT-PCR:

The primers were designed using Primer-BLAST Software from NCBI.

5' GGACCTTGTACCATGCCTGC3'

5' TCCAGACCTGGCAGAGGAAT3'

#### **Double fluorescent in situ hybridization on section**

Embryos were fixed in MEMFA, store in methanol overnight in – 20°C, rehydrated and embedded in O.C.T Compound (VWR Chemicals Prolabo). The sections were performed at 12µm thickness in a cryostat (CM3050SLeica) and frozen in – 80°C. Fluorescent in situ hybridization was carry out using Tyramide Signal Amplification - TSA<sup>TM</sup> Plus Cyanine 3/Fluorescein System (PerkinElmer, Waltham, MA USA). The antisense or sense (control) RNA probes from Steel1 and  $\alpha$ -tubulin (Deblandre et al.1999) were generated from linearized plasmids using digoxigenin or fluorescein RNA-labeling mix (Roche). The sections (stage 13, 16, 19, 24) were hybridized with Digoxegenin and Fluorescein probes at the same time at 60°C overnight. The first probe was detected with DIG horse-radish peroxidase (POD) antibody (1:500, Roche

Germany) and Cy3 Fluorophore Amplification Reagent (TSA™ Plus). The second probe was detected by incubation with fluorescein POD antibody (1:500, Roche Germany) followed by reaction with Cy5 Fluorophore Amplification Reagent (TSA™ Plus). After hybridization the immunostaining with anti-gfp antibody was performed.

### **Morpholino antisense oligos (MO)**

Morpholino oligonucleotides against miR-449 (GeneTools, LLC) were antisense to *Xenopus tropicalis* miR-449:

miR-449a morpholino oligonucleotide, 5'-ACCAGCTAACATTACACTGCCT-3'

morpholino oligonucleotide control, 5'-TGCACGTTTCAATACAGACCGT-3'

MiR-449 a MO were injected at a concentration 10ng/9,2µl of each at 8-cell stage.

The protector morpholino oligonucleotides directed against miR-449-binding sites in STEEL1 3'-UTR have the following sequences

5'- TGGAAATTTGGCAGTGCATTCCAGA -3'

The protector MO was injected at a concentration 30ng/9,2µl at 8-cell stage.

CONTROL for STEEL1 PO MO

5'CCAAAGAAATGCCCTTGTGAATACA3'

### **In fluorescent *in situ* hybridization on whole-mount embryos**

(adapted from Castillo-Briceno et Kodjabachian, 2013).

RNA probes were synthesized and labelled with digoxigenin (DIG) or fluorescein (FLUO) from plasmids containing the appropriate hybridizing sequences for the Steel1 and  $\alpha$ tubulin (gift from Christopher Kintner, Salk Institute for Biological Studies, U.S). The samples stored in ethanol at -20°C were progressively rehydrated in 75%, 50% and 25% ethanol in PBT (0.1% Tween 20 in 1× PBS), and then in PBT; they were then treated with 0.1 M triethanolamine (TEA) pH8 for 5 min. and 0.5% acetic anhydride in 0.1 M TEA for 10 minutes, and washed in PBT; they were then treated with proteinase K (PK) at 2 µg/ml final concentration for 8 min., washed with PBT and placed in bleaching solution (600 µl RNase free water, 325 µl H<sub>2</sub>O<sub>2</sub>, 50 µl

formamide and 25 µl 20X SSC) under bright light, washed and re-fixed in formaldehyde 4% for 20 min. After that, samples were successively placed in HM hybridization mix (1% w/v Roche blocking agent, 25% 20X SSC, 50% Formamide, 0.01% heparin, 0.1% Torula RNA, 0.1% Tween 20, 0.1% CHAPS, 5 mM EDTA pH8, in bi-distilled water) 50% in PBS and HM 100%. The samples were subsequently incubated with the respective probes in HM 100% at 60°C for 18 h. On day 2, samples were successively washed in HM 50% (in 2x SSC and CHAPS 0.1%) at 37°C, in 2x SSC and CHAPS 0.1% at 37°C, in 0.2x SSC and CHAPS 0.1% at 60°C, MABX (0.1% TritonX-100, maleic acid 0.1 M and NaCl 0.15 M) 50% in 0.2x SSC and CHAPS 0.1% at RT and, finally, in MABX. Embryos were then placed in blocking buffer (2% Roche blocking reagent, 10% fetal bovine serum and 5% DMSO in MABX) during 1.5 h and then incubated with anti-DIG or anti-FLUO labelling antibodies from sheep at 4°C for 18 h and washed with MABX. Fluorescent ISH (FISH) was performed with horse-radish peroxidase (POD) conjugated antibodies at 1:500 in blocking buffer and detected with TSA Plus fluorescein or Cy3 kits (PerkinElmer) for FLUO or DIG tagged probes, respectively. Samples were incubated with the TSA substrate for 1 h and then washed with MABX; then, the reaction was stopped with 2% H<sub>2</sub>O<sub>2</sub> in PBS for 0.5 h and washed in MABX. From TSA substrate addition until imaging, samples were kept protected from the light.

For chromogenic ISH (CISH), TEA treatment was omitted. ISH was carried-out with alkaline phosphatase (AP) conjugated antibodies at 1:5000 in blocking buffer, and detected with 0.5x BM-purple substrate in water.

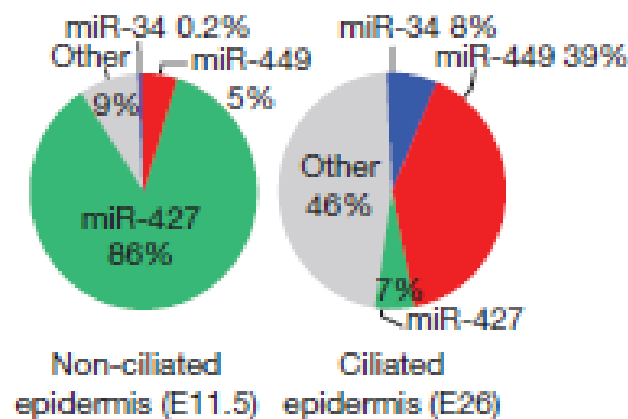
## Discussion



## IV. Discussion

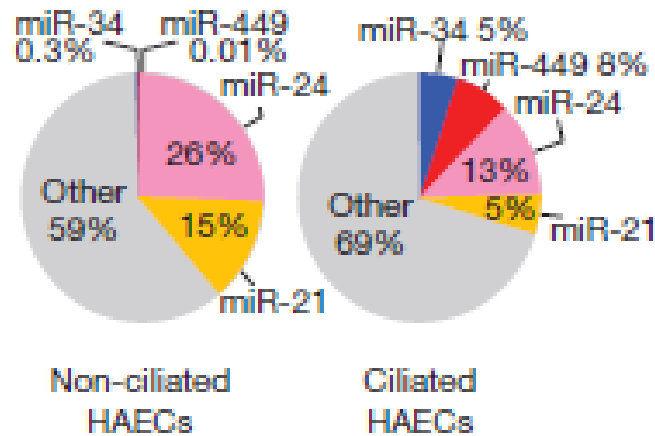
### miR-449 involvement in multiciliogenesis

The first attempts to characterize the possible regulatory role of miR-449 in *Xenopus laevis* epidermal multiciliogenesis have been made using RNAseq, microarray and quantitative PCR assays on explanted ectoderm at stage 11,5 (gastrulation), before the multiciliated cells appearance and stage 26 (tailbud), when the multiciliated epidermis is fully developed (Fig.XVII) ( Marcet et al, 2011).



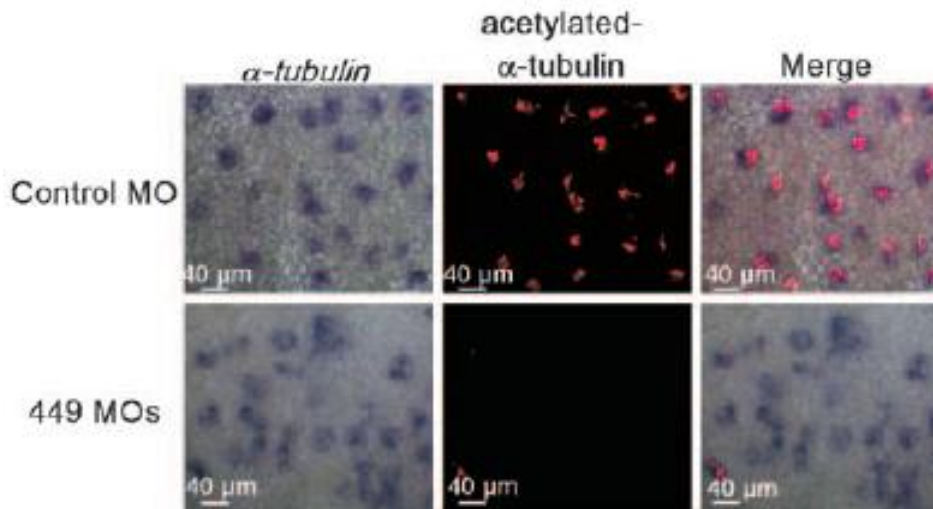
**Figure XVII.** The relative microRNAs abundance (percentage of miRNAs reads) in *Xenopus laevis* larval epidermis at different stages of development, before and after MCCs differentiation. miR-449 and miR-34, the most up-regulated are indicated in red and blue, respectively (Marcet et al, 2011).

This study showed that miR-449 was robustly increased during multiciliated cell differentiation, increasing from 5% of the total miRNA content up to 39%. Moreover, it was shown that the miR-449 family (consisting of three members: miR-449a, miR-449b and miR-449c) is conserved among vertebrates and that up-regulation of miR449 expression also occurs in cultures of regenerating human airways mucociliary epithelial cells (HAECs) (Marcet et al, 2011) (Fig.XVIII).



**Figure XVIII.** The relative microRNAs abundance (percentage of miRNAs reads) in Human airway epithelium at different stages of development, before and after MCCs differentiation. miR-449 and miR-34, the most up-regulated miRNAs are indicated in red and blue, respectively (Marcet et al, 2011).

Microinjection with morpholino antisense oligonucleotides, designed to knock-down the miR-449 binding activity on all its targets, demonstrates the requirement of this family of miRNAs for the development of multiple motile cilia. (Fig.XIX) (Marcet et al, 2011). Moreover, it was shown that miR-449 controls multiciliogenesis through the Notch/Delta signaling pathway. The Notch receptor as well as its ligand - Delta1 are bona fide target of miR-449 in human upper airways and *Xenopus laevis* embryonic skin. It was thus shown that miR-449 dependent inhibition of Delta1 expression in MCCs is required for their terminal differentiation (Marcet et al, 2011).

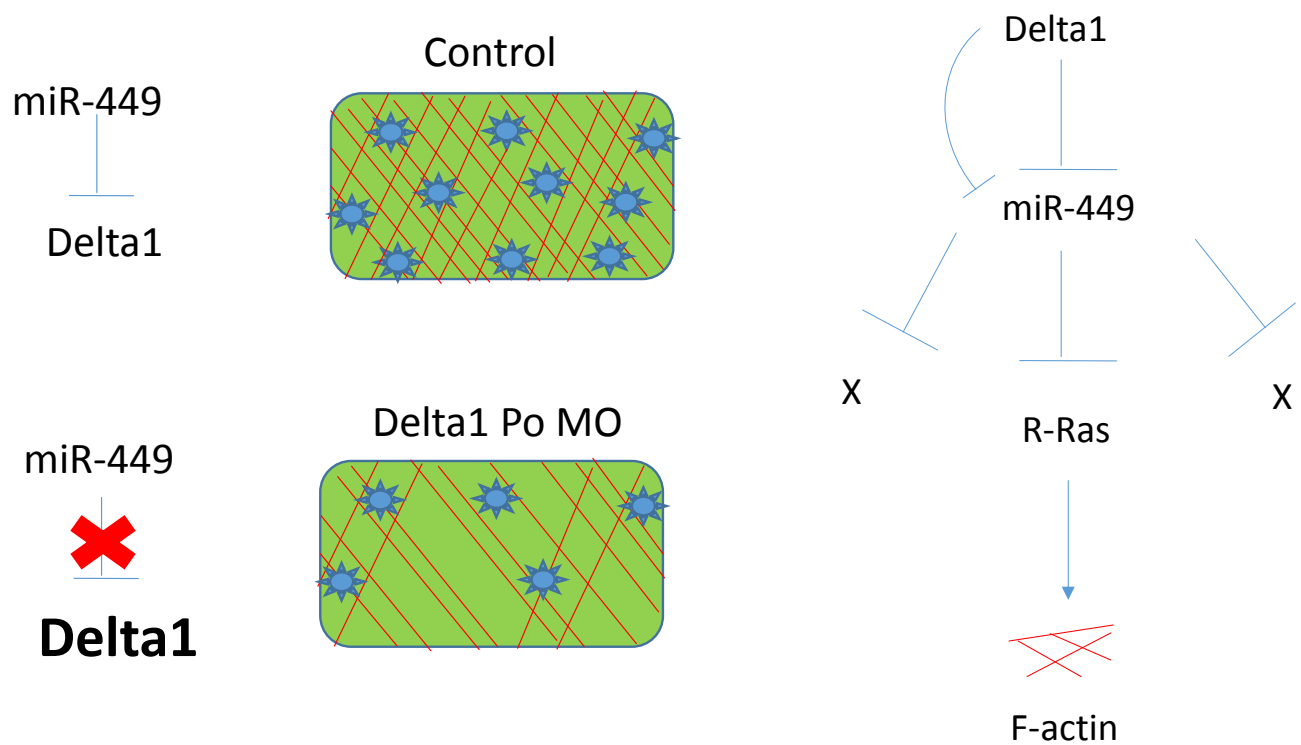


**Figure XIX.** miR-449 deficient cells maintain a ciliated cells progenitor identity, but do not make cilia. Therefore, the MCCs specification has not been affected (Marcet et al, 2011).

### The Notch/Delta signaling pathway involvement in multiciliogenesis

In a previous joint publication from the Kodjabachian and Barbry laboratories, it was shown that miR-449 is involved in the terminal differentiation of MCCs through inhibition of the Notch/Delta1 signaling (Marcet et al, 2011).

More recently, we were able to demonstrate the existence of an inhibitory feedback loop between miR-449 and its target Delta1. Indeed, we noticed that Delta1 protection from miR-449 led to down-regulation of miR-449 itself (data not shown in the current version of manuscript). Therefore, we conclude that not only miR-449 inhibits its target Delta1, but also that Delta1 is able to repress the expression of its regulator miR-449. Based on this discovery we proposed to place Delta1 in the position of “Master regulator” and miR-449 in a position of “Master controller” of multiciliogenesis (Scheme III).



**Scheme III.** Interaction between miR-449 and its target Delta1 during the reorganization of actin network of MCCs. A) Control MCC B) Impact on actin network reorganization in MCC upon Delta1 protection from miR-449 binding by injection R-Ras Po MO. C) Schematic representation of proposed role of Delta1 in the process of actin cap formation in MCCs of frog mucociliary epithelium.

## **Actin cap reorganization at the apical surface of multiciliated cells is controlled by miR-449**

Many lines of evidence demonstrate the importance of miRNAs in the modulation of several signaling pathways, among which those known to be involved in actin cytoskeleton reorganization and ciliogenesis. For example, miR-129-3p controls primary cilia assembly by regulating CP110 and repressing branched F-actin formation (Cao et al, 2011). Another miRNA, miR-8 regulates the cross-talk between ERM/Nherf activity and Wnt/PCP signaling during actin reorganization in zebrafish epidermis (Flynt et Patton, 2010). miR-34a controls RhoA/Rac1 crosstalk and actin cytoskeleton reorganization in the developing chondrocytes (Kim et al, 2012). Finally, miR-124 modulates the activity of Rho and expression level of cdc42 during neuronal differentiation (Yuet al, 2008).

It is known that miR-449 controls several aspects of ciliogenesis. We have experimentally shown using morpholinos against the members of the miR-449 family (miR-449a/b/c), that miR-449 controls one of the crucial step of multiciliogenesis characterized by formation of a dense meshwork of actin at the apical surface of the multiciliated cells (MCCs). This step of multiciliogenesis occurs after cell specification and before MCCs terminal differentiation.

In order to know better the period of time when a dense meshwork of actin is formed, we performed time-course immunohistochemistry on the explanted ectoderm of *Xenopus laevis* embryos, from stage 15 (early neurula) until stage 25 (tailbud). We have shown that formation of a dense meshwork of filamentous actin occurs in the late neurula stage, between stage 17 and 18.

To better understand the action of miR-449 on the actin cytoskeleton, we have been searching for possible targets of miR-449 within the genes, whose repression could be linked to actin cytoskeleton reorganization on the MCCs apical surface. Hence, by using different target prediction tools we have found a few promising candidates to be miR-449 targets.

## **The role of different GTPases in the multiciliogenesis**

Previous reports on primary cultures of mouse airway epithelial cells indicated the involvement of RhoA GTPase in the crucial step of multiciliogenesis related to the cortical actin reorganization at the apical surface of ciliated cells (Pan et al, 2007). It was suggested that Rho GTPase signaling, in cooperation with planar cell polarity (PCP) pathway, controls the assembly of apical actin filaments (Park et al, 2008). Furthermore, it was shown that specific accumulation of the filamentous actin at the apical surface of ciliated cells is required for basal body docking and spacing, thus allowing the growth of the ciliary axoneme (Pan et al, 2007; Park et al, 2008; Vladar et al, 2008).

The regulatory function of GTPases in the actin dynamics during the multiciliogenesis and MCCs differentiation became one of the objects of our research (Brody et al, 2000; Pan et al, 2007). Since it was expected that RhoA is not the only regulator of the actin cytoskeleton, we assumed that RhoA, together with other GTPases can orchestrate the overall reorganization of the actin cytoskeleton during multiciliogenesis. Therefore, we have been looking for the putative targets of miR-449 within the family of GDP-dissociation inhibitors as well as within the other members of small G proteins family.

Together with Pascal Barbry's team we decided to study the involvement of two putative targets of miR-449, a Rho-GDI called Arhgd1B and a GTPase called R-Ras in the actin cytoskeleton reorganization during multiciliogenesis in the human airways epithelial cells (HAECs) and *Xenopus laevis* mucociliary epithelium.

The potential link between RhoA and its regulators (RhoGEFs, RhoGAPs and RhoGDIs) or other GTPases during the actin reorganization in MCCs of human and frog mucociliary epithelium has been never studied before.

## **The targets of mir-449 involved in actin cap formation.**

Arhgdib is a Rho GDP-dissociation inhibitor that can control a wide range of cellular processes, including the cell adhesion, migration, proliferation and differentiation (Ota et al, 2004; Garcia-Mata et al, 2011). A recent report demonstrated Arhgdib specific enrichment in mouse airway non-ciliated cells (Hoh et al, 2012).

Our *in silico* preliminary data indicated the presence of a miR-449 binding site on the Arhgdib 3'UTR. Therefore, this finding encouraged us to further study the possible role of Arhgdib in human and frog multiciliogenesis.

We began our studies by on studying Arhgdib expression in HAECs and *Xenopus* embryos.

In human airway epithelium Arhgdib is significantly expressed in HAECs, with a specific decrease of its expression levels at the beginning of MCCs differentiation. The immunohistochemistry on HAECs revealed that Arhgdib protein is enriched in the non-ciliated basal cells (data not shown). However, in *Xenopus* larval epidermis the expression of Arhgdib is not detectable at any developmental stages. Moreover, Arhgdib expression is restricted to the migrating blood cells (see the results). We concluded that Arhgdib participates in the development of the hematopoietic cells rather than of the MCCs and therefore chose not to pursue our work on this gene any further.

R-Ras is a small GTPase belonging to the R-Ras like GTPase family. It was previously shown, that R-Ras interacts with Rho and Rac small GTPase pathways, filamin A and the actin network (Gawecka et al, 2010; Griffiths et al, 2011; Self et al, 1993). These evidences prompted the assumption that R-Ras could indirectly modulate the organization of filamentous actin at the apical surface of MCCs through RhoA or filamin A.

Our *in silico* approach reveals the existence of a conserved miR-449 binding site on the 3'UTR of human and frog R-Ras. Therefore, we decided to determine the involvement of R-Ras as a putative target of miR-449 in the actin cytoskeleton reorganization during the multiciliogenesis of the human airway and *Xenopus laevis* epidermis.

Firstly, we have shown that R-ras is highly expressed in the human and frog mucociliary epithelium and that its expression is tightly regulated by miR-449 silencing in both models. Secondly, by performing a double fluorescent *In situ* hybridization on sections, we demonstrated that R-Ras expression is higher in the cells negative for the CCPs marker  $\alpha$ tubulin.

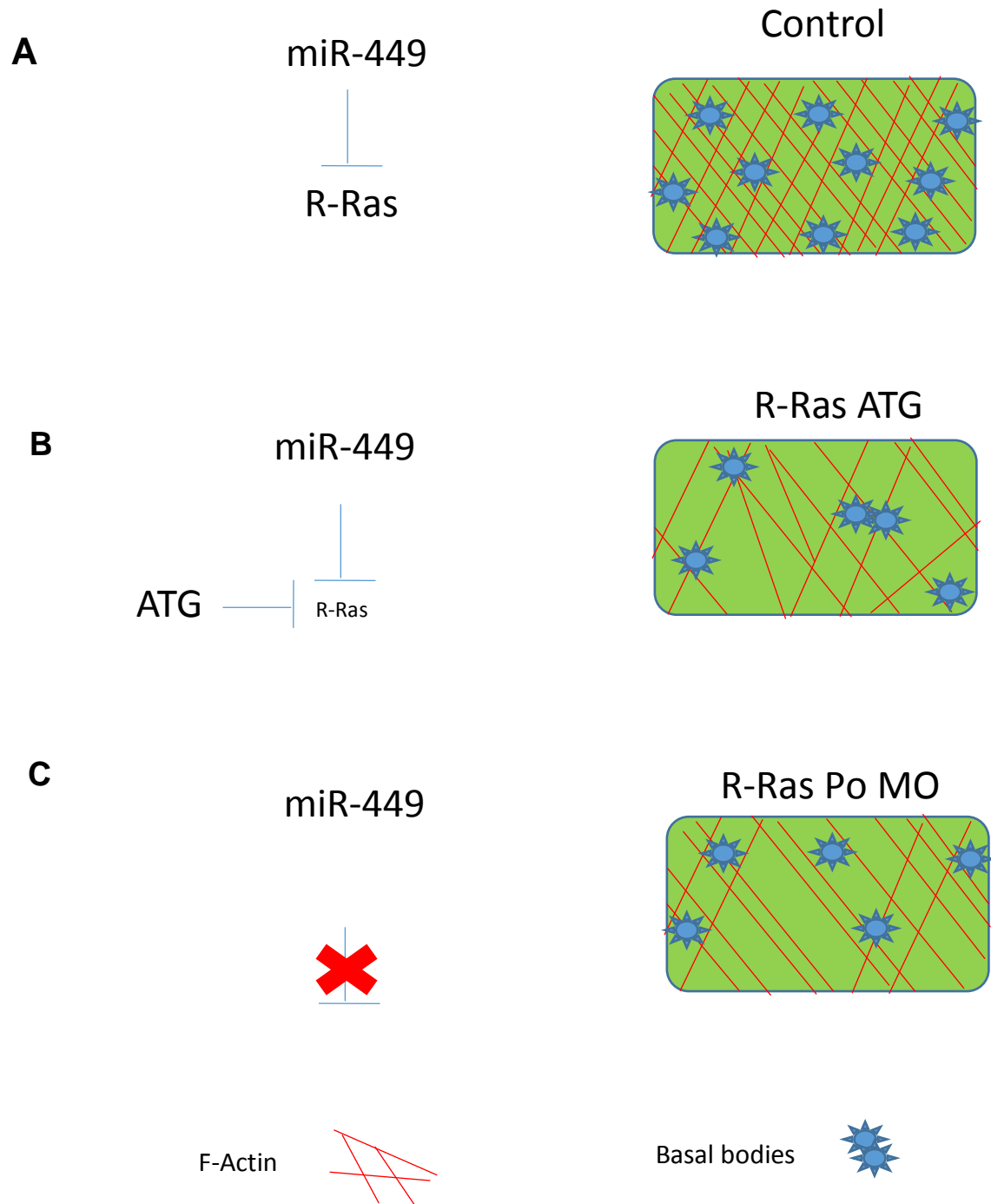
We demonstrated that the R-Ras GTPase is a bona-fide target of miR-449 and we showed its impact on filamentous actin reorganization. We demonstrated that R-Ras indirect up-regulation through protection from the miR-449 binding results in the entire loss of the dense meshwork of actin at the apical surface of MCCs of *Xenopus* larval skin.

We concluded that miR-449 tightly regulates the proper level of R-Ras transcripts during multiciliogenesis in human and *Xenopus* mucociliary epithelium (Scheme IV). This finding was supported by the results obtained from quantitative RT-PCR and western blotting on explanted frog ectoderm after R-ras down-regulation and indirect up-regulation following protection from miR-449 binding. We showed that R-Ras transcripts and proteins level decreased or increased, respectively after the manipulations (see the manuscript).

Recently, Antoniadou and colleagues showed that MCCs in frog MCE possess two distinct pools of actin: apical and subapical. The apical pool controls basal bodies docking, while the subapical pool controls their spacial distribution (Antoniadou et al, 2014). We indicated that R-Ras down-regulation as well as up-regulation caused defects in both the apical and subapical actin network formation.

To determine the molecular mechanisms by which miR-449 controls apical actin cytoskeleton reorganization, we tested the presence of a possible link between R-Ras and RhoA GTPase in HAECs. We found that R-Ras silencing had no significant effect on RhoA activity in HAECs (see manuscript). We suggest another explanation on R-Ras impact on actin cap formation through the interaction with Filamin A, a well-known actin cross-linker. In some of the previous reports, it was shown that Filamin A is involved in controlling the epithelial cell shape, actin cytoskeleton remodeling and primary cilia formation (Gawecka et al, 2010; Griffiths et al, 2011).





**Scheme. IV** Interaction between miR-449 and its target R-Ras during the reorganization of actin network in MCCs. A) Control MCC B) Impact on actin network reorganization in MCC upon blocking R-Ras translation by injection R-Ras ATG MO C) Impact on actin network reorganization in MCC upon protection R-Ras from miR-449.

## **Regulators of the multiciliated cells intercalation form the inner into the outer epidermal layer**

To better understand the complex process of cilia formation it is necessary to unmask the molecular regulators of this event. It is also important to clarify the relation between MCCs and their neighboring cells within the epithelium.

*Xenopus* MCCs generated in the inner ectodermal layer have to be translocated into the outer ectodermal layer, where they achieve differentiation and exert their functions. In the best-studied case of the MCCs, this translocation, called radial intercalation, occurs after cell specification and during differentiation.

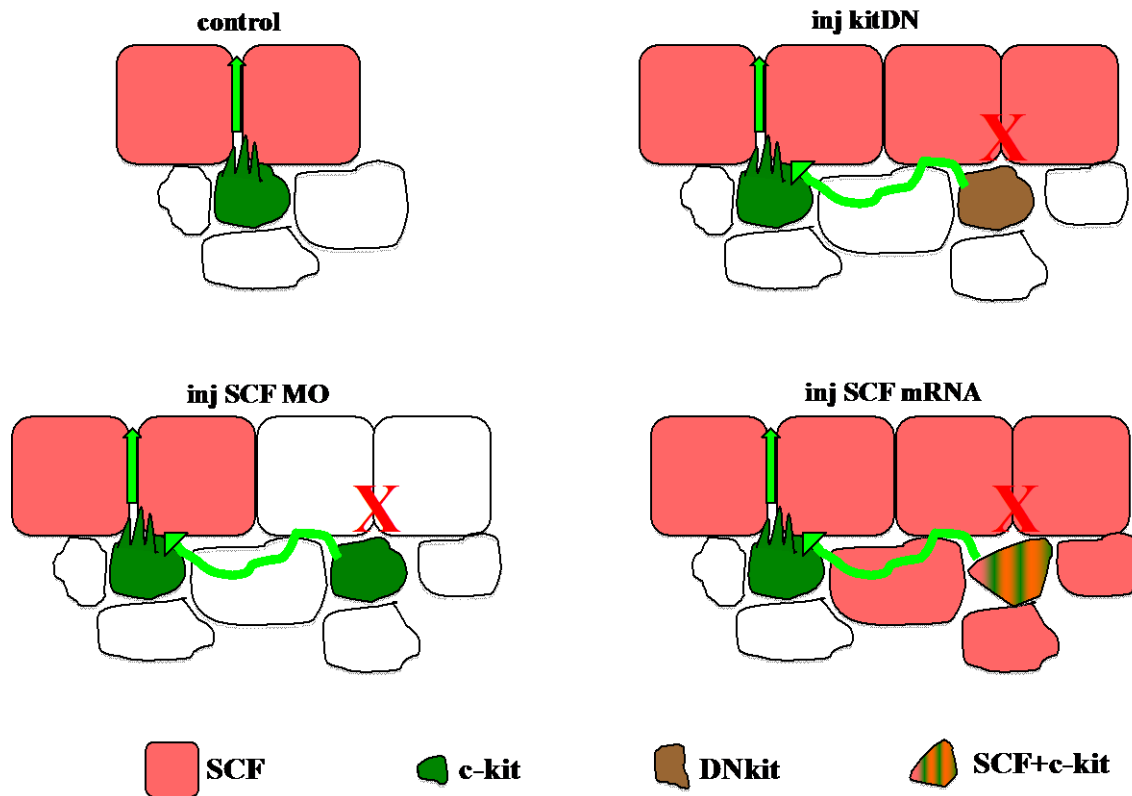
Given the role of miR449 as regulator of multiple steps of multiciliogenesis, we wondered whether it can also control the radial intercalation of MCCs. Steel factor (or Scf), the ligand for the KIT tyrosine kinase receptor, is a promising candidate for a miR-449 target involved in this step of ectoderm development. It has been shown that Steel is expressed in the ectoderm of early *Xenopus* embryos (gastrulation).

Our preliminary data indicated the presence of a miR-449 binding site at the 3'UTR of Steel1 (one of two KIT ligand coding genes in *Xenopus*). Furthermore, we demonstrated by performing double fluorescent *in situ* hybridization that Steel1 RNA is mostly present in the outer ectodermal layer, in the neighborhood of the CCPs.

The expression pattern of Steel1 changes following the microinjection with two types of morpholinos interfering with the activity of miR449. The first morpholino blocks the binding of miR-449 on all of its possible targets, while the second one specifically inhibits miR-449 interaction with the Steel1 3'UTR. These manipulations altered the expression pattern of Steel1 in the frog embryonic ectoderm by inducing its upregulation in the CCPs.

The protection of Steel1 from miR-449 binding caused mild effects on CCPs intercalation, and some of the CCPs injected by morpholinos seem to be trapped in the inner ectodermal layer. Moreover, the data obtained by Steel1 down-regulation, through injection with morpholinos against Steel1 translation showed a disrupted pattern of the MCCs within *Xenopus* embryonic skin (at late stages of development). In this case, the MCCs instead of intercalating separately intercalate in groups of three or four (data obtained from Dr. Andrea Pasini) (Scheme V).

Since all of the presented data have been done on Steel1 transcripts level, to conclude Steel1 role in MCE development, further investigations (at the proteins level) need to be performed.



**Scheme.V** The hypothesis on SCF/c-kit signaling in *Xenopus laevis* mucociliary epithelium by presenting the effects on MCE cells organization upon steel/c-kit expression manipulations through morpholinos or DN microinjection. SCF/c-kit signal must be polarized to allow MCCs directional movements and penetration into outer layer (adapted from Dr. Andrea Pasini). kitDN- dominant-negative receptor kit, SCF MO- injection of Steel translation blocking morpholinos, SCF mRNA or Steel1 Po morpholinos to overexpressed Steel1 in MCE.

## V. Conclusions and perspectives

We have been focusing on few of many different targets of miR-449 relevant for multiciliogenesis. However, it is known that miRNAs are interacting at the same time with many other targets. In other words, miRNAs regulate expression of many different genes and it is unlikely that miR-449 has a massive effect only on one single target.

We showed that miR-449 is a conserved controller of multiciliogenesis, however not all its targets are conserved between species. For example, *Arhgd1B* is targeted by miR-449 in human airway epithelial cells, but in mucociliary epithelium of *Xenopus* larval skin *Arhgd1B* expression is not detectable.

The post-transcriptional regulation of genes in mucociliary epithelium is not completely understood, thus raising many questions. For instance, how many targets of each particular miRNAs have to be down-regulated during differentiation of MCCs and MCE development? And also, which and how many signaling pathways are regulated by miR-449?

We chose just a few of the putative miR-449 targets for our investigation, however the list of candidate targets of miR-449 is long. There are genes involved in cell cycle regulation including: *Areg*, *Ccnb1*, *Ccne2*, *Cdc25a* and EGF receptor ligand (Marcet et al, 2011).

Moreover, recently it was showed that the miRNAs from the same family are redundant in frog mucociliary epithelium. Therefore, inhibition of miR-449 can be compensated by other members of the same family of miRNA for example miR-34b (Song et al, 2014).

Also, the relation between miR-449 and other genes of the same locus should be further investigated. This is particularly true, for example, the regulatory relation between miR-449 and its host gene *CDC20B*.

Therefore, the investigation on miR-449 and its targets function in MCCs differentiation and MCE development is not complete.

## References

## VI. References

1. Jianfeng Lin, Thomas Heuser, Blanca I. Carbajal-González, Kangkang Song and Daniela Nicastro(2012), The structural heterogeneity of radial spokes in cilia and flagella is conserved, *Cytoskeleton*, Vol.69, Issue 2, 88-1
2. Neeraj Sharma, Nicolas F. Berbari, Bradley K. Yoder (2008), Chapter 13 Ciliary Dysfunction in Developmental Abnormalities and Diseases, *Curr Topics in Developmental Biology*, Volume 85, 2008, Pages 371–427
3. Tetsuo Kobayashi, Brian D.Dynlacht, (2011). Regulating the transition from centriole to basal body, *The Journal of Cell Biology*, Vol.193, No.3, 435-444
4. Sigrid Hoyer-Fender, (2010). Centriole maturation and transformation to basal body, *Seminars in Cell and Developmental Biology* 21, 142-147
5. Helen R.Dawe, Helen Farr, Keith Gull, (2007). Centriole/basal body morphogenesis and migration during ciliogenesis in animal cells. *Journal of Cell Science*,
6. Nicolas F.Berbari, Amber K.O'Connor, Courtney J.Haycraft, Bradley K.Yoder (2009). The primary cilium as a complex signaling center. *Current Biology* 19, R526-R535
7. Julie M. Hyes, Su Kyoung Kim, Philip B.Abitua, Tae Joo Park, Emily R.Herrington, Atsushi Kitayama, Matthew W. Grow, Naoto Ueno, John B. Wallingford (2007). Identification of novel ciliogenesis factors using a new in vivo model for mucociliary epithelial development. *Dev Biology* December 1; 312(1): 115-130
8. M.E Werner and B.J Mitchell (2012). Understanding ciliated epithelia: The power of *Xenopus*. *Genesis* 50: 176-185
9. Eamon Dubaissi, Karine Rousseau, Robert Lea, Ximena Soto, Siddarth Nardeosingh, Axel Schweickert, Enrique Amaya, Davis J. Thornton, Nancy Papalopulu (2014). A

secretory cell type develops alongside multiciliated cells, ionocytes and goblet cells, and provides a protective, antiinfective function in the frog embryonic mucociliary epidermis. *Development* 141, 1514-1525

10. Peter Walentek, Susanne Bogusch, Thomas Thumberger, Philipp Vick, Eamon Dubaissi, Tina Beyer, Martin Blum, Axel Schweickert (2014). *Development* 141, 1526-1533

11. Saburo Nagata, Misato Nakanishi, Reiko Nanba, Naoko Fujita (2003). Developmental expression of XEEL, a novel molecule of the *Xenopus* oocyte cortical granule lectin family. *Dev Genes Evol* 213: 368-370

12. Gisele A. Deblandre, Daniel A. Wettstein, Naoko Koyano-Nakagawa, Chris Kintner (1999). A two-step mechanism generates the spacing pattern of the ciliated cells in the skin of *Xenopus* embryos. *Development* 126, 4715-4728

13. Andrew D. Chalmers, Bernhard Strauss, Nancy Papalopulu (2003). Oriented cell divisions asymmetrically segregate aPKC and generate cell fate diversity in the early *Xenopus* embryo. *Development* 130, 2657-2668

14. Ian K. Quigley, Jennifer L. Stubbs, Chris Kintner (2011). Specification of ion transport cells in the *Xenopus* larval skin. *Development* 138, 705-714

15. Cathy Sirour, Magdalena Hidalgo, Valerie Bello, Nicolas Buisson, Thierry Darribere, Nicole Moreau (2011). Dystroglycan is involved in skin morphogenesis downstream of the Notch signaling pathway. *MboC* Vol.22, August 15, 2957-2969

16. J.L Stubbs, E.K Vladar, J.D Axelrod, C.Kintner (2012). Multicilin promotes centriole assembly and ciliogenesis during multiciliate cell differentiation. *Nature Cell Biology*, January 2012, 1-8

17. Chia-Ying Chu, Tariq M. Rana (2007). Small RNAs: Regulators and guardians of the genome. *Journal of Cellular Physiology*, 213: 412-419
18. Muriel Lize, Alexander Klimke, Matthias Dobbelsstein (2011). MicroRNA-449 in cell fate determination. *Cell Cycle* Vol.10 Issue 17, 2874-2882
19. Lina Ma, Ian Quigley, Heymut Omran, Chris Kintner (2014). Multicilin drives centriole biogenesis via E2f proteins. *Genes & Development* April 17, 1-11
20. Jennifer L. Stubbs, Isao Oishi, Juan Carlos Izpisua Belmonte, Chris Kintner (2008). The forkhead protein Foxj1 specifies node-like cilia in *Xenopus* and zebrafish embryos. *Nature genetics* Vol.40, Number 12, 1454-1460
21. Joelle Thomas, Laurette Morle, Fabien Soulavie, Anne Laurencon, Sebastien Sagnol, Benedicte Durand (2010). Transcriptional control of genes involved in ciliogenesis: a first step in making cilia. *Biol.Cell* 102: 499-513
22. Julia Wallmeier, Dalal A Al-Mutairi, Chun-Ting Chen, Niki Tomas Loges, Petra Pennekamp, Tabea Menchen, Lina Ma, Hanan E Shamseldin, Heike Olbrich, Gerard W Dougherty, Claudius Werner, Basel H Alsabah, Gabriele Kohler, Martine Jaspers, Mieke Boon, Matthias Griesse, Sabina Schmitt-Grohe, Theodor Zimmermann, Cordula Koerner-Rettberg, Elisabeth Horak, Chris Kintner, Fowzan S Alkuraya, Heymut Omran (2014). Mutations in CCNO result in congenital mucociliary clearance disorder with reduced generation of multiple motile cilia. *Nature genetics* April 2014, 1-8
23. Rui Song, Peter Walentek, Nicole Sponer, Alexander Klimke, Joon Sub Lee, Gary Dixon, Richard Harland, Ying Wan, Polina Lishko, Muriel Lize, Micheal Kessel, Lin He (2014). MiR-34/449 miRNAs are required for motile ciliogenesis by repressing cp110. *Nature* 115: Vol 510,
24. Muriel Lize, Christian Herr, Alexander Klimke, Robert Bals, Matthias Dobbelsstein (2010). MicroRNA-449a levels increase by several orders of magnitude during mucociliary differentiation of airway epithelia. *Cell Cycle* 9:22, 4579-4582



25. Brigitte N.Gomperts, Xiulan Gong-Cooper, Brian P.Hackett (2004). Foxj1 regulates basal body anchoring to the cytoskeleton of ciliated pulmonary epithelial cells. *Journal of Cell Science* 117, 1329-1337
26. Mei-I Chung, Sara M. Peyrot, Sarah LeBoeuf, Tae Joo Park, Kriston L. McGary, Edward M.Marcotte, John B. Wallingford (2011). RFX2 is broadly required for ciliogenesis during vertebrate development. *Developmental Biology* Vol.363, Issue 1, 155-165
27. Alex S.Flynt, Eric C.Lai (2008). Biological principles of microRNA-mediated regulation: shared themes amid diversity. *Nat Rev Genet.* 9(11):831-842
28. Semil P.Choksi, Gilbert Lauter, Peter Swoboda, Sudipto Roy (2014). Switching on cilia: transcriptional networks regulating ciliogenesis. *Development* 141, 1427-1441
29. Jiehong Pan, Yingjian You, Tao Huang, Steven L.Brody (2007). RhoA-mediated apical actin enrichment is required for ciliogenesis and promoted by Foxj1. *Journal of Cell Science*, 120, 1868-1876
30. T.J Mitchison, H.M Mitchison (2010). How cilia beat. *Nature* Vol.463.21
31. Deborah A. Klos Dehring, Eszter K.Vladar, Micheal E.Werner, Jennifer W.Mitchell, Peter Hwang, Brian J.Mitchell (2013). Deuterosome-mediated centriole biogenesis. *Developmental Cell* 27, 103-112
32. Sen Takeda, Keishi Narita (2012). Structure and function of vertebrate cilia, towards a new taxonomy. *Differentiation* 83, S4-S11
33. Peter Satir, Soren Tvorup Christensen (2007). Overview of structure and function of mammalian cilia. *Annu.Rev. Physiol.*69: 377-400
34. Sehyun Kim, Brian David Dynlacht (2013). Assembling a primary cilium. *Current Opinion in Cell Biology*, 25:506-511

35. Juliette Azimzadeh, Michel Bornens (2007). Structure and duplication of the centrosome. *Journal of Cell Science* 120:2139-2142
36. Moe R.Mahjoub (2013). The importance of a single primary cilium. *Organogenesis* 9:2, 61-69
37. Sarah C.Goetz, Kathryn V.Anderson (2010). The primary cilium: a signaling center during vertebrate development. *Nat Rev Genet.* 11(5):331-344
38. Katarzyna Szymanska, Colin A Johnson (2012). The transition zone: an essential functional compartment of cilia. *Cilia* 1:10, 1-8
39. Hiroaki Ishikawa, Wallace F.Marshall (2011). Ciliogenesis: building the cell's antenna. *Nature Reviews* Vol.12, 222-234
40. Erica E.Davis, Martina Brueckner, Nicholas Katsanis (2006). The emerging complexity of the vertebrate cilium: New functional roles for an ancient organelle. *Developmental Cell* 11, 9-19
41. Devorah C.Goldman, Linnea K.Berg, Micheal C.Heinrich, Jan L. Christian (2006). Ectodermally derived steel/stem cell factor functions non-cell autonomously during primitive erythropoiesis in *Xenopus*. *Blood* 107 (8): 1-11
42. Stuart A.Berger (2006). Signaling pathways influencing SLF and c-kit-mediated survival and proliferation. *Immunologic Research* 35; 1-11
43. Benjamin L.Martin, Richard M.Harland (2004). The developmental expression of two *Xenopus laevis* steel homologues, *Xsl-1* and *Xsl-2*. *Gene Expression Patterns* 5: 239-243
44. Leonie K. Ashman (1999). The biology of stem cell factor and its receptor c-kit. *The international journal of biochemistry and cell biology* 31:1037-1051

45. L Ronnstrand (2004). Signal transduction via the stem cell factor receptor/c-kit. *CMLS Cellular and Molecular Life Sciences* 61:2535-2548
46. Hyuk Wan Ko (2012). The primary cilium as a multiple cellular signaling scaffold in development and disease. *BMB Reports* 427-432
47. Tae Joo Park, Brian J.Mitchell, Philip B.Abitua, Chris Kintner, John B.Wallingford (2008). Dishevelled controls apical docking and planar polarization of basal bodies in ciliated epithelial cells. *Nat Genet* 40(7):871-879
48. John B. Wallingford, Brian Mitchell (2011). Strange as it may seem: the many links between Wnt signaling, planar cell polarity, and cilia. *Genes&Development* 25:201-213
49. Evelyne Fischer, Marco Pontoglio (2009). Planar cell polarity and cilia. *Seminars in Cell&Developmental Biology* 20:998-1005
50. Ioanna Antoniadou, Panayiota Stylianou, Paris A. Skourides (2014). Making the connection: ciliary adhesion complexes anchor basal bodies to the actin cytoskeleton. *Developmental cell* 28: 70-80
51. Nan Tang, Wallace F.Marshall (2012). Centrosome positioning in vertebrate development. *Journal of Cell Science* 125: 4951-4961
52. Alex Braiman, Zvi Priel (2008). Efficient mucociliary transport relies on efficient regulation of ciliary beating. *Respiratory Physiology & Neurobiology* 163: 202-207
53. Andriani Ioannou, Niovi Santama, Paris A. Skourides (2013). *Xenopus laevis* nucleotide binding protein 1 (xNubp1) is important for convergent extension movements and controls ciliogenesis via regulation of the actin cytoskeleton. *Developmental Biology* 380: 243-258
54. Fraser E.Tan, Eszter K.Vladar, Lina Ma, Luis C.Fuentealba, Ramona Hoh, F.Hernan Espinoza, Jeffrey D.Axelrod, Arturo Alvarez-Buylla, Tim Stearns, Chris Kintner, Mark A.

Krasnow (2013). Myb promotes centriole amplification and later steps of the multiciliogenesis program. *Development* 140: 4277-4286

55. Jantje M.Gerdes, Erica E.Davis, Nicholas Katsanis (2009). The vertebrate primary cilium in development, homeostasis, and disease. *Cell* 137(1): 32-45

56. Maxence V.nachury, E.Scott Seeley, Hua Jin (2010). Trafficking to the ciliary membrane: How to get across the periciliary diffusion barrier? *Annu Rev Cell Dev Biol* 26:59-87

57. John A. Follit, Richard A. Tuft, Kevin E. Fogarty, Gregory J.Pazour (2006). The intraflagellar transport protein IFT20 is associated with the Golgi complex and is required for cilia assembly. *Molecular Biology of the Cell* Vol.17, 3781-3792

58. Takahide Ota, Masayo Maeda, Shiho Suto, Masaaki Tatsuka (2004). LyGDI functions in cancer metastasis by anchoring Rho proteins to the cell membrane. *Molecular Carcinogenesis* 39:206-220

59. Philip S.Hodkinson, Paul A.Elliott, Yatish Lad, Brian J. McHugh, Alison C.MacKinnon, Christopher Haslett, Tariq Sethi (2007). Mammalian NOTCH-1 activates  $\beta 1$  integrins via the small GTPase R-Ras. *The Journal of Biology Chemistry* Vol.82, No.39:28991-29001

60. Michele A.Wozniak, Lina Kwong, David Chodniewicz, Richard L.Klemke, Patricia J.Keely (2005). R-Ras controls membrane protrusion and cell migration through the spatial regulation of Rac and Rho. *Molecular Biology of the Cell* Vol.16, 84-96

61. David Sprinzak, Amit Lakhanpal, Lauren LeBon, Leah A.Santat, Michelle E.Fontes, Graham A.Anderson, Jordi Garcia-Ojalvo, Michael B.Elowitz (2010). Cis-interactions between Notch and Delta generate mutually exclusive signalling states. *Nature Letters* Vol.456, 86-91

62. Brice Marcet, Benoit Chevalier, Christelle Coraux, Laurent Kodjabachian, Pascal Barbry (2011). MicroRNA-based silencing of Delta/Notch signaling promotes multiple cilia formation. *Cell Cycle* 10:17: 2858-2864
63. Gary W.Reuther, Channing J.Der (2000). The Ras branch of small GTPases: Ras family members don't fall far from the tree. *Current Opinion in Cell Biology* 12:157-165
64. Annette Ehrhardt, Gotz R.A.Ehrhardt, Xuecui Guo, John W.Schrader (2002). Ras and relatives – job sharing and networking keep an old family together. *Experimental Hematology* 30:1089-1106
65. Shialou Yuan, Zhaoxia Sun (2013). Expanding horizons: ciliary proteins reach beyond cilia. *Annu.Rev.Genet* 47:353-376
66. Yusuke Ohba, Naoki Mochizuki, Shigeko Yamashita, Andrew M.Chan, John W.Schrader, Seisuke Hattori, Kazuo Nagashima, Michiyuki Matsuda (2000). Regulatory proteins of R-Ras. TC21/R-Ras2, and M-Ras/R-Ras3\*. *The Journal of Biological Chemistry* Vol.275, No.26, 20020-20026
67. Johannes L.Bos (1997). Ras-like GTPases. *Biochimica et Biophysica Acta* 1333: M19-M31
68. Fernando R.Balestra, Pierre Gonczy (2014). Multiciliogenesis: multicilin directs transcriptional activation of centriole formation. *Current Biology* Vol.24, No 16,
69. Marie Cibois, Pierluigi Scerbo, Virginie Thome, Andrea Pasini, Laurent Kodjabachian (2014). Induction and Differentiation of the *Xenopus* ciliated embryonic epidermis. *Xenopus Development* Wiley Blackwell
70. Eamon Dubaissi, Nancy Papalopulu (2011). Embryonic frog epidermis: a model for the study of cell-cell interactions in the development of mucociliary disease. *Disease Models&Mechanisms* 4: 179-192

71. Leah T.Haimo, Joel L.Rosenbaum (1981). Cilia, Flagella, and Microtubules. The Journal of Cell Biology Vol.91, No.3, 125-130
72. T.Cavalier-Smith (2002). The phagotrophic origin of eukaryotes and phylogenetic classification of Protozoa. International Journal of Systematic and Evolutionary Mircobiology 52: 297-354
73. Ryoko Kuriyama, Gary G. Borisky (1981). Centriole cycle In Chinese Hamster Ovary Cells as determinedby whole-mount electron microscopy. The Journal of Cell Biology Vol.91, 814-821
74. Norton B.Gilula, Peter Satir (1972). The ciliary necklace. The Journal of Cell Biology.Vol.58, 494-509
75. Stefan Westermann, Klaus Weber (2003). Post-translational modifications regulate microtubule function. Nature Reviews Molecular Cell Biology 4: 938-948
76. Jianfeng Lin, Thomas Heuser, Blanca I. Carbajal-González, Kangkang Song, Daniela Nicastro (2012). The structural heterogeneity of radial spokes in cilia and flagella is conserved. Cytoskeleton Vol.69, Issue 2, 88-100
77. Shigenori Nonaka, Yosuke Tanaka, Yasushi Okada, Sen Takeda, Akihiro Harada, Yoshimitsu Kanai, Mizuho Kido, Nobutaka Hirokawa (1998). Randomization of left-right asymmetry due to loss of nodal cilia generating leftward flow of extraembryonic fluid in mice lacking KIF3B motor protein. Cell 95(6), 829-837
78. Keishi Narita, Toyoko Kawate, Naoto Kakinuma, Sen Takeda (2010). Multiple Primary Cilia Modulate the Fluid Transcytosis in Choroid Plexus Epithelium.Traffic Vol.11, Issue 2, 287-301
79. Sen Takeda, Keishi Narita (2012). Structure and function of vertebrate cilia, towards a new taxonomy. Differentiation Vol.83, Issue 2, S4-S11

80. Sudipto Roy (2009). The motile cilium in development and disease: emerging new insights. *BioEssays* 31: 694-699
81. Norann A. Zaghloul, Samantha A Brugmann (2011). The emerging face of primary cilia. *Genesis* Vol.49, Issue 4, 231-246
82. Gregory J. Pazour, Bethany L. Dickert, Yvonne Vucica, E. Scott Seeley, Joel L. Rosenbaum, George B. Witman, Douglas G. Cole (2000). *Chlamydomonas* IFT88 and Its Mouse Homologue, Polycystic Kidney Disease Gene *Tg737*, Are Required for Assembly of Cilia and Flagella. *The Journal of Cell Biology* 151(3): 709-718
83. Jeffrey J.Schrick, L.F.Onuchic, S.T.Reeders, J.Korenberg, X-N.Chen, J.H.Moyer, J.E.Wilkinson, Richard P.Woychik (1995). Characterization of the human homologue of the mouse *Tg737* candidate polycystic kidney disease gene. *Human Molecular Genetics* Vol.4, No 4, 559-567
84. Danwei Huangfu, Aimin Liu, Andrew S. Rakeman, Noel S. Murcia, Lee Niswander, Kathryn V. Anderson (2003). Hedgehog signaling in the mouse requires intraflagellar transport proteins. *Nature* 426:83-87
85. Kevin C. Corbit, Pia Aanstad, Veena Singla, Andrew R. Norman, Didier Y. R. Stainier, Jeremy F. Reiter (2005). Vertebrate Smoothed functions at the primary cilium. *Nature* 437:1018-1021
86. Aimin Liu, Baolin Wang, Lee A. Niswander (2005). Mouse intraflagellar transport proteins regulate both the activator and repressor functions of Gli transcription factors. *Development* 132:3103-3111
87. Eszter K. Vladar, Dragana Antic, Jeffrey D. Axelrod (2009). Planar Cell Polarity Signaling: The Developing Cell's Compass. *Cold Spring Harbor Perspectives in Biology*
88. Michael T. Veeman, William C. Smith (2013). Whole-organ cell shape analysis *Vol.373, Issue 2, 281-289*

89. Brian Mitchell, Jennifer L. Stubbs, Fawn Huisman, Peter Taborek, Clare Yu, Chris Kintner (2009). The PCP Pathway Instructs the Planar Orientation of Ciliated Cells in the *Xenopus* Larval Skin. *Current Biology* Vol.19, Issue 11, 924-929
90. Alison J Ross, Helen May-Simera, Erica R Eichers, Masatake Kai, Josephine Hill, Daniel J Jagger, Carmen C Leitch, J Paul Chapple, Peter M Munro, Shannon Fisher, Perciliz L Tan, Helen M Phillips, Michel R Leroux, Deborah J Henderson, Jennifer N Murdoch, Andrew J Copp, Marie-Madeleine Eliot, James R Lupski, David T Kemp, Hélène Dollfus, Masazumi Tada, Nicholas Katsanis, Andrew Forge, Philip L Beales (2005). Disruption of Bardet-Biedl syndrome ciliary proteins perturbs planar cell polarity in vertebrates. *Nature Genetics* 37: 1135-1140
91. Michael R. Deans, Dragana Antic, Kaye Suyama, Matthew P. Scott, Jeffrey D. Axelrod, Lisa V. Goodrich (2007). Asymmetric Distribution of Prickle-Like 2 Reveals an Early Underlying Polarization of Vestibular Sensory Epithelia in the Inner Ear. *The Journal of Neuroscience* 27(12): 3139-3147 reveals the developmental basis of ascidian notochord taper. *Developmental Biology*
92. Michelle Tallquist, Andrius Kazlauskas (2004). PDGF signaling in cells and mice. *Cytokine and growth factor reviews* 15(4): 205-213
93. Ian C. Schneider, Jason M. Haugh (2005). Quantitative elucidation of a distinct spatial gradient-sensing mechanism in fibroblasts. *The Journal of Cell Biology* 171(5): 883-892
94. Judith M. Neugebauer, Jeffrey D. Amack, Annita G. Peterson, Brent W. Bisgrove, H. Joseph Yost (2009). FGF signaling during embryo development regulates cilia length in diverse epithelia. *Nature Letter* 458: 651-654



95. Praetorius Helle A, Spring Kenneth R (2003). The renal cell primary cilium functions as a flow sensor. *Current Opinion in Nephrology and & Hypertension* Vol.12, Issue 5, 517-520
96. Surya M. Nauli, Francis J. Alenghat, Ying Luo, Eric Williams, Peter Vassilev, Xiaogang Li, Andrew E. H. Elia, Weining Lu, Edward M. Brown, Stephen J. Quinn, Donald E. Ingber, Jing Zhou (2003). Polycystins 1 and 2 mediate mechanosensation in the primary cilium of kidney cells. *Nature Genetics* 33: 129-137
97. Glen G. Ernstrom and Martin Chalfie (2002). Genetics of sensory mechanotransduction. *Annual Review of Genetics* Vol.36, 411-453
98. Jung-Bum Shin, Dany Adams, Martin Paukert, Maria Siba, Samuel Sidi, Michael Levin, Peter G. Gillespie, Stefan Gründer (2005). *Xenopus* TRPN1 (NOMPC) localizes to microtubule-based cilia in epithelial cells, including inner-earhair cells. *PNAS* 102(35): 12572-12577
99. Heather M Kulaga, Carmen C Leitch, Erica R Eichers, Jose L Badano, Alysa Lesemann, Bethan E Hoskins, James R Lupski, Philip L Beales, Randall R Reed, Nicholas Katsanis (2004). Loss of BBS proteins causes anosmia in humans and defects in olfactory cilia structure and function in the mouse. *Nature Genetics* 36(9): 994-998
100. Basudha Basu, Martina Brueckner (2009). Fibroblast “Cilia Growth” Factor in the Development of Left-Right Asymmetry. *Developmental Cell* Vol.16, Issue 4, 489-490
101. Alok S Shah, Yehuda Ben-Shahar, Thomas O Moninger, Joel N Kline, Michael J Welsh (2009). Motile Cilia of Human Airway Epithelia Are Chemosensory. *Science* 325(5944) 1131-1134
102. Friedhelm Hildebrandt, M.D., Thomas Benzing, M.D., and Nicholas Katsanis (2011). Ciliopathies. *The New England journal of medicine* 364(16), 1533-1543

103. Neeraj Sharma, Nicolas F. Berbari, Bradley K. Yoder (2008). Chapter 13 Ciliary Dysfunction in Developmental Abnormalities and Diseases. *Current Topics in Developmental Biology* Vol.85, 371-427
104. Friedhelm Hildebrandt, Weibin Zhou (2007). Nephronophthisis-Associated Ciliopathies. *Journal of the American Society of nephrology* Vol.18, NO 6; 1855-1871
105. Ansley SJ, Badano JL, Blacque OE, Hill J, Hoskins BE, Leitch CC, Kim JC, Ross AJ, Eichers ER, Teslovich TM, Mah AK, Johnsen RC, Cavender JC, Lewis RA, Leroux MR, Beales PL, Katsanis N (2003). Basal body dysfunction is a likely cause of pleiotropic Bardet-Biedl syndrome. *Nature* 425; 628-633
106. Norann A. Zaghloul, Nicholas Katsanis (2009). Mechanistic insights into Bardet-Biedl syndrome, a model ciliopathy. *The Journal of Clinical Investigation* 119(3); 428-437
107. Michel Paintrand, Mohammed Moudjou, Hervé Delacroix, Michael Bornens (1992). Centrosome organization and centriole architecture: Their sensitivity to divalent cations. *Journal of Structural Biology* Vol.108, Issue 2, 107-128
108. Nonaka S, Tanaka Y, Okada Y, Takeda S, Harada A, Kanai Y, Kido M, Hirokawa N (1998). Randomization of left-right asymmetry due to loss of nodal cilia generating leftward flow of extraembryonic fluid in mice lacking KIF3B motor protein. *Cell* 95:829–837.
109. Clement A, Solnica-Krezel L, Gould KL (2011). The Cdc14B phosphatase contributes to ciliogenesis in zebrafish. *Development* 138:291–302.

110. Prachee Avasthi, Wallace F. Marshall (2012). Stages of Ciliogenesis and Regulation of Ciliary Length. *Differentiation* 82(2); 30-42
111. Stephen Doxsey, Wendy Zimmerman, Keith Mikule (2005). Centrosome control of the cell cycle. *Trends in Cell Biology* Vol.15, Issue 6, 303-311
112. Jadranka Loncarek, Alexey Khodjakov (2009). *Ab ovo* or *de novo*? Mechanisms of centriole duplication. *Molecules and Cells* 28, 27(2); 135-142
113. Meng-Fu Bryan Tsou, Tim Stearns (2005). Controlling centrosome number: licenses and blocks. *Current Opinion in Cell Biology* Vol.18, Issue 1, 74-78
114. Nina Peel, Naomi R. Stevens, Basto Renata, Jordan W. Raff (2007). Overexpressing Centriole-Replication Proteins In Vivo Induces Centriole Overduplication and De Novo Formation. *Current Biology* 17(10); 834-843
115. Tomer Avidor-Reiss, Jayachandran Gopalakrishnan (2013). Building a Centriole. *Current Opinion in Cell Biology* 25(1); 72-77
116. Anja Puklowski, Yahya Homsy, Debora Keller, Martin May, Sangeeta Chauhan, Uta Kossatz, Viktor Grünwald, Stefan Kubicka, Andreas Pich, Michael P. Manns, Ingrid Hoffmann, Pierre Gönczy, Nisar P. Malek (2011). The SCF–FBXW5 E3-ubiquitin ligase is regulated by PLK4 and targets HsSAS-6 to control centrosome duplication. *Nature Cell Biology* 13; 1004-1009
117. Rodrigues-Martins A, Riparbelli M, Callaini G, Glover DM, Bettencourt-Dias M (2007). Revisiting the role of the mother centriole in centriole biogenesis. *Science* 316(5824); 1046-1050
118. Eszter K. Vladar, Tim Stearns (2007). Molecular characterization of centriole assembly in ciliated epithelial cells. *Journal of Cell Biology* Vol.178, no1, 31-42

119. Richard G.W Anderson, Robert M.Brenner (1971). The formation of basal bodies (centrioles) in the Rhesus monkey oviduct. *Journal of Cell Biology* 50(1), 10-34
120. Julia Kleylein-Sohn, Jens Westendorf, Mikael Le Clech, Robert Habedanck, York-Dieter Stierhof, Erich A. Nigg (2007). Plk4-Induced Centriole Biogenesis in Human Cells. *Developmental Cell* Vol.13, Issue 2, 190-202
121. Veena Singla, Miriam Romaguera-Ros, Garcia-Verdugo JM, Jeremy F. Reiter (2010). *Odf1*, a human disease gene, regulates the length and distal structure of centrioles. *Developmental Cell* 18(3); 410-424
122. Hiroaki Ishikawa, Akiharu Kubo, Shoichiro, Tsukita Sachiko Tsukita (2005). *Odf2*-deficient mother centrioles lack distal/subdistal appendages and the ability to generate primary cilia. *Nature Cell Biology* 7; 517-524
123. Koshi Kunimoto, Yuji Yamazaki, Tomoki Nishida, Kyosuke Shinohara, Hiroaki Ishikawa, Toshiaki Hasegawa, Takeshi Okanoue, Hiroshi Hamada, Tetsuo Noda, Atsushi Tamura, Shoichiro Tsukita, Sachiko Tsukita (2012). Coordinated Ciliary Beating Requires *Odf2*-Mediated Polarization of Basal Bodies via Basal Feet. *Cell* Vol.148, Issue 1-2, 189-200
124. Susanne Graser, York-Dieter Stierhof, Sébastien B. Lavoie, Oliver S. Gassner, Stefan Lamla, Mikael Le Clech, Erich A. Nigg (2007). *Cep164*, a novel centriole appendage protein required for primary cilium formation. *Journal of Cell Biology* Vol.179, no 2, 321-330
125. Elena N. Pugacheva, Sandra A. Jablonski, Tiffiney R. Hartman, Elizabeth P. Henske, Erica A. Golemis (2007). HEF1-Dependent Aurora A Activation Induces Disassembly of the Primary Cilium. *Cell* Vol. 129, Issue 7, 1351-1363

126. Thomas D. Pollard, John A. Cooper (2009). Actin, a Central Player in Cell Shape and Movement. *Science* 326(5957); 1208-1212
127. Thomas D. Pollard (2007). Regulation of Actin Filament Assembly by Arp2/3 Complex and Formins. *Annual Reviews, Biophysics and Biomolecular Structure*. Vol.36; 451-477
128. Matthew P. Taylor, Orkide O. Koyuncu, Lynn W. Enquist (2011). Subversion of the actin cytoskeleton during viral infection. *Nature Review Microbiology* 9; 427-439
129. Yili Yin, Fiona Bangs, I. Robert Paton, Alan Prescott, John James, Megan G. Davey, Paul Whitley, Grigory Genikhovich, Ulrich Technau, David W. Burt, Cheryll Tickle (2009). The *Talpid3* gene (*KIAA0586*) encodes a centrosomal protein that is essential for primary cilia formation. *Development* 136(4); 655-664
130. Catherine Klotz, Nicole Bordes, Marie-Christine Laine, Daniel Sandoz, Michel Bornens (1986). Myosin at the Apical Pole of Ciliated Epithelial Cells As Revealed by a Monoclonal Antibody. *The Journal of Cell Biology* 103(2); 613-619
131. Emmanuelle Boisvieux-Ulrich, Marie-Christine Laine, Daniel Sandoz (1990). Cytochalasin D inhibits basal body migration and ciliary elongation in quail oviduct epithelium. *Cell and tissue research* 259(3); 443-454
132. Michael E. Werner, Peter Hwang, Fawn Huisman, Peter Taborek, Clare C. Yu, Brian J. Mitchell (2011). Actin and microtubules drive differential aspects of planar cell polarity in multiciliated cells. *The Journal of Cell Biology* Vol.195, NO 1, 19-26
133. Gregory J. Pazour, Nathan Agrin, John Leszyk, George B. Witman (2005). Proteomic analysis of a eukaryotic cilium. *The Journal of Cell Biology* Vol.170, NO.1, 103-113
134. John B. Wallingford (2010). Planar cell polarity signaling, cilia and polarized ciliary beating. *Current Opinion In Cell Biology* Vol.22, Issue 5, 597-604

135. Zaman Mirzadeh, Young-Goo Han, Mario Soriano-Navarro, Jose Manuel García-Verdugo, Arturo Alvarez-Buylla (2010). Cilia Organize Ependymal Planar Polarity. *The Journal of Neuroscience*. 17; 30(7), 2600-2610
136. Chonnetia Jones, Venus C Roper, Isabelle Foucher, Dong Qian, Boglarka Banizs, Christine Petit, Bradley K Yoder , Ping Chen (2008). Ciliary proteins link basal body polarization to planar cell polarity regulation. *Nature Genetics* 40; 69-77
137. Keiths G. Kozminski, Karl A. Johnson, Paul Forscher, Joel L. Rosenbaum (1993). A motility in the eukaryotic flagellum unrelated to flagellar beating. *Proceedings of the National Academy of Sciences of the United States of America* 15;90(12); 5519-5523
138. Wallace F. Marshall, Joel S. Rosenbaum (2001). Intraflagellar transport balances continuous turnover of outer doublet microtubules implications for flagellar length control. *Journal of Cell Biology* 155(3); 405-414
139. Hongmin Qin, Dennis R. Diener, Stefan Geimer, Douglas G. Cole, Joel L. Rosenbaum (2004). Intraflagellar transport (IFT) cargo: IFT transports flagellar precursors to the tip and turnover products to the cell body. *The Journal of Cell Biology* Vol.164, NO.2, 255-266
140. Hongmin Qin, Dylan T. Burnette, Young-Kyung Bae, Paul Forscher, Maureen M. Barr Joel L. Rosenbaum (2005). Intraflagellar Transport Is Required for the Vectorial Movement of TRPV Channels in the Ciliary Membrane. *Current Biology* Vol.15, Issue 18, 1695-1699

141. John F. Dishinger, Hooi Lynn Kee, Paul M. Jenkins, Shuling Fan, Toby W. Hurd, Jennetta W. Hammond, Yen Nhu-Thi Truong, Ben Margolis, Jeffrey R. Martens, Kristen J. Verhey (2010). Ciliary entry of the kinesin-2 motor KIF17 is regulated by importin- $\beta$ 2 and RanGTP. *Nature Cell Biology* 12; 703-710
142. Benjamin D. Engel, William B. Ludington, Wallace F. Marshall (2009). Intraflagellar transport particle size scales inversely with flagellar length: revisiting the balance-point length control model. *The Journal of Cell Biology* Vol.187, NO.1, 81-89
143. Corey L. Williams, Svetlana V. Masyukova, Bradley K. Yoder (2009). Normal Ciliogenesis Requires Synergy between the Cystic Kidney Disease Genes *MKS-3* and *NPHP-4*. *Journal of American Society of Nephrology*. 21(5); 782-793
144. Christine Blaineau, Magali Tessier, Pascal Dubessay, Lena Tasse, Lucien Crobu, Michel Pagès, Patrick Bastien (2007). A Novel Microtubule-Depolymerizing Kinesin Involved in Length Control of a Eukaryotic Flagellum. *Current Biology* Vol.17, Issue 9, 778-782
145. Weiyuan Ma, Shai D. Silberberg, Zvi Priel (2002). Distinct Axonemal Processes Underlie Spontaneous and Stimulated Airway Ciliary Activity. *The Journal of general physiology* 120(6); 875-885
146. Andreas Schmid, Matthias Salathe (2011). Ciliary beat co-ordination by calcium. *Biology of the cell* 103; 159-169
147. M. J. Sanderson, M. A. Sleight (1981). Ciliary activity of cultured rabbit tracheal epithelium: beat pattern and metachrony. *Journal of cell science* 47; 331-347

148. Dan Eshel, Zvi Priel (1987). Characterization of metachronal wave of beating cilia on frog's palate epithelium in tissue culture. *The journal of physiology*. 388; 1-8
149. Tong Ihn Lee, Richard A. Young (2013). Transcriptional Regulation and Its Misregulation in Disease. *Cell* Vol.152, Issue 6; 1237-1251
150. Laura R. Keller, Jeffery A. Schloss, Carolyn D. Silflow, Joel L. Rosenbaum (1984). Transcription of  $\alpha$ - and  $\beta$ -Tubulin Genes In Vitro in Isolated *Chlamydomonas reinhardi* Nuclei. *The Journal of Cell Biology* 93(3); 1138-1143
151. Wim G. M. Damen, Leo A. van Grunsven, André E. van Loon (1994). Transcriptional regulation of tubulin gene expression in differentiating trochoblasts during early development of *Patella vulgata*. *Development* 120, 2835-2845
152. Peter Swoboda Haskell T. Adler, James H. Thomas (2000). The RFX-Type Transcription Factor DAF-19 Regulates Sensory Neuron Cilium Formation in *C. elegans*. *Molecular Cell* Vol.5, Issue 3, 411-421
153. Brian P. Piasecki, Jan Burghoorn, Peter Swoboda (2010). Regulatory Factor X (RFX)-mediated transcriptional rewiring of ciliary genes in animals. *PNAS* 107(29); 12969-12974
154. E. Bonnafé, M. Touka, A. AitLounis, D. Baas, E. Barras, C. Ucla, A. Moreau, F. Flamant, R. Dubruille, P. Couble, J. Collignon, B. Durand, W. Reith (2004). The Transcription Factor RFX3 Directs Nodal Cilium Development and Left-Right Asymmetry Specification. *Molecular and Cellular Biology* 24(10); 4417-4427
155. Amir M. Ashique, Youngshik Choe, Mattias Karlen, Scott R. May, Khanhky Phamluong, Mark J. Solloway, Johan Ericson, Andrew S. Peterson (2009). The Rfx4 Transcription Factor Modulates Shh Signaling by Regional Control of Ciliogenesis. *Science* Vol.2, Issue 95;



156. Jun Yang, Jiangang Gao, Michael Adamian, Xiao-Hong Wen, Basil Pawlyk, Luo Zhang, Michael J. Sanderson, Jian Zuo, Clint L. Makino, Tiansen Li (2005). The ciliary rootlet maintains long-term stability of sensory cilia. *Molecular and cellular biology* 25(10); 4129-4137
157. Derek B. Murphy, Stefanie Seemann, Stefan Wiese, Renate Kirschner, Karl H. Grzeschik, Ulrike Thies (1997). The Human Hepatocyte Nuclear Factor 3/Fork Head Gene FKHL13: Genomic Structure and Pattern of Expression. *Genomics* Vol.30, Issue 3; 462-469
158. Steven L. Brody, Xiu Hua Yan, Mary K. Wuerffel, Sheng-Kwei Song, Steven D. Shapiro (2000). Ciliogenesis and Left–Right Axis Defects in Forkhead Factor HFH-4–Null Mice. *American Journal of respiratory cell and molecular biology* Vol.23, Issue1, 45-51
159. Xianwen Yu, Chee Peng Ng, Hermann Habacher, Sudipto Roy (2008). Foxj1 transcription factors are master regulators of the motile ciliogenic program. *Nature genetics* 40; 1445-1453
160. Robert G. Ramsay, Thomas J. Gonda (2008). MYB function in normal and cancer cells. *Nature review cancer* 8; 523-534
161. Andrew Fire, SiQun Xu, Mary K. Montgomery, Steven A. Kostas, Samuel E. Driver, Craig C. Mello (1998) Potent and specific genetic interference by double-stranded RNA in *Caenorhabditis elegans*. *Nature* 391; 806-811
162. Witold Filipowicz, Lukasz Jaskiewicz, Fabrice A Kolb, Ramesh S Pillai (2005). Post-transcriptional gene silencing by siRNAs and miRNAs. *Current Opinion in Structural Biology* Vol.15, Issue 3, 331-341
163. Antony Rodriguez, Sam Griffiths-Jones, Jennifer L. Ashurst, Allan Bradley (2004). Identification of Mammalian microRNA Host Genes and Transcription Units. *Genome research* 14(10A); 1902-1910

164. Alex S. Flynt, Eric C. Lai (2008). Biological principles of microRNA-mediated regulation: shared themes amid diversity. *Nature reviews genetics* 9(11); 831-842
165. Benjamin P. Lewis, Christopher B. Burge, David P. Bartel (2005). Conserved Seed Pairing, Often Flanked by Adenosines, Indicates that Thousands of Human Genes are MicroRNA Targets. *Cell* Vol.120, Issue 1, 15-20
166. Marco Antonio Valencia-Sanchez, Jidong Liu, Gregory J. Hannon, Roy Parker (2006). Control of translation and mRNA degradation by miRNAs and siRNAs. *Genes & Development* 20(5); 515-524
167. Lin He, Xingyue He, Lee P. Lim, Elisa de Stanchina, Zhenyu Xuan, Yu Liang, Wen Xue, Lars Zender, Jill Magnus, Dana Ridzon, Aimee L. Jackson, Peter S. Linsley, Caifu Chen, Scott W. Lowe, Michele A. Cleary, Gregory J. Hannon (2007). A microRNA component of the p53 tumour suppressor network. *Nature* 447; 1130-1134
168. Lei Wang, Cong Fu, Hongbo Fan, Tingting Du, Mei Dong Yi Chen, Yi Jin, Yi Zhou, Min Deng, Aihua Gu, Qing Jing, Tingxi Liu, Yong Zhou (2013). miR-34b regulates multiciliogenesis during organ formation in zebrafish. *Development* 140(13); 2755-2764
169. Brice Marcet, Benoît Chevalier, Guillaume Luxardi, Christelle Coraux, Laure-Emmanuelle Zaragosi, Marie Cibois, Karine Robbe-Sermesant, Thomas Jolly, Bruno Cardinaud, Chimène Moreilhon, Lisa Giovannini-Chami, Béatrice Nawrocki-Raby, Philippe Birembaut, Rainer Waldmann, Laurent Kodjabachian, Pascal Barbry (2011). Control of vertebrate multiciliogenesis by miR-449 through direct repression of the Delta/Notch pathway. *Nature Cell Biology* 13(6); 693-699
170. Nicholas Redshaw, Guy Wheeler, Mohammad K. Hajihosseini, Tamas Dalmay (2009). microRNA-449 is a putative regulator of choroid plexus development and function. *Brain Research* Vol.1250, 20-26

171. Guowei Fang, Hongtao Yu, Marc W Kirschner (1998). Direct Binding of CDC20 Protein Family Members Activates the Anaphase-Promoting Complex in Mitosis and G1. *Molecular Cell* Vol.2, Issue 2; 163-171
172. Mieke Boon, Julia Wallmeier, Lina Ma, Niki Tomas Loges, Martine Jaspers, Heike Olbrich, Gerard W. Dougherty, Johanna Raidt, Claudius Werner, Israel Amirav, Avigdor Hevroni, Revital Abitbul, Avraham Avital, Ruth Soferman, Marja Wessels, Christopher O'Callaghan, Eddie M. K. Chung, Andrew Rutman, Robert A. Hirst, Eduardo Moya, Hannah M. Mitchison, Sabine Van Daele, Kris De Boeck, Mark Jorissen, Chris Kintner, Harry Cuppens, Heymut Omran (2014). *MCIDAS* mutations result in a mucociliary clearance disorder with reduced generation of multiple motile cilia. *Nature Communications* 5; 4418
173. Chazel L.Sive, Robert M. Grainger, Richard M.Harland (2000). Early development of *Xenopus laevis*. A laboratory manual. Cold Spring Harbor Laboratory Press
174. Julie M.Hayes, Su Kyoung Kim, Philip B.Abitua, Tae Joo Park, Emily R.Herrington, Atsushi Kitayama, Matthew W. Grow, Naoto Ueno, John B. Wallingford (2007). Identification of novel ciliogenesis factors using a new in vivo model for mucociliary epithelial development. *Developmental Biology* 312(1); 115-130
175. F S Billett, R P Gould (1971). Fine structural changes in the differentiating epidermis of *Xenopus laevis* embryos. *Journal of Anatomy*. 108; 465-480
176. Eamon Dubaissi, Nancy Papalopulu (2010). Embryonic frog epidermis: a model for the study of cell-cell interactions in the development of mucociliary disease. *Disease Models and Mechanisms*. 4(2); 172-192
177. Kessel, HW Beams, CY Shih (1974). The origin, distribution and disappearance of surface cilia during embryonic development of *Rana pipiens* as revealed by scanning electron microscopy. *The American Journal of Anatomy* 141; 341-359

178. David R. Curran, Lauren Cohn (2010). Advances in Mucous Cell Metaplasia A Plug for Mucus as a Therapeutic Focus in Chronic Airway Disease. *American Journal of respiratory cell and molecular biology*. 42(3), 268-275
179. Thomas Vaccari, Serena Duchi, Katia Cortese, Carlo Tacchetti, David Bilder (2010). The vacuolar ATPase is required for physiological as well as pathological activation of the Notch receptor. *Development* 137(11); 1825-1832
180. Andrew D. Chalmers, Bernhard Strauss, Nancy Papalopulu (2003). Oriented cell divisions asymmetrically segregate aPKC and generate cell fate diversity in the early *Xenopus* embryo. *Development* 130(12); 2657-2668
181. Alfons T.L. Van Lommel (2002). *From Cells to Organs. A histology textbook and atlas*. Kluwer Academic Publisher
182. Olga Ossipova, Jacqui Tabler, Jeremy B. A. Green, Sergei Y. Sokol (2007). PAR1 specifies ciliated cells in vertebrate ectoderm downstream of aPKC. *Development* 134(23); 4297-4306
183. Sarah J. Bray (2006). Notch signalling: a simple pathway becomes complex. *Nature Reviews Molecular Cell Biology* 7, 678-689  
184. Raphael Kopan, Xenia G. Ilagan (2009). The Canonical Notch Signaling Pathway: Unfolding the Activation Mechanism. *Cell* Vol.137, Issue 2, 216-233

185. Jason R. Rock, Mark W. Onaitis, Emma L. Rawlins, Yun Lu, Cheryl P. Clark, Yan Xue, Scott H. Randell, Brigid L. M. Hogan (2009). Basal cells as stem cells of the mouse trachea and human airway epithelium. PNAS 106(31); 12771-12775
186. Anne Schohl, François Fagotto (2002).  $\beta$ -catenin, MAPK and Smad signaling during early *Xenopus* development. Development 129(1); 37-52
187. Thomas A. Drysdale, Richard P. Elinson (1992). Cell migration and induction in the development of the surface ectodermal pattern of the *Xenopus laevis* tadpole. Development, Growth & Differentiation 34; 51-59
188. Kyeongmi Kim, Blue B. Lake, Tomomi Haremak, Daniel C. Weinstein, Sergei Y. Sokol (2012). Rab11 Regulates Planar Polarity and Migratory Behavior of Multiciliated Cells in *Xenopus* Embryonic Epidermis. Developmental Dynamics 241(9); 1385-1395
189. Patricia Castillo-Briceno, Laurent Kodjabachian (2014). *Xenopus* embryonic epidermis as a mucociliary cellular ecosystem to assess the effect of sex hormones in a non-reproductive context. Frontiers in zoology 6,11

## **Résumé:**

Le processus de formation des cils mobiles multiples (multiciliogénèse) est composé de nombreuses étapes. Récemment, nous avons démontré que les microARNs de la famille miR-449 contrôlent plusieurs de ces étapes. Au cours de mon travail, je me suis concentré sur le rôle joué par miR-449 dans deux aspects particuliers du développement de l'épithélium embryonnaire multicilié de l'amphibien *Xenopus laevis*: la formation d'un réseau d'actine sous la surface apicale des cellules multiciliées et l'intercalation des cellules multiciliées au sein de la couche muqueuse de l'épiderme en développement.

Dans les cellules multiciliées, un réseau dense d'actine sous-jacent l'aspect apicale de la membrane cellulaire (coiffe d'actine) est nécessaire pour l'ancrage des multiples corps basaux, et donc pour une ciliogénèse approprié. Les petites GTPases jouent un rôle important dans la formation de la coiffe d'actine. Dans le cadre de mon travail, j'ai participé à l'identification de la petite GTPase R-Ras comme une des véritables cibles de miR-449. J'ai démontré que la réorganisation de la coiffe d'actine et l'ensemble du processus de multiciliogénèse étaient compromis lorsque l'ARN messager de R-Ras se trouve protégé de la liaison avec miR-449. En outre, la formation de la coiffe d'actine et le processus de multiciliogénèse redeviennent normaux lorsque la traduction des ARN messagers de R-RAS protégés contre miR-449 est empêchée.

J'ai aussi contribué à identifier une nouvelle cible de miR-449, le gène *Steel*, qui code pour le ligand du récepteur transmembranaire à activité tyrosine-kinase KIT. La repression de *Steel* par miR449 est impliquée dans le processus par lequel les cellules multiciliées atteignent leur position finale dans l'épiderme embryonnaire de *Xenopus*. *STEEL*, qui agit probablement comme une molécule de guidage pour les cellules multiciliées qui expriment KIT, doit être réprimé par miR-449 dans ces mêmes cellules en cours de migration pour assurer leur déplacement directionnel approprié. En conclusion, mon travail a contribué à élucider le rôle complexe joué par le miARN miR-449 dans le processus de multiciliogénèse chez les vertébrés.

## **Summary:**

The process of multiple motile cilia formation (multiciliogenesis) is composed of many different steps. Recently, we demonstrated that microRNAs of the miR-449 family control several of these steps. During my work, I focused on the role played by miR-449 in two particular aspects of the development of the multiciliated embryonic epithelium of the amphibian *Xenopus laevis*: the formation of an actin network underneath the apical surface of multiciliated cells and the intercalation of the developing multiciliated cells within the mucous layer of the epidermis.

In multiciliated cells, a dense actin network underlying the apical aspect of the cell membrane (actin cap) is required for the anchoring of the multiple basal bodies, and therefore for proper ciliogenesis. Small GTPases play important role in the formation of the actin cap. In the course of my work, I took part in the identification of transcripts coding the small GTPase R-Ras as bona fide targets of miR-449. I demonstrated that apical and subapical actin network reorganization and multiciliogenesis were impaired when R-Ras mRNA was protected from miR-449 binding. Moreover, the actin cap formation and multiciliogenesis were rescued when the translation of protected R-Ras transcripts was prevented. I also contributed to the finding that a new miR-449 target, the KIT receptor tyrosin kinase ligand *STEEL*, is involved in the process through which the multiciliated cells reach their final position within the developing frog epidermis. *STEEL*, which likely acts as a guidance molecule for the KIT-expressing multiciliated cells, needs to be repressed by miR-449 within the migrating cells to ensure their proper directional migration.

Altogether, my work contributed to elucidate the complex role played by the miR-449 miRNA in the process of vertebrate multiciliogenesis.

